RWE

Awel y Môr Offshore Wind Farm

Category 6: Environmental Statement

Volume 4, Annex 2.3: Physical Processes Modelling Results

Date: **April 2022**

Revision: **B**

Application Reference: 6.4.2.3

Pursuant to: APFP Regulation 5(2)(a)

REVISION	DATE	STATUS/ REASON FOR ISSUE	AUTHOR:	CHECKED BY:	APPROVED BY:
A	August 2021	PEIR	ABPmer	RWE	RWE
B	March 2022	ES	ABPmer	RWE	RWE

www.awelymor.cymru

RWE Renewables UK
Swindon Limited

Windmill Hill Business Park
Whitehill Way
Swindon
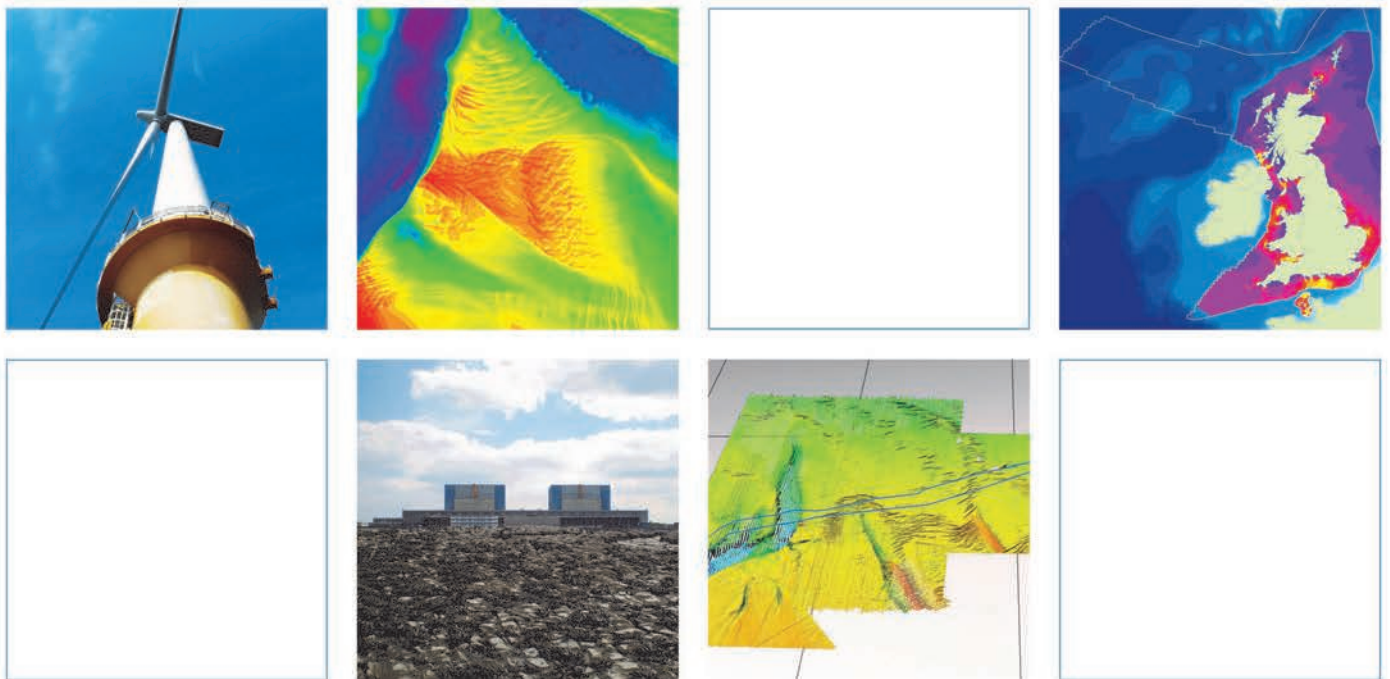Wiltshire SN5 6PB
T +44 (0)8456 720 090
www.rwe.com

Registered office:
RWE Renewables UK
Swindon Limited Windmill
Hill Business Park Whitehill
Way
Swindon

 Fferm Wynt Alltraeth
AWEL Y MÔR
Offshore Wind Farm

GoBe Consultants Ltd

Awel y Môr Offshore Windfarm Environmental Impact Assessment

Volume 4, Annex 2.3: Marine Geology, Oceanography and Physical Processes Technical Assessment
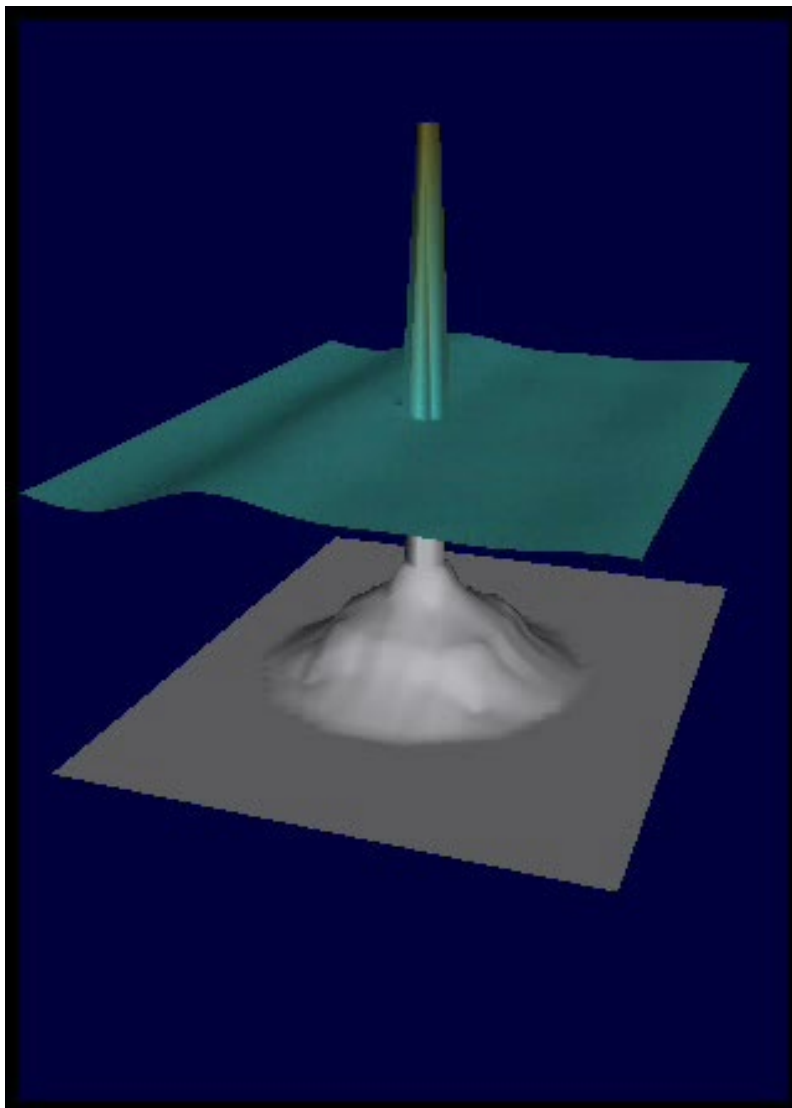
March 2022

Innovative Thinking - Sustainable Solutions

Page intentionally left blank

Awel y Môr Offshore Windfarm Environmental Impact Assessment

Volume 4, Annex 2.3: Marine Geology, Oceanography and Physical Processes Technical Assessment

March 2022

Document Information

Document History and Authorisation		
Title	Awel y Môr Offshore Windfarm Environmental Impact Assessment	
	Volume 4, Annex 2.3: Marine Geology, Oceanography and Physical Processes Technical Assessment	
Commissioned by	GoBe Consultants Ltd	
Issue date	March 2022	
Document ref	R.3628	
Project no	R/4913/1	
Date	**Version**	**Revision Details**
09/04/2021	0.1	V0.1 Issue for Client review
16/04/2021	0.2	V0.2 GoBe Comments
23/04/2021	0.3	V0.3 Addresses GoBe Comments
12/04/2021	0.4	V1.2 Addresses RWE comments
09/06/2021	0.5	V2.1 Boundary updates
09/07/2021	1	V3.1 Issued for Client use
23/03/2021	2	V0.1 Boundary updates Issued for Client use

Prepared (PM)	Approved (QM)	Authorised (PD)
Anthony Brooks	David Lambkin	Heidi Roberts

Suggested Citation

ABPmer, (2021).   Awel y Môr Offshore Windfarm Environmental Impact Assessment, Volume 4, Annex 2.3: Marine Geology, Oceanography and Physical Processes Technical Assessment, ABPmer Report No. R3628. A report produced by ABPmer for GoBe Consultants Ltd, March 2022.

Notice

ABPmer
Quayside Suite, Medina Chambers, Town Quay, Southampton, Hampshire   SO14 2AQ

Contents

Appendices

Tables

Figures

1 Introduction

1.1 Overview

ABPmer has been commissioned to deliver the Marine Geology, Oceanography and Physical Processes Environmental Impact Assessment (EIA) for the Awel y Môr Offshore Wind Farm (referred to as AyM) (Figure 1). This annex provides supporting technical analysis underpinning the following coastal processes assessments presented in the Preliminary Environmental Information Report (PEIR) Volume 2, Chapter 2: Marine Geology, Oceanography and Physical Processes:

- Changes to suspended sediment concentrations, bed levels and sediment type (Section 2);
- Changes to the wave regime (Section 3);
- Changes to the tidal regime and tidally driven sediment transport regime (Section 4); and
- Scour and seabed alteration (Section 5).

The assessments presented in this technical annex have been informed by:

- The collation and analysis of baseline information (as set out in Volume 4, Annex 2.1: Marine Geology, Oceanography and Physical Processes Baseline); and
- Hydrodynamic, wave and sediment plume modelling (the setup of which is set out in Volume 4, Annex 2.2: Model calibration).

1.2 Approach

In order to assess the potential changes relative to the baseline (existing) coastal and marine environment, a combination of complementary approaches have been adopted for the AyM marine physical processes assessment. These include:

- The 'evidence base' containing monitoring data collected during the construction, and operation and maintenance of other offshore wind farm developments. The evidence base also includes results from numerical modelling and desk-based analyses undertaken to support other offshore wind farm EIAs, especially that used to support the consenting processes for the adjacent operational Gwynt y Môr (referred to as GyM) OWF;
- New numerical modelling to consider potential changes to hydrodynamics and waves and sediment transport in response to the construction, operation and decommissioning of AyM;
- Analytical assessments of AyM project-specific data, including the application of rule-based and spreadsheet based numerical models; and
- Standard empirical equations describing the relationship between (for example) hydrodynamic forcing and sediment transport or settling and mobilisation characteristics of sediment particles released during construction activities (e.g. Soulsby, 1997).

Awel y Môr Offshore Windfarm Environmental Impact Assessment:
Volume 4, Annex 2.3: Marine Geology, Oceanography and Physical Processes Technical Assessment

GoBe Consultants Ltd

Figure 1.   **Study area**

2   Sediment Disturbance

2.1   Overview

This section presents a study of the likely nature of sediment plumes (footprint, concentration, duration) and resulting sediment deposition (footprint and thickness) as a result of Maximum Design Scenario (MDS) sediment disturbance during the construction of AyM OWF (described in Section 2.2).

Maps of potential increase in suspended sediment concentration (SSC) and thickness of sediment deposition are produced for various sediment disturbance scenarios and tidal conditions.

The MDS(s) are determined using the information contained in the full project design description (Volume 2, Chapter 1: Offshore Project Description). For each activity, the rate and duration of sediment disturbance and the total sediment volume is calculated for individual occurrences and for all occurrences of the activity, including the range of design permutations (e.g. a smaller number of larger foundations or a larger number of smaller foundations). Scenarios are identified that are likely to correspond to the realistic 'worst case' in terms of instantaneous and overall effects. The effect of all other options in the design envelope are therefore expected to be equal to or less than the results presented in this report.

2.2   Sediment disturbance scenarios

The following MDS sediment releases were considered:

- Four activity types:
    - Pre-lay cable trenching using an MFE tool at the seabed;
    - Sandwave clearance using an MFE tool at the seabed;
    - Dredge spoil disposal at the water surface related to seabed preparation for cables or foundations (including sandwave clearance);
    - Drill arisings release at the water surface during drilling for monopile foundations;
- At locations in the array area, along the length of and in the middle of the export cable corridor (ECC), and near to the landfall; and
- Occurring (separately) on and around representative spring and neap tidal periods.

A range of information has been used to characterise the nature of the surficial and sub-seabed sediments within the array and offshore ECC. These include benthic samples collected to inform the GyM EIA (RWE, 2005) and by BGS, as well as interpreted geophysical data collected as part of the AyM site characterisation survey work (Fugro, 2020a and b). The range of sediment grain size categories used in the model are shown in Table 1.

Table 1.   Sediment grain size fractions used

Sediment Fraction Name	Representative Grain Size (µm)	Representative Settling Velocity (m/s)
Gravel	~8,000	0.5
Coarse sand	~1,000	0.1
Medium sand	~250	0.03
Fine sand	~150	0.01
Silt	~10	0.0001

Further details of the sedimentary environment of the array and offshore ECC, including data sources and the distribution of different sediment types, are provided in Volume 4, Annex 2.1: Marine Geology, Oceanography and Physical Processes Baseline. The representative proportion of different grain size fractions present in the AyM array areas and offshore ECC for the purposes of sediment disturbance modelling is described below.

The subsequent plume settlement and dispersion is simulated over a further period following the end of the sediment disturbance to characterise the persistence and dispersion rate of the plume. Where fines are present, a three-day period is sufficient for the purposes of the EIA assessment. Sands and gravels will have redeposited to the seabed within a much shorter timescale (time depending on water depth, approximately 2 to 20 minutes for sands in 5 to 50 m water depth, respectively; gravel will settle faster than sands).

Table 2 provides a summary of the sediment plume scenarios, the location of each release, the mass of sediment and the type of sediment at each site.

Table 2. **Sediment disturbance scenarios**

Scenario Number	Mean Tidal Condition	Activity	Location of Release (UTM[3]1N)	Rate and Duration of Disturbance	Grain Size Fractions (% of Total)
1	Neap	Pre-lay trenching (MFE)	X 450000 Y 5926000 (Central array area)	875 kg/s for 24 hours 50 min, 400 m/hr, @3 m above bed	(Surficial sediments) Gravel (25%) Coarse sand (10%) Medium sand (63%) Silt (2%)
2	Spring				
3	Neap	Sandwave clearance (MFE)		1,000 kg/s for 12 hours 20 min, static, @3 m above bed	
4	Spring				
5	Neap	Drilling a large monopile	X 450428 Y 5923240 (Central array area)	207.2 kg/s for 34 hours, static, @water surface	(Disaggregated glacial till) Gravel (20%) Coarse sand (20%) Medium sand (20%) Fine Sand (20%) Silt (20%)
6	Spring				
7	Neap, Peak Flood	Dredge spoil disposal (TSHD)		1,749,000 kg sudden release*, static, @water surface	(Surficial sediments) Gravel (25%) Coarse sand (10%) Medium sand (63%) Silt (2%)
8	Spring, Peak Flood				
9	Neap	Pre-lay trenching (MFE)	ECC (along whole length)	875 kg/s for 53 hours 40 min	(Surficial sediments) Medium sand (95%) Silt (5%)
10	Spring				
11	Neap	Sandwave clearance (MFE)	X 460882 Y 5914783 ECC (mid length)	1,000 kg/s for 12 hours 20 min, static, @3 m above bed	
12	Spring				
13	Neap, Peak Flood			1,749,000 kg sudden release*,	

Scenario Number	Mean Tidal Condition	Activity	Location of Release (UTM³1N)	Rate and Duration of Disturbance	Grain Size Fractions (% of Total)
14	Spring, Peak Flood	Dredge spoil disposal (TSHD)		static, @water surface	
15	Neap	Sandwave clearance (MFE)	X 467862 Y 5910772 Nearshore (~2.5 km from landfall)	1,000 kg/s for 12 hours 20 min, static, @3 m above bed	
16	Spring				
17	Neap, Peak Flood	Dredge spoil disposal (TSHD)		1,749,000 kg sudden release*, static, @water surface	
18	Spring, Peak Flood				
*	At the time of peak flood current speed (to the east).				

The following notes also apply:

- The MFE in Scenarios 1 and 2 is represented as a moving source over a 24:50 hr period (two tidal cycles), moving initially from south to north (across the current axis) for one tide (including one ebb and one flood) and then from west to east (with the current axis) for one tide, at a constant (maximum) rate of 400 m/hr (covering ~10 km during the simulation period).
- The location of the static releases in Scenarios 3 to 8 (local sandwave clearance, drilling and dredge spoil disposal) is approximately central in the AyM array area.
- The MFE in Scenarios 9 and 10 is represented as a moving source over a 53:40 hr period (over 4 to 5 tidal cycles), moving from the landfall to the edge of the array area, at a constant (maximum) rate of 400 m/hr (covering ~21.5 km during the simulation period).
- The location of the static releases in Scenarios 11 to 14 (local sandwave clearance and dredge spoil disposal) is approximately halfway along, and central within, the AyM export cable corridor.
- The location of the static releases in Scenarios 15 to 18 (local sandwave clearance and dredge spoil disposal) is in the shallow nearshore area, approximately 2.5 km offshore of the landfall for the AyM export cable corridor.
- The distribution of grain size fractions for surficial sediments (all activity types except drilling) are representative of the general sediment types in the array area and ECC; a conservative minimum proportion of fines has been identified for each area in order to provide a conservatively realistic description of far field plume SSC and sediment deposition thickness.
- The distribution of grain size fractions for sub-surface sediments (drilling) are a uniform mixture of all sediment types, representing the poorly sorted glacial tills that form the majority of the material to be drilled. The proportion of fines that will be fully disaggregated or otherwise created from the drilling process is not known, however, the chosen value is considered to provide a conservatively realistic description of far field plume SSC and sediment deposition thickness.

The rate of sediment disturbance (1000 kg/s) by an active MFE tool was conservatively estimated based on the MDS trench cross section dimensions, the speed of progress of the tool, and the bulk density of the local sediment type at each of the three locations. This estimate is conservative in comparison to the working rate of the device (1000 m³/hr, which corresponds to approximately 440 kg/s).

All of the disturbed sediment is initially released at 3 m above the local seabed level. In practice, an MFE will also displace some proportion of sediment from the trench to the adjacent seabed through liquefaction and nearbed gravity flow (rather than necessarily putting sediment into suspension higher

into the water column). This scenario therefore provides a conservative representation of the nearfield plume effect of the MFE process.

The mass of sediment placed into suspension by a spoil release scenario is estimated as follows:

- A representative large hopper sediment volume of 11,000 m³ is released suddenly (within a single 10-minute timestep in the model).
- The total mass of sediment released is estimated as 11,000 m³ sediment x 0.6 solidity ratio x 2,650 kg/m³ solid density = 17,490,000 kg.
- The majority (90%) of the sediment volume is realistically assumed to descend directly to the bed in the 'active phase' of the plume as a single mass of sediment, which does not contribute to the more diffuse SSC effects considered by the plume model.
- The remaining 10% of sediment (10% of 17,490,000 kg =1,749,000 kg) is assumed to be dispersed into the water column at the point of release, allowing sediment grains to remain in suspension for longer, forming the 'passive phase' of the plume.
- It is assumed that the sediment is sufficiently mixed by the dredging process that the proportion of sediment fractions in the active and passive phases are the same as the original seabed sediment.

The proportion of sediment assumed to be in the passive and active phases is a conservatively representative value that may vary in practice. The chosen value (up to 10% in the passive phase) is consistent with studies on this topic by Becker *et al.* (2015).

The assumed sediment type at each location is presently informed by grab sample results along the ECC and within the array area, collected and analysed for the adjacent GyM OWF (overlapping with the AyM array area). The proportion of sediment mass in each grain size fraction is accounted for in the number and mass of the individual particles released at each timestep. A low minimum 5% fines content is conservatively assumed in sediment disturbed within the ECC, although a much lower proportion (<1%) is more typical of the surficial sediments.

2.3 Sediment plume model results

2.3.1 Overview

The following results are provided as images in Appendix A:

- Results for each model scenario in Table 2.
- Maps of SSC at the end of sediment disturbance, and one and three days later.
- Maps of instantaneous maximum SSC at any time throughout the model simulation period.
- Timeseries of SSC at a central location in the area of sediment disturbance (centre of the MFE route or at the location of drilling or spoil disposal).

The following results are provided as images in Appendix B:

- Maps of settled sediment thickness at the end of the model simulation period.

The sediment plume modelling was originally undertaken for PEIR. There are no relevant changes to the MDS with respect to the sediment disturbance assessed. As such, the images in Appendix A still show the PEIR array area and ECC boundary for AyM. See other images in this report for the location of the ES array area boundary.

Results for SSC describe an increase in SSC relative to the ambient naturally occurring condition.

2.3.2   Summary of results: SSC of plumes from longer duration disturbance (moving and static point sources over multiple flood/ebb cycles)

Table 3.   Summary of results: SSC of plumes from longer duration disturbance (moving and static point sources over multiple flood/ebb cycles)

Parameter	Summary
Change or effect	Pre-lay cable trenching using an MFE (moving nearbed source) Local sandwave clearance using an MFE (static nearbed source) Continuous drilling at one location (static surface source)
Phase	Construction
Location	Array area and export cable corridor
Maximum Design Scenario	Pre-lay cable trenching: disturbance rate 1000 kg/s; duration 25 hr in array area, 53 hr in export cable corridor; release at 3 m above bed level; 400 m/hr. Local sandwave clearance: disturbance rate 875 kg/s; duration 12 hr in array area, 12 hr in export cable corridor; release at 3 m above bed level; static. Drilling: disturbance rate 207.2 kg/s; duration 34 hr; release at water surface; static. Trenching and sandwave clearance scenarios: [gravel (25%), coarse sand (10%), medium sand (63%), silt (2%)] in array area, [medium sand (95%), silt (5%)] in export cable corridor. Drilling scenarios: [gravel (20%), coarse sand (20%), medium sand (20%), silt (20%)] in array area.
Maximum sediment plume extent	Up to one tidal excursion distance along the flood/ebb tidal axis from the activity (on spring tides: 11-12 km in the array area; 9-10 km in the offshore export cable corridor; 6-7 km in the nearshore export cable corridor.
Details of increase in SSC	Within small distances (<50 m) of the activity, SSC can be in the order of thousands to hundreds of thousands of mg/l, reducing rapidly with time and distance (through settlement and dispersion) to the order of hundreds or tens of mg/l. Where there is only a relatively low height of initial suspension from the seabed, SSC is unlikely to exceed 150 mg/l beyond approximately 5 m away for gravels, 30 m for coarse sand, 90 m for medium sand, and ~250-300 m for finer sands. The time required for redeposition of sands and gravels following low height disturbance is in the order of seconds to a few minutes. Where sediment is released at the water surface, SSC is unlikely to exceed 150 mg/l beyond approximately 100 m away for gravels, 500 m for coarse sand, 1.5-2 km for medium sand, and ~5 km for finer sands. The time required for redeposition of sands and gravels following release at the water surface is in the order of a few minutes to 1.5 hours. Only finer (silt and mud) sized sediments are likely to persist in suspension for long enough to cause any effect in SSC beyond the above distances. SSC due to the limited quantity of fines present is expected to be up to 50 mg/l, up to approximately 2 km downstream of the activity; decreasing to 1 to 5 mg/l within 1 to 3 days through progressive dilution and dispersion.

Parameter	Summary
Scenario results figures	Maps of the increase in SSC as a result of pre-lay cable trenching using an MFE (moving nearbed source) are provided by Scenarios 1 and 2 for the array area, and Scenarios 9 and 10 for the export cable corridor, for neap and spring tidal conditions, respectively, in Appendix A.
Maps of the increase in SSC as a result of local sandwave clearance using an MFE (static nearbed source) are provided by Scenarios 3 and 4 for the array area, Scenarios 11 and 12 for the middle of the export cable corridor, and Scenarios 15 and 16 for the nearshore end of the export cable corridor, for neap and spring tidal conditions, respectively, in Appendix A.
Maps of the increase in SSC as a result of continuous drilling at one location (static surface source) are provided by Scenarios 5 and 6 for the array area, for neap and spring tidal conditions, respectively, in Appendix A.

The following summary provides a general description and characterisation of the more detailed results shown in the scenario results images listed above. See the individual figures for site and scenario specific details of SSC and plume dimensions.

The plume feature resulting from continuous sediment disturbance activities is characterised as a long, relatively thin plume extending downstream from the point of active disturbance. Where the source is moving, the path of active disturbance in the simulation period is visible in the results images as a line of higher maximum instantaneous SSC.

Gravels and sands will settle relatively rapidly towards the seabed (see Table 1, settling velocities from 0.01 to 0.5 m/s). From the maximum expected height of initial suspension (3 m above bed), sediment of these grain sizes is likely to resettle to the seabed (no longer contributing to an increase in SSC) within 1 to 5 minutes. At a representative higher current speed of 0.9 m/s on spring tides, these sediment grades will settle to the bed (and not cause any effect on SSC) within 5 m (gravel) to ~250-300 m (finer sands) from the trench. This distance will be proportionally reduced during periods of lower current speed (e.g. times other than peak flow speed and generally around neap tides).

The level of SSC caused by all sediment types together is realistically expected to be locally very high at the location of active trenching (where sediment is being put into suspension at a rate of the order 800 to 1,000 kg/s). Within 5 m of the activity, SSC might be millions of mg/l or more locally, i.e. more sediment than water in parts of the local plume. The effect is very localised and would last only while the MFE is active over that section of the trench. As sediment in the plume is redeposited and dispersed both vertically and horizontally with distance and time downstream, SSC is expected to reduce to thousands or high hundreds of mg/l within tens to low hundreds of metres. These detailed nearfield processes are only relatively coarsely resolved in the model (at a resolution of approximately 100 m).

Where there is only a relatively low height of initial suspension from the seabed, only silt sized sediments are likely to persist in suspension for long enough to cause any effect on SSC beyond approximately 5 m for gravels, 30 m for coarse sand, 90 m for medium sand, and ~250-300 m for finer sands, from the trench.

The width of the plume of finer material (silt) is initially in the order of 10 to 50 m (within 10 to 20 minutes of release, up to 500 to 1,000 m downstream). The SSC in this section of plume is relatively high (up to 1,000 mg/l for all sediment types and up to 100 mg/l for silts alone).

During the first half tidal cycle (~6 hours), the width of the plume increases through dispersion to 50-100 m, all non-silt sediments have settled to the seabed, and SSC consequentially reduces rapidly to 5-10 mg/l.

After 3 days, the width of the measurable plume will spread to 250-500 m wide and SSC reduces to 1-2 mg/l as a result of ongoing sediment dispersion and settlement.

During spring tidal conditions, the disturbed sediment is carried away from the working area at a faster rate, dispersing the sediment mass over a larger area and water volume, and so the resulting SSC in the plume is relatively lower than on a comparable neap tide.

During slack water (on both neap and spring tides), water is not moving sediment away from the area of disturbance, resulting in suspended sediment accumulating in a local area of relatively higher SSC (approximately 100-200 m across, order of 5 to 10 mg/l). This local area of higher SSC is subsequently advected by the tide and may take longer to reduce to background levels than other parts of the plume generated during non-slack water conditions.

The limited width/footprint of the plume feature means that specific locations will only be affected by the described increase in SSC for the limited duration it takes for the plume to be advected past by the tide.

The path followed by the tidal ellipse is not the same on every tide, so it is unlikely that the same area of seabed will be affected by higher SSC more localised plume for more than one or two consecutive tides.

2.3.3   Summary of results: SSC of plumes from spoil disposal

Table 4.   Summary of results: SSC of plumes from spoil disposal

Parameter	Summary
Change or effect	Dredge spoil disposal at the water surface from a TSHD (static surface source)
Phase	Construction
Location	Array area and export cable corridor
Maximum Design Scenario	Dredge spoil release: disturbance 1,749,000 kg as a sudden release (10% of the full volume of the hopper becomes suspended); release at water surface; static release; [gravel (25%), coarse sand (10%), medium sand (63%), silt (2%)] in array area, [medium sand (95%), silt (5%)] in export cable corridor.
Maximum sediment plume extent	Up to one tidal excursion distance along the flood/ebb tidal axis from the activity (on spring tides: 11-12 km in the array area; 9-10 km in the offshore export cable corridor; 6-7 km in the nearshore export cable corridor.
Details of increase in SSC	Within small distances (<50 m) of the activity, SSC can be in the order of hundreds of thousands to millions of mg/l, reducing rapidly with time and distance (through settlement and dispersion) to the order of hundreds or tens of mg/l. Although the sediment mass is released at the water surface, sediment is shed from the mass into suspension evenly through the water column. SSC is unlikely to exceed 150 mg/l beyond approximately 100 m away for gravels, 500 m for coarse sand, 1.5-2 km for medium sand, and ~5 km for finer sands. The time required for redeposition of sands and gravels following release at the water surface is in the order of a few minutes to 1.5 hours. Only finer (silt and mud) sized sediments are likely to persist in suspension for long enough to cause any effect in SSC beyond the above distances. SSC due to the limited quantity of fines present is expected to be up to 50 mg/l, up to approximately 2 km downstream of the activity; decreasing to 1 to 5 mg/l within 1 to 3 days through progressive dilution and dispersion.

Parameter	Summary
Details of increase in deposition	The main mass (90% volume) of spoil deposit will descend directly to the seabed and result in a sizable deposit of variable (not predictable) shape, extent and thickness. The sediment in suspension may settle out over a wider area with greater extent but proportionally smaller thickness. Distances and extents will likely be within the above described distances for SSC. In practice, the thickness and extent will depend on the volume actually released, the spread of the material on impact with the seabed, the current speed at the time of the release, and the nature of the sediment put into suspension. Thicknesses greater than 0.05 m and 0.3 m are possible in all cases, but the maximum area of effect is inherently limited by the finite volume of sediment released (see the detailed results for a range of possible outcomes). Fines in the suspended plume are expected to become widely dispersed and so will not resettle with measurable thickness locally. Fines in the main body of the spoil deposit will remain buried within that mass.
Scenario results figures	Maps of the increase in SSC as a result of spoil disposal at the water surface from a TSHD are provided by Scenarios 7 and 8 for the array area, Scenarios 13 and 14 for the central export cable corridor, and Scenarios 17 and 18 for nearshore areas close to the landfall, for neap and spring tidal conditions, respectively, in Appendix A.

The following summary provides a general description and characterisation of the more detailed results for each location shown in the figures listed above. See the individual figures for site and scenario specific details of SSC and plume dimensions.

The passive phase plume feature resulting from a spoil disposal event is characterised as an isolated circular plume, initially with higher concentration in the centre, decreasing with radial distance outwards.

Gravels and sands will settle relatively rapidly towards the seabed (see Table 1, settling velocities from 0.01 to 0.5 m/s). From the maximum expected height of initial suspension (approximately 35 m above bed within the AyM array area), sediment of these grain sizes is likely to resettle to the seabed (no longer contributing to an increase in SSC) within approximately 1 to 60 minutes. At a representative higher current speed of 0.9 m/s on spring tides, these sediment grades will settle to the bed (and not cause any effect on SSC) within approximately 65 m for gravel, 315 m for coarse sand, 1,050 m for medium sand and 3,150 m for finer sands, from the trench. This distance will be proportionally reduced during periods of lower current speed (e.g. times other than peak flow speed and generally around neap tides).

Fine sand and silt sized sediments persist in suspension for longer than relatively coarser sediment grain sizes (i.e. medium sand, coarse sand and gravels) and so control the majority of the effect on SSC beyond the above durations/distances.

The proportion of silt in the seabed sediment being disturbed is lower in the array area (2%) than in the cable corridor (5%), and the water depth is also greater, leading to proportionally lower SSC in the plume in the array from otherwise similar activities (a smaller proportion of the total disturbed sediment might persist in suspension for longer periods and the plume can be more dispersed, to lower concentrations, through the greater water depth).

The dimensions of the plume are realistically expected to be in the order of tens of metres in diameter at the point of release (not resolved directly by the model). The plume model indicates that dispersion will increase the plume width to approximately 1 to 2 km after one tidal cycle (approximately 12 hours), 3 km after one day and to approximately 5 km after 3 days, with an associated reduction in SSC.

The level of SSC associated with all sediment fractions is realistically expected to be locally very high at the location of the spoil release (millions of mg/l within 5 m of the activity, i.e. more sediment than water in the local plume. This level of detail is not resolved directly by the sediment plume model, which indicates a more dispersed initial concentration of 1,000 to 10,000 mg/l.

Due to ongoing dispersion and the settlement of non-silt sediment to the seabed during the first half tidal cycle, the level of SSC associated with the remaining silt in the advected plume will reduce with time from 50 to 100 mg/l in central parts of the plume after one day, to less than 2 mg/l after 3 days.

The limited width/footprint of the plume feature means that specific locations will only be affected by the described increase in SSC for the limited duration it takes for the plume to be advected past by the tide. The limited width of the spoil disposal plume also means that only locations closely aligned to the disposal location along the tidal axis are likely to be measurably affected.

The path followed by the tidal ellipse is not the same on every tide, so it is unlikely that the same area of seabed will be affected by higher SSC more localised plume for more than one or two consecutive tides.

2.3.4 Summary of results: Settlement thickness resulting from plumes from MFE trenching

Table 5.   Summary of results: Settlement thickness resulting from plumes from MFE trenching

Parameter	Summary
Change or effect	Pre-lay cable trenching using an MFE (moving nearbed source)
Phase	Construction
Location	Array area and export cable corridor
Maximum Design Scenario	Pre-lay cable trenching: disturbance rate 1000 kg/s; duration 25 hr in array area, 53 hr in export cable corridor; release at 3 m above bed level; 400 m/hr; [gravel (25%), coarse sand (10%), medium sand (63%), silt (2%)] in array area, [medium sand (95%), silt (5%)] in export cable corridor.
Maximum sediment deposition extent	Where there is only a relatively low height of initial suspension from the seabed, sediments are likely to deposit within a distance proportional to their grain size/settling rate. Assuming a 3 m height of ejection and representative 1 m/s current speed at the time of disturbance, the maximum extent is approximately 5 m for gravels, 30 m for coarse sand, 90 m for medium sand, and ~250-300 m for finer sands. The time required for redeposition of sands and gravels following low height disturbance is in the order of seconds to a few minutes.
Details of increase in deposition	Sands and gravels may cause a measurable thickness of sediment deposition within the above described distances for SSC. In practice, the thickness and extent will depend on the volume of sediment locally displaced, the height of ejection, the current speed at the time of the release, and the nature of the sediment. Thicknesses greater than 0.05 m and 0.3 m are possible in all cases, but the maximum area of effect is inherently limited by the finite volume of sediment disturbed (see the detailed results for a range of realistically possible outcomes). Fines are expected to become widely dispersed and so will not resettle with measurable thickness locally.

Parameter	Summary
Scenario results figures	Maps of settlement thickness as a result of pre-lay cable trenching using an MFE are provided by Scenarios 1 and 2 for the array area, and Scenarios 9 and 10 for the export cable corridor, for neap and spring tidal conditions, respectively, in Appendix B. Maps of settlement thickness as a result of localised sandwave clearance using an MFE are provided by Scenarios 3 and 4 for the array area, Scenarios 11 and 12 for the middle of the export cable corridor, and Scenarios 15 and 16 for the nearshore end of the export cable corridor, for neap and spring tidal conditions, respectively, in Appendix B.

Estimates of the footprint and thickness of sediment deposition from MFE trenching are provided based on:

- The results of the sediment plume model; and
- Direct estimates (for all sediment types).

The sediment plume model results provide the more reliable description of settlement thickness in the far field, i.e. for sediments that are subject to advection and dispersion over timescales greater than 1 hour and distances greater than 500 to 1,000 m.

The direct estimates provide a more generalised but demonstrably realistic range of potential deposition area/thickness combinations in the nearfield, i.e. for sediment of any type that is deposited more rapidly to the seabed in timescales less than 1 hour and distances less than 500 to 1,000 m. Such direct estimates can provide a more reliable description of details in the nearfield that are not resolved spatially or temporally by the sediment plume model.

MFE - sediment plume model estimates of settlement thickness

The following summary provides a general description and characterisation of the more detailed results for each location shown in the figures listed above. See the individual figures for site and scenario specific details of settlement thickness and extent.

The results show the thickness of sediment following initial deposition. In practice (and specifically excluded from the plume model scenarios) the same sediment may be subsequently re-eroded and resettled elsewhere as part of the ongoing natural sediment transport regime.

The predicted thickness of settlement is limited. The coarser sand and gravel fractions at each site settle to the seabed within a limited time of release (from seconds up to 5 minutes, i.e. within the 10 minute timestep of the sediment plume model) and so tend to be deposited within a relatively small footprint (from metres up to 200 m), resulting in a relatively greater local average thickness of 50 to 100 mm in the AyM array area and 50 to 150 mm within the export cable corridor. The predicted thickness of settlement for only the finer sediments dispersed more widely in the passive phase plume at these locations is very limited, in the order of <1 mm in all sites, over a dispersed area of effect.

Sediment accumulation of this magnitude would not cause a measurable change in bed level or sediment type in practice. Fine sediments that do settle are also likely to experience further erosion and dispersion during subsequent tides. The area and thickness of sediment settlement from the active phase and coarser sediments in the passive phase of the plume which are not resolved in detail by the plume model are considered below.

MFE - direct estimates of settlement thickness

As discussed in Section 2.3.2, coarser sediments (gravels and sands) will settle form the maximum height of disturbance (3 m) relatively rapidly towards the seabed and so the distance of advection and dispersion is realistically limited to distances within 5 m (gravel) to ~250-300 m (finer sands) downstream from the trench during representative stronger tidal current conditions (0.9 m/s). Distances will be proportionally less at times of lower current speed. The plume model does not resolve spatial details less than the resolution of the model mesh (approximately 100 m) and tidal current speed varies widely over flood and ebb, and spring and neap cycles. The following method provides a range of realistic direct estimates.

The volume of sediment displaced from the trench is finite and proportional to the trench cross section (up to 6 m²) and so it is possible to estimate the maximum average sediment thickness for a range of realistic downstream dispersion distances. Results are presented in Table 6.

The calculations in Table 6 assume that 100% of the sediment volume is fully displaced from the trench cross section and that 100% of the displaced sediment is deposited within the downstream dispersion distance indicated. In practice, if the cable simultaneously laid, a large proportion of the sediment in the trench cross section would be intentionally retained or actively backfilled to provide the intended level of cover, proportionally reducing the volume, area and thickness of sediment deposited elsewhere. A small proportion of the disturbed material (2 to 5%) may be finer material that remains in suspension and also does not contribute to the volume, area and thickness of sediment deposited outside but nearby to the trench.

This calculations in Table 6 also assume that the downstream dispersion is perpendicular to the trench axis (the AyM ECC makes a slightly shallower angle, approximately 45 degrees, to the tidal axis along most of its length, so the predicted distances may be reduced, with a corresponding increase in thickness). Where the current direction is more oblique to the trench, the perpendicular distance from the trench to the edge of the deposit might be reduced, with a proportional increase in average thickness. In all cases, a larger footprint or extent of effect for any reason will result in a proportionally smaller average thickness of deposition, and *vice versa*.

Table 6.   Maximum average sediment deposit thickness for a range of realistic downstream dispersion distances (assuming 100% sediment is ejected and locally redeposited)

Downstream Dispersion Distance (m)	Maximum Average Thickness of Sediment Accumulation (mm) for Varying Trench Cross Sections		
	4 m²	5 m²	6 m²
5	800	1,000	1,200
10	400	5,00	600
25	160	2,00	240
50	80	100	120
100	40	50	60
150	27	33	40
200	20	25	30
250	16	20	24
300	13	17	20

2.3.5 Summary of results: Settlement thickness resulting from plumes from spoil disposal

Table 7.   Summary of results: Settlement thickness resulting from plumes from spoil disposal

Parameter	Summary
Change or effect	Dredge spoil disposal at the water surface from a TSHD (static surface source)
Phase	Construction
Location	Array area and export cable corridor
Maximum Design Scenario	Dredge spoil release: disturbance 1,749,000 kg as a sudden release (10% of the full volume of the hopper becomes suspended); release at water surface; static release; [gravel (25%), coarse sand (10%), medium sand (63%), silt (2%)] in array area, [medium sand (95%), silt (5%)] in export cable corridor.
Maximum sediment deposition extent	Sediments deposit within a distance proportional to their grainsize/settling rate, the vertical distance to settle, and the ambient current speed at the time of release. Assuming a conservatively large 50 m water depth and representative 1 m/s current speed, the extent is approximately 100 m for gravels, 500 m for coarse sand, 1.5-2 km for medium sand, and ~5 km for finer sands. The time required for redeposition of sands and gravels following release at the water surface is in the order of a few minutes to 1.5 hours.
Details of increase in deposition	The main mass (90%) of the spoil deposit will descend directly to the seabed and result in a likely sizable deposit of variable (and not predictable) shape, extent and thickness. The remaining 10% of sediment in suspension may settle out over a wider area with potentially greater extent but proportionally smaller thickness. Distances and extents will likely be within the distances described above. In practice, the thickness and extent will depend on the volume actually released, the spread of the material on impact with the seabed, the current speed at the time of the release, and the nature of the sediment put into suspension. Thicknesses greater than 0.05 m and 0.3 m are possible in all cases, but the maximum area of effect is inherently limited by the finite volume of sediment released (see the detailed results for a range of realistically possible outcomes). Fines in the suspended plume are expected to become widely dispersed and so will not resettle with measurable thickness locally. Fines in the main body of the spoil deposit will remain buried within that mass.
Scenario results figures	Maps of settlement thickness resulting from the passive phase of the plume (~10% of the sediment volume) during dredge spoil disposal are provided by Scenarios 1 and 2 for the array area, and Scenarios 9 and 10 for the export cable corridor, for neap and spring tidal conditions, respectively, in Appendix B. (The settlement thickness resulting from the active phase of the plume (~90% of the sediment volume) is considered separately in another section below).

Estimates of the footprint and thickness of sediment deposition from dredge spoil disposal are provided based on:

- The results of the sediment plume model for the passive phase of the plume only (for all sediment types and for silts alone).
- Direct estimates for the passive phase of the plume only (for all sediment types); and
- Direct estimates for the active phase of the plume only (for all sediment types).

The sediment plume model results provide the more reliable description of settlement thickness in the far field, i.e. for sediments that are subject to advection and dispersion over timescales greater than 1 hour and distances greater than 500 to 1,000 m.

The direct estimates provide a more generalised but demonstrably realistic range of potential deposition area/thickness combinations in the nearfield, i.e. for sediment of any type that is deposited more rapidly to the seabed in timescales less than 1 hour and distances less than 500 to 1,000 m. Such direct estimates provide a more reliable description of details in the nearfield that are not resolved spatially or temporally by the sediment plume model.

The results from the plume model relate only to the sediment in the passive phase of the plume (i.e. 10% of the total sediment volume/mass being deposited). Results for the passive and active phases of the plume (described separately below) should be considered together in order to describe the full effect of the dredge spoil release.

Spoil disposal passive phase - sediment plume model estimates of settlement thickness

The following summary provides a general description and characterisation of the more detailed results for each location and activity shown in the figures. See the individual figures for site and scenario specific details of settlement thickness and extent.

The results show the thickness of sediment following initial deposition. The same sediment is expected to immediately re-join the natural sedimentary environment and will be subsequently re-eroded and resettled elsewhere as part of the ongoing natural sediment transport regime.

The predicted thickness of settlement accounting for all sediment types in the passive phase plume is limited. The coarser sand and gravel fractions at each site settle to the seabed within a limited time of release (from minutes to 1 hour) and so tend to be deposited within a relatively small footprint. In the AyM array area the deposit has a length scale of 200 to 300 m or less, resulting in a local average thickness of 70 to 100 mm. In the export cable corridor, possibly due to shallower water depths and lowers current speed, the deposit is less dispersed less between the surface and the seabed, forming a smaller deposit with a length scale 100 m, resulting in a greater average local thickness of 200 to 300 mm. The predicted average thickness of settlement for the finer sediments dispersed more widely in the passive phase plume at these locations is very limited, in the order of <1 mm in all sites, over a dispersed area of effect.

Sediment accumulation of this magnitude would not cause a measurable change in bed level or sediment type in practice. Fine sediments that do settle are also likely to experience further erosion and dispersion during subsequent tides. The area and thickness of sediment settlement from the active phase and coarser sediments in the passive phase of the plume which are not resolved in detail by the plume model are considered below.

Spoil disposal passive phase – direct estimates of settlement thickness

As discussed in Section 2.3.3, coarser sediments (gravels and sands) in the passive plume will settle from the water surface (up to 35 m above the seabed in the AyM array area) relatively rapidly towards the seabed and so the distance of advection and dispersion is realistically limited to distances within 65 m (gravel) to ~3,150 m (finer sands) downstream from the disposal site during representative stronger tidal current conditions (0.9 m/s on spring tides). Distances will be proportionally less at times of lower current speed (and during neap tides). The plume model does not resolve spatial details less than the resolution of the model mesh (approximately 100 m) and tidal current speed varies widely over flood and ebb, and spring and neap cycles. The following method provides a range of realistic direct estimates.

As noted in Section 2.2, the total volume of sediment in the passive phase of the plume is limited (10% of 11,000 m³ = 1,100 m³) and so it is possible to estimate the maximum average sediment thickness for a range of realistic dispersion footprint dimensions. Results are presented in Table 8. These estimates conservatively assume that all sediment in the passive phase is deposited to the seabed, however, the silt fraction (comprising up to 2 to 5% of the sediment mass in the passive phase, depending on the location, see Table 2) will remain in suspension for longer (as described by the plume model results above) and will not contribute to these estimates.

Table 8.   **Maximum average sediment deposit thickness as a result of the passive plume for a range of realistic downstream dispersion distances**

Downstream Dispersion Distance (m)	Maximum Average Thickness of Sediment Accumulation (mm) for Varying Dispersion Widths.		
	50 m	100 m	200 m
100	220	110	55
250	88	44	22
500	44	22	11
750	29	15	7
1,000	22	11	6
2,000	11	6	3
3,000	7	4	2
4,000	6	3	1
5,000	4	2	1

Spoil disposal active phase – direct estimates of settlement thickness

The active phase of the plume will descend rapidly and directly to the seabed, where it will spread laterally, initially with the force of impact and then under gravity. The final shape or dimensions of the deposit therefore cannot be predicted in detail. The volume of sediment in the active phase of the plume is also limited (90% of 11,000 m³ = 9,900 m³) and so it is also possible to estimate the maximum average sediment thickness for a range of realistic dispersion footprint areas. Results are presented in Table 9.

Table 9.   **Maximum average sediment deposit thickness for a range of realistic active phase deposit dimensions and areas**

Deposit Length Scale (m)	Deposit Footprint Area (m²)*	Maximum Average Thickness of Sediment Accumulation (mm)
50	2,500	3,960
100	10,000	990
150	22,500	440
200	40,000	248
222	49,500	200
315	99,000	100
445	198,000	50
* Deposit footprint area] = [Deposit length scale²)		

2.3.6   Tidal excursion distance and plume advection

The tidal excursion distance is the approximate distance over which a package of water (or a section of plume with elevated SSC) is advected during one flood or ebb tide.

The local extent of the sediment plume at any given time is the limited area within which changes to instantaneous local magnitude and extent of elevated SSC are experienced. As described in Sections 2.3.2 and 2.3.3, the plume is being almost continuously moved (advected) by the ambient currents. This section considers the distances and directions that the plume might be displaced from the source before it is dissipated to near background concentrations, and therefore the overall spatial extent that any local plume effects might be (temporarily) experienced.

The relative motion (local speed and direction) of the plume at any given time in the tidal cycle will vary depending not only on the relative time in the flood ebb cycle, but also the spatially varying flow characteristics along the path of advection. In open water, plume advection typically describes an approximately elliptical path (the tidal ellipse), which may or may not be closed, i.e. returning to approximately the same position at the end of the tidal cycle. In areas of more complex flow, the path may be more complex, e.g. following coastline or bathymetric features, and the path may not be necessarily closed. The overall distance that the plume is advected from the disturbance source (both along the tidal axis and laterally across it) is the tidal excursion distance and describes the area over which any effects on SSC are likely to occur. Conversely, areas beyond the tidal excursion distance and footprint are unlikely to experience any effect on SSC from the plume.

A summary map of idealised tidal excursion ellipses is shown in Figure 2.

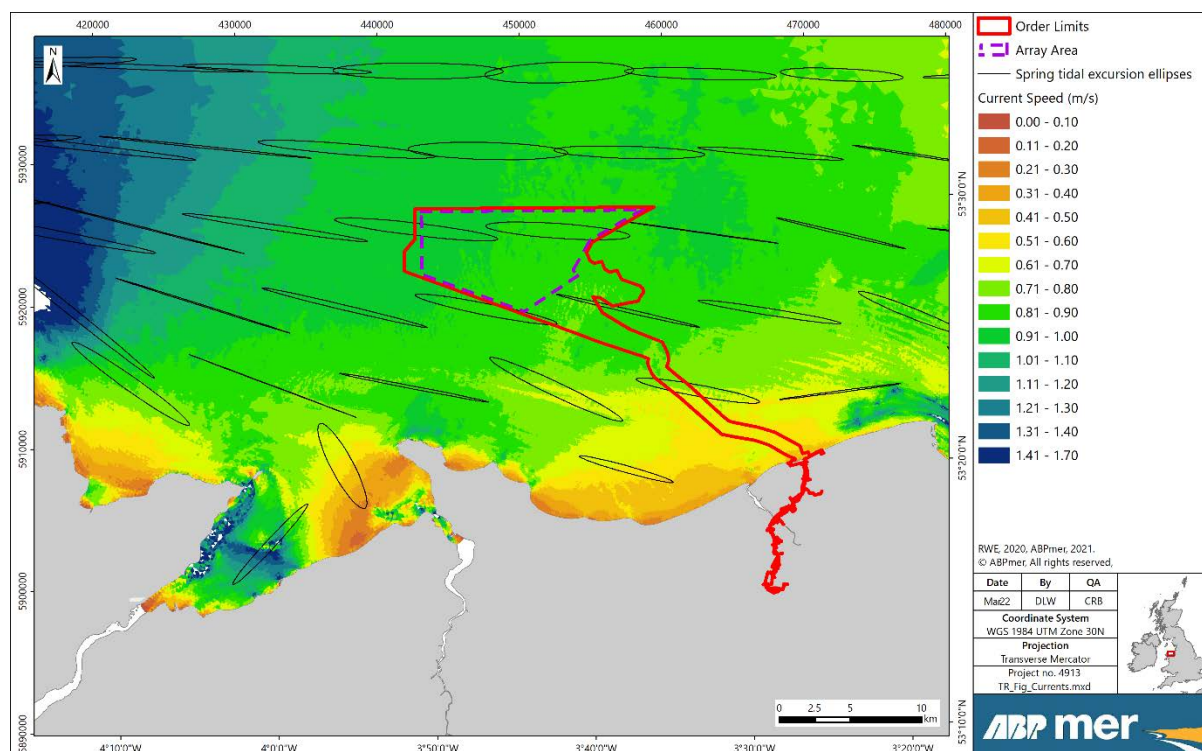**Figure 2.**   **Peak current speed on a mean spring tide and associated tidal excursion ellipses**

The tidal axis is indicated by the orientation of the long axis of the ellipse. The tidal axis is generally parallel to the adjacent coastlines in offshore areas but will of course vary closer to headlands and estuaries. The ellipses are relatively long and thin, suggesting a rectilinear pattern of tidal currents (well

defined ebb and flood directions with minimal rotation of the tide through the tidal cycle). The ellipses in the study area are relatively similar in size (length) across the offshore area but become smaller as a result of lower peak current speeds nearshore and in shallower water. In practice, patterns of tidal flow (described in more detail in Section 4.3) are more complex and the path taken by water will be affected by detailed patterns of flow over distances less than one (idealised) tidal excursion in some areas.

The displacement of the plume features by tidal currents also provides another proxy measure of the tidal excursion distance from each of the release locations for representative neap and spring range conditions. The path of the plume (including changes in flow speed and direction elsewhere in the model domain) provides a 'Lagrangian' estimate. In areas of more complex flow (e.g. near to headlands and estuaries), this can provide a more realistic measure than the alternative 'Eularian' estimate (based on the net displacement of water past a particular location).

The values below were determined based on the observed advection of the plumes features in the sediment plume model results, over multiple flood and ebb cycles, during representative mean neap and mean spring tidal range conditions. There can be variation in the peak current speed between consecutive flood and ebb tides (see Volume 4, Annex 2.2: Model calibration), therefore, a small range of tidal excursion distances are presented for tidal ranges representative of mean neap and mean spring conditions.

The tidal excursion distance varies in proportion to the peak current speed during particular flood or ebb cycles. As such, the distance may also be smaller than the mean neap conditions (on smaller than mean neap tidal ranges) and occasionally larger than the mean spring condition (on larger than mean spring tidal ranges).

In the AyM array area:

- On neap tides, the tidal excursion distance is between ~5 to 6 km, depending on the peak flow speed during that half tidal cycle.
- On spring tides, the tidal excursion distance is between ~11 to 12 km, depending on the peak flow speed during that half tidal cycle.

In the middle part of AyM export cable corridor:

- On neap tides, the tidal excursion distance is between ~4 to 5 km, depending on the peak flow speed during that half tidal cycle.
- On spring tides, the tidal excursion distance is between ~9 to 10 km, depending on the peak flow speed during that half tidal cycle.

In the nearshore area close to the landfall of the AyM export cable corridor:

- On neap tides, the tidal excursion distance is ~2.5 to 3 km.
- On spring tides, the tidal excursion distance is ~6 to 7 km.

The spatial variation in Lagrangian tidal excursion provides a more generalised basis for the description of the extent of potential effect on SSC and sediment deposition.

3   Changes to the Wave Regime

3.1   Overview

This section sets out the assessment of changes to the wave regime within the study area, based on spectral wave modelling of the MDS for blockage within the AyM array.

The wave model has been built using the MIKE21FM Spectral Wave (SW) module, which simulates the development, propagation and dispersion of wave energy throughout the model domain.

More detailed information about the design and validation of the wave model may be found in Volume 4, Annex 2.2: Model Design and Validation.

The wave model creates discrete simulations of wave height, period and direction throughout the domain, for a representative range of selected everyday and extreme wave conditions (return periods and directions). The wave condition scenarios considered by the model for the assessment are:

- Wave coming directions (SW, SSW, S, SSE, SE); and
- Return periods (50% non-exceedance, 0.1 yr; 1 yr; 10 yr; 50 yr; 100 yr).

The details of each condition as defined in a central location of the northern offshore wave boundary, approximately 5 km north of AyM, are presented in Table 10.

Table 10.   **Wave and wind boundary conditions for each of the directional return period seastate conditions tested**

Directional Sector	Case (Return Period)	Significant Wave Height (m)	Peak Wave Period (Tp, s)	Mean Wave Direction (°N)	Wind Speed @10 m (m/s)	Wind Direction (°N)
W	50% no exc	0.80	4.66	270	5.9	270
	0.1 yr RP	2.09	6.04	270	11	270
	1 yr RP	3.52	7.84	270	15	270
	10 yr RP	4.84	9.20	270	17	270
	50 yr RP	5.72	10.00	270	21.4	270
	100 yr RP	6.16	10.38	270	21.4	270
WNW	50% no exc	0.91	5.14	292.5	6.5	292.5
	0.1 yr RP	2.64	7.03	292.5	12.7	292.5
	1 yr RP	4.40	9.07	292.5	17.3	292.5
	10 yr RP	6.16	10.73	292.5	21.4	292.5
	50 yr RP	7.26	11.65	292.5	22.3	292.5
	100 yr RP	7.81	12.08	292.5	26	292.5
NW	50% no exc	0.73	4.65	315	4.9	315
	0.1 yr RP	2.42	6.74	315	12	315
	1 yr RP	3.96	8.62	315	16.3	315
	10 yr RP	5.50	10.16	315	21	315
	50 yr RP	6.60	11.13	315	22.3	315
	100 yr RP	7.04	11.50	315	22.3	315

Directional Sector	Case (Return Period)	Significant Wave Height (m)	Peak Wave Period (Tp, s)	Mean Wave Direction (°N)	Wind Speed @10 m (m/s)	Wind Direction (°N)
NNW	50% no exc	0.66	4.37	337.5	5.3	337.5
	0.1 yr RP	2.20	6.40	337.5	11	337.5
	1 yr RP	3.63	8.22	337.5	15.5	337.5
	10 yr RP	5.06	9.71	337.5	19.8	337.5
	50 yr RP	6.05	10.62	337.5	24	337.5
	100 yr RP	6.49	10.99	337.5	21.3	337.5
N	50% no exc	0.57	4.02	0	4.37	0
	0.1 yr RP	2.09	6.25	0	11	0
	1 yr RP	3.52	8.11	0	15	0
	10 yr RP	4.84	9.51	0	17	0
	50 yr RP	5.72	10.34	0	21.4	0
	100 yr RP	6.16	10.73	0	21.4	0

3.2   Baseline conditions

Plots showing the spatial distribution of wave height and direction for each of the baseline wave conditions without any wind farm infrastructure present are shown in Appendix C (Figure C1 to Figure C5). In the figures, solid lines show the array area extents for each wind farm; the dotted line indicates the extent of Constable Bank.

As shown in the following assessment section and confirmed in baseline model scenarios that include the effect of nearby operational windfarms (not shown), the monopile foundations installed in the nearby operational windfarms cause no measurable difference (<2.5% wave height, <0.1 s wave period and <3 deg wave direction) in the baseline condition.

3.3   Assessment

3.3.1   Awel y Môr foundation type and number

The AyM design envelope includes a range of wind turbine generator (WTG) and offshore substation platform (OSP) foundation types, numbers and dimensions. The MDS is identified as the combination of options presenting the greatest total potential blockage to waves passing through the array area.

The MDS for AyM is:

- 50 x smaller WTGs on conical gravity base
    - 45 m base diameter at seabed, tapering to 15 m at sea surface;
    - Scour protection 2 m high in centre, tapered to edge, 112.5 m diameter; and
    - Combined equivalent blockage width 35.5 m per foundation.
- 2 x OSP on jacket foundations with suction buckets
    - 6 legs, 3.5 m diameter;
    - Cross bracing, 1.0 m diameter;
    - Base dimensions at seabed 50 m x 80 m;
    - Scour protection 2 m high in centre, tapered to edge, 40 m diameter around each leg; and
    - Combined equivalent blockage width 55.5 m per foundation.

- 1 x met mast on monopile
    - 5 m diameter;
    - Scour protection 2 m high, 25 m diameter; and
    - Combined equivalent blockage width 6.3 m per foundation.

Any other combination of foundation type and number would result in a smaller total blockage.

3.3.2   Other operational wind farm foundation type and number

The actual built dimensions of individual foundations in a wind farm are not normally publicly listed and, in any case, may vary slightly within an array to account for differences in water depth or ground conditions. Conservatively representative WTG, OSP and met mast foundation details for the nearby existing operational offshore wind farms are used as follows.

Gwynt y Môr:

- 160 x WTGs on monopile foundations
    - 6.0 m diameter
- 2 x OSP on jacket foundation
    - 4 legs, 2.0 m diameter
    - Cross bracing, 1.0 m diameter
    - Combined equivalent blockage width 16.0 m per foundation
- 1 x met mast on monopile foundation
    - 2.0 m diameter

Rhyl Flats:

- 25 x WTGs on monopile foundations
    - 4.7 m diameter
- 1 x met mast on monopile foundation
    - 2.0 m diameter

North Hoyle:

- 30 x WTGs on monopile foundations
    - 4.0 m diameter
- 1 x met mast on monopile foundation
    - 2.0 m diameter

Burbo Bank:

- 25 x WTGs on monopile foundations
    - 4.7 m diameter

Burbo Bank Extension:

- 32 x WTGs on monopile foundations
    - 7.1 m diameter
- 1 x OSP on jacket foundation
    - 4 legs, 2.0 m diameter
    - Cross bracing, 1.0 m diameter
    - Combined equivalent blockage width 16.0 m per foundation

No scour protection is included in the above combined equivalent blockage width calculations for nearby existing operational offshore wind farms. The details of scour protection (height, slope, diameter, armour type, proportion and location of foundations applied to) are not publicly available. Although (very) conservatively included for AyM, nearbed scour protection is unlikely to make a measurable change to local water depths or contribution to blockage of waves (or currents) for the purposes of this assessment.

3.3.3   Foundation layouts

For AyM, the indicative layout pattern for smaller WTGs and areas of likely locations for the OSPs are used in conjunction with the MDS type and number of foundations (shown in Figure 3). This layout is considered to be realistically representative of any that might be eventually considered.
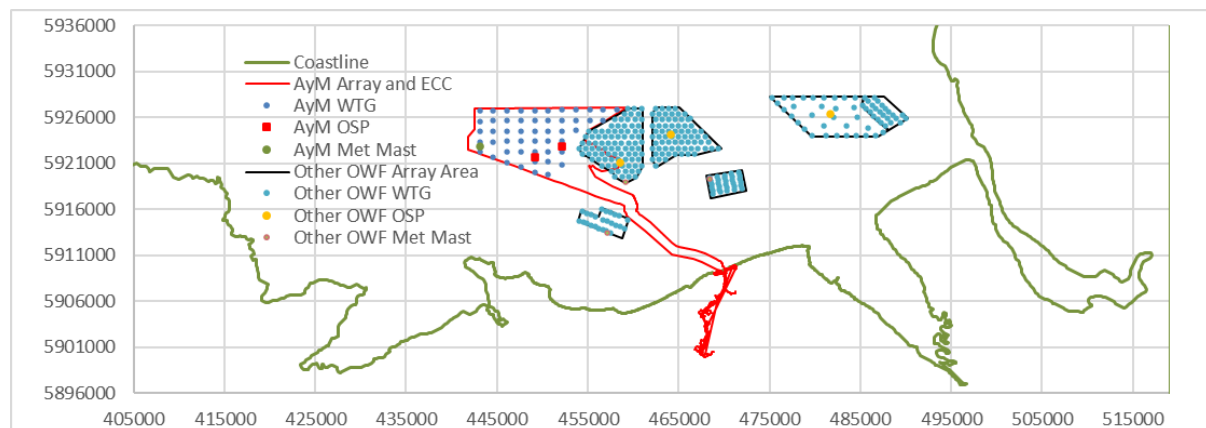

Figure 3.   Layout of AyM MDS foundations, and the location of foundations in all other nearby operational wind farms

The actual location of all foundations in other nearby operational wind farms are known and used directly in the model.

3.3.4   Changes to the wave regime

Plots showing the spatial distribution of changes to wave height for each of the baseline wave conditions as a result of MDS foundation type, number and layout for AyM, and other nearby operational wind farms, are shown in Appendix C (Figure C6 to Figure C10). In the figures, solid black lines show the array area extents for each wind farm; the dotted black line indicates the extent of Constable Bank.

Changes less than 5% of the baseline wave height would be indistinguishable from natural variability both within the seastate (difference between individual waves) and compared to normal rates of change (over timescales of one hour or less); such small differences would not be measurable in practice. Changes less than 2.5% are also less than the reasonably expected accuracy of the model and so are excluded from the colour scale.

The images show that wave height is progressively decreased with distance through the array area in the direction from which the waves are coming. As a result, the maximum reduction in wave height is found downwind of individual WTGs in the central downwind part of the array area (5 to 7.5%). The maximum reduction outside of the array area in the full range of wave directions and return periods considered is only 2.5 to 5%. The scale of the change is dependent on the nature of the wave height/period condition, and the main direction of the wave energy with respect to the shape/thickness

of the array and the alignment of the foundations. The maximum corresponding changes to wave period and wave direction (not shown) are less than 0.1 s and 3 deg respectively, at all locations, in all cases.

Wave height begins to recover immediately downwind of the array area. Recovery occurs mainly due to a wave energy spreading from areas to the side less or unaffected by interaction with the wind farm. For smaller seastates, recovery of the dominant wave condition can also occur as a result of ongoing wind energy input.

In the area where changes to wave height are greatest (typically within and immediately to the south or south-west of the array area), water depths are also relatively large (15 to 30 mLAT, with an additional 1 to 7 m depth depending on the state of the tide). In such water depths, a minimum wave period (approximately 6 s and larger in 30 m depth) is required to penetrate deeply enough to cause any water movement at the seabed. Even longer waves in conjunction with a sufficient wave height are needed to cause sufficient motion at the seabed to contribute to sediment transport.

As the wave period will not be affected (by more than 0.1 s), the ability of individual waves to reach the seabed will be unaffected. Where an individual wave is large enough to reach the seabed, the predicted change in wave height (proportional to the resulting amplitude of water movement) is locally only up to 5 to 10 %. The difference is therefore unlikely to result in a measurably different motion of water. Further south and south east, the water depth progressively decreases (to 10 mLAT) and so more/smaller waves may interact with the seabed more strongly and more frequently; however, wave height also recovers rapidly with distance downwind of the array area and the relative difference in wave height in shallower areas is even more limited (2.5 to 5% or less).

The greatest differences in wave height at Constable Bank are limited to the lower end of the 2.5 to 5% range and tend to occur mainly during north westerly through northerly wave conditions (occurring 10 to 15 % of the time) and only then with a difference of 2.5 to 5% wave height and no associated change in wave period or wave direction (<0.1 s, <3 deg). No difference in wave height (<2.5%) is predicted in the majority of wave scenarios modelled, or therefore, in the 75% of time that waves are not from these directions. Larger differences may occur within AyM (e.g. in response to larger waves from the west), however, such larger effects do not then extend in the direction of Constable Bank.

Differences in wave height are less than 2.5 % in nearshore areas (up to 5 km from the coast) and at the adjacent coastlines.

Sediment transport by waves alone in deep water results in a to-and-fro motion with minimal net transport. In conjunction with tidal currents, waves increase the overall rate of sediment transport but the combined net transport rate and direction is largely controlled by the speed and direction of the coincident tidal current.

The differences in wave height, period and direction described above are small in absolute and relative terms and (as a small additional contribution to the tidally dominated transport) could only cause an even smaller change to overall instantaneous sediment transport rates or directions. The differences would not be measurable in practice and are easily within the range of natural variability in wave height from wave to wave, from hour to hour during the passage of a storm, and in the context of seasonal and interannual variation of wave climate.

Further discussion of the results is provided in the PEIR impact assessment (Volume 2, Chapter 2: Marine Geology, Oceanography and Physical Processes).

4   Changes to the Tidal Regime

4.1   Overview

This section sets out the assessment of changes to the tidal regime within the study area, based on hydrodynamic modelling of the PEIR MDS for blockage within the AyM array. The PEIR MDS blockage (described below) was based on a larger number of WTGs (95 in PEIR versus 50 in the ES) and therefore the results in this section provide a conservative assessment of potential impacts of the ES MDS.

The hydrodynamic model has been built using the MIKE21FM Hydrodynamic (HD) module, which simulates the development, propagation and dispersion of the tidal wave, and associated movements of water, throughout the model domain.

More detailed information about the design and validation of the wave model may be found in Volume 4, Annex 2.2: Model Design and Validation.

The hydrodynamic model creates a continuous simulation of tidal water level, depth average current speed and current direction throughout the domain, for a representative spring-neap cycle (approximately mean neap and mean spring conditions) during the model validation period.

4.2   Baseline conditions

Plots showing the spatial distribution of current speed and direction for representative neap and spring conditions, during low water, peak flood, high water and peak ebb periods, without any wind farm infrastructure present are shown in Appendix D (Figure D1 and Figure D2). In the figures, solid lines show the array area extents for each wind farm; the dotted line indicates the extent of Constable Bank. The images in Appendix D still show the PEIR array area boundary for AyM. See other images in this report for the ES array area location.

As shown in the following assessment section and as confirmed in baseline model scenarios that include the effect of nearby operational windfarms (not shown), the monopile foundations installed in the nearby operational windfarms cause no measurable difference (<0.01 m water level, <0.01 current speed and <1 deg current direction) at the resolution of the model (100 m) in the baseline condition. As discussed below in Section 4.3.2, although not explicitly resolved by the model, a very localised narrow wake is expected behind (and similar to the width of) individual foundations, associated with a small reduction in average current speed and a corresponding small increase in turbulence intensity. The wake signature will dissipate and recover with distance downstream, becoming indistinguishable to ambient conditions within tens to a few hundreds of metres. The dimensions and characteristics of such wake features were measured (by ABPmer) in the Burbo Offshore Wind Farm, reported in SeaScape Energy (2008).

4.3   Assessment

4.3.1   Awel y Môr and other operational wind farm foundation type, number and layout

The AyM design envelope includes a range of wind turbine generator (WTG) and offshore substation platform (OSP) foundation types, numbers and dimensions. The MDS is identified as the combination of options presenting the greatest total potential blockage to water movement through the array area.

The PEIR MDS foundation type, number and layout for AyM is the same as described and used for modelling changes to the wave regime in Section 3.3, except with 95 WTGs (of the same dimensions) in a slightly larger array area. Any other combination of foundation type and number in the design envelope (for PEIR and for the ES) would result in a smaller total blockage.

Conservatively representative WTG, OSP and met mast foundation type, dimensions and numbers are used for the nearby existing operational offshore wind farms, as described and used for modelling changes to the wave regime in Section 3.3. The actual location of all foundations in other nearby operational wind farms are known and used directly in the model (see Figure 3).

4.3.2   Changes to the tidal regime

Further discussion of the results is also provided in the ES impact assessment (Volume 2, Chapter 2: Marine Geology, Oceanography and Physical Processes).

Instantaneous current speed and direction

Plots showing the spatial distribution of changes to current speed for selected tidal conditions as a result of the PEIR MDS foundation type, number and layout for AyM, and other nearby operational wind farms, are shown in Appendix D (Figure D3 and Figure D4). In the figures, solid black lines show the array area extents for each wind farm; the dotted black line indicates the extent of Constable Bank. The images in Appendix D still show the PEIR array area boundary for AyM. See other images in this report for the ES array area location.

The model has a relatively high spatial resolution of 100 m in the study area including AyM and all of the nearby operational wind farms. The model therefore describes the change caused by the individual foundations, and the propagation and recovery of wake features, at a similar scale. In practice, at a more local sub-grid scale (order of metres), slightly greater changes might be expected in the very local flow field of the individual foundations (e.g. a narrow wake approximately as wide as the foundation, and turbulent eddies in the order of tens of centimetres to a few metres within the wake footprint, all recovering to ambient conditions within the order of tens to a few hundreds of metres downstream).

Changes less than 5% of the baseline condition (approximately 0.4 m spring tidal range, 0.05 m/s current speed or 5 deg current direction) would be largely indistinguishable from frequent and high natural rates of change over various timescales, including: flood/ebb/slack; spring-neap; solstice-equinox; interannual/metonic cycle; and, variability in response to meteorological (surge) influence. Such small absolute differences would also not be accurately measurable in practice. Changes less than 0.01 m/s are also less than the reasonably expected accuracy of the model and so are excluded from the colour scale.

The result figures show that changes to current speed at the resolution of the model (at length scales greater than 100 m) will be less than 0.01 m/s, which is very small in both absolute and relative terms, within the range of natural variability, and not measurable in practice. Corresponding changes to current direction (not shown in the figures) are less than 1 deg.

Residual current speed and direction

The timeseries of current speed and direction throughout the model domain was also used to determine the residual current speed and direction (the long term drift rate and direction of water over one spring neap cycle). The results are equally valid for baseline conditions with or without the nearby other built wind farms which cause no measurable difference in currents (<0.01 m water level, <0.01 current speed

and <1 deg current direction) at the resolution of the model (approximately 100 m). Consistent with the very limited scale of change in instantaneous current speed and direction described above as a result of the MDS foundation type, number and layout for AyM (MDS foundation type, number and layout for AyM), no measurable change in residual current speed or direction is predicted either within the AyM array, or elsewhere.

A plot showing the spatial distribution of residual current speed and direction for selected tidal conditions are shown in Appendix D (Figure D5). In the figures, solid black lines show the array area extents for each wind farm; the dotted black line indicates the extent of Constable Bank.

Tidally driven sediment transport rate and direction

The timeseries of current speed and direction throughout the model domain was also used in conjunction with a simple sediment transport model (using the MIKE21FM Sand Transport (ST) module). The model simulates a time series of total load transport rate and direction for 250 μm diameter quartz sand in response to the shear stress caused by the tidal currents described by the hydrodynamic model).

The model results were used to determine the residual sand transport rate and direction (the long term transport rate and direction for representative medium to fine sand over one spring neap cycle). Consistent with the very limited scale of change in instantaneous current speed and direction described above, no measurable change in residual sand transport rate or direction is predicted either within the AyM array, or elsewhere, at the resolution of the model (approximately 100 m). Localised narrow wake features not resolved by the model may have a similarly localised effect on the texture (but not the morphology) of the seabed within their footprint; the wake is only likely to result in changes to seabed morphology immediately around the foundation base in the form of scour (described in Section 5).

Plots showing the spatial distribution of instantaneous sediment transport rate and direction for selected tidal conditions, and the residual sediment transport rate and direction over a representative spring-neap cycle, are shown in Appendix D (Figure D6 to Figure D8). In the figures, solid black lines show the array area extents for each wind farm; the dotted black line indicates the extent of Constable Bank.

5   Scour and Seabed Alteration

5.1   Overview

The purpose of this section is to conservatively and quantifiably estimate the area of seabed that will altered during the operational phase of the wind farm as a result of sediment scour that may develop adjacent to turbine foundations (in the absence of any scour protection).

The term scour refers here to the development of pits, troughs or other depressions in the seabed sediments around the base of turbine foundations. Scour is the result of net sediment removal over time (typically in the order of hours to days from installation in mobile sediments) due to the complex three-dimensional interaction between the foundation and ambient flows (currents and/or waves). Such interactions result in locally accelerated time-mean flow and locally elevated turbulence levels that enhance sediment transport potential in the area of influence. The resulting dimensions of the scour features and their rate of development are, generally, dependent upon the characteristics of the:

- Obstacle (dimensions, shape and orientation);
- Ambient flow (depth, magnitude, orientation and variation including tidal currents, waves, or combined conditions); and
- Seabed sediment (geotextural and geotechnical properties).

Based on the existing literature and evidence base, an equilibrium depth and pattern of scour can be empirically approximated for given combinations of these parameters. Natural variability in the above parameters means that the predicted equilibrium scour condition may also vary over time on, for example, spring-neap, seasonal or annual time-scales. The time required for the equilibrium scour condition to initially develop is also dependant on these parameters and may vary from hours to years.

Scour assessment for EIA purposes is considered here for three foundation types: monopiles; piled jacket foundations (a four-legged version); and gravity base foundation structures. Each foundation type may produce different scour patterns therefore monopiles, gravity base foundations and jacket foundations have all been considered. Suction caisson foundations (for monopods and jackets) have not been considered in the assessment below because these will fall within the envelope of change associated with the other three foundation types.

The concerns under consideration include the seabed area that may become modified from its natural state (potentially impacting sensitive receptors through habitat alteration) and the volume and rate of additional sediment resuspension, as a result of scour. The seabed area directly affected by scour may be modified from the baseline (pre-development) or ambient state in several ways, including:

- A different (coarser) surface sediment grain size distribution may develop due to winnowing of finer material by the more energetic flow within the scour pit;
- A different surface character will be present if scour protection (e.g. rock protection) is used;
- Seabed slopes may be locally steeper in the scour pit; and
- Flow speed and turbulence may be locally elevated.

The magnitude of any change will vary depending upon the foundation type, the local baseline oceanographic and sedimentary environments and the type of scour protection implemented (if needed). In some cases, the modified sediment character within a scour pit may not be so different from the surrounding seabed; however, changes relating to bed slope and elevated flow speed and

turbulence close to the foundation are still likely to apply. No direct assessment is offered within this document as to the potential impact on sensitive ecological receptors.

The assessment presented here is not intended for use in detailed engineering design. However, methodologies similar to those recommended for the design of offshore wind foundations (e.g. DNV, 2016) have been used in some cases where they are applicable. The methods applied to assess scour are set out in Appendix C.

5.2   Baseline conditions

Where obstacles are not present on the seabed, normal sediment transport processes can cause spatial and temporal variations in seabed level and sediment character in the baseline environment. Scour is a similar but localised change resulting from particular local patterns of sediment transport. Scour may also occur in the baseline environment in response to natural obstacles such as rocky outcrops or boulders. Key features of the baseline environment pertinent to the assessment of scour due to the presence of wind farm infrastructure are summarised below:

- The AyM array is characterised by the presence of coarse-grained unconsolidated sediments with both sand and sandy gravel particularly prevalent;
- Surficial sediment units are of variable thickness: the greatest thicknesses are found in south central and eastern areas of the array (4 to 6 m, up to 9 m) whilst in the north and west, pre-Holocene material is at or close to the surface (thickness <2 m); and
- Based on the prevalence and mobility of bedform features of varying scale in the available geophysical survey data, the seabed level is expected to vary naturally on hourly timescales to the order of centimetres to decimetres. This is primarily due to the movement of small scale bedforms due to the action of tidal currents and wave induced orbital currents. It will also vary over longer-timescales (order of decimetres to metres) in response to the migration of larger sand wave features.

5.3   Evidence base

The operational GyM was constructed using monopile foundations up to 6 m diameter. Of the 160 turbine foundations, about 70 have scour protection installed. The combined total of rock protection used for the GyM array and export cables during the construction campaign (2012 to 2015) was 388,758 tonnes. Monitoring evidence for GyM (and other nearby OWFs) is currently not publicly available and therefore the extent to which (i) scour has developed in locations without scour protection; and/or (ii) secondary scour has developed in locations with scour protection is presently unknown.

Whitehouse (1998) provides a synthesis of a range of research papers, industry reports, monitoring studies and other evidence available at that time, describing the patterns and dimensions of scour that result from a variety of obstacle shapes, sizes and environmental conditions. Building upon a theoretical understanding of the processes involved, the accepted methods for the prediction of scour mainly rely on stochastic relationships and approaches (i.e. relationships that are based on and describe the available evidence). As such, scour analysis is an evidence-based science where suitable analogues provide the most robust basis for prediction.

Since the publication of Whitehouse (1998), evidence continues to be collected and other predictive relationships have been developed and reported by the research community. In general, more recent observations have confirmed the approaches (and associated ranges of uncertainty) presented in Whitehouse (1998). As the evidence base has grown, additional approaches and relationships have been

developed to better predict scour for a wider range of more specific obstacle shapes, sizes and environmental conditions.

Monitoring evidence regarding scour development around unprotected wind farm monopile installations is provided by HR Wallingford *et al.* (2007) and ABPmer *et al.*, (2010) in a series of monitoring data synthesis reports for DTI and COWRIE. HR Wallingford *et al.*, (2007) note that the available data support the view that scour is a progressive process that can occur where the seabed sediment is potentially erodible and there is an adequate thickness of that sediment for scouring to occur. Where the seabed comprises consolidated pre-Holocene sedimentary units, the scour will be slower to develop and limited in depth. For instance, geotechnical surveys at Kentish Flats offshore wind farm (Outer Thames) show that the seabed consists of non-cohesive sands over more resistant London Clay. The post construction monitoring evidence generally indicates that maximum scour rates around the monopiles (of diameter 4.3 m) occurred during the first year from installation and then rapidly slowed with near stability occurring by the third anniversary of the works. Scour depths ranged from 1.5 to 1.9 m at the monitoring locations and the results indicate that the scour depth is restricted by the cohesive underlying clay formation.

A research paper by Whitehouse *et al.*, (2011) provides a summary of the field evidence for scour around gravity base foundations in the North Sea used in oil and gas projects. This review emphasized the sensitivity of scour to foundation shape, with foundations in very close proximity sharing similar hydrodynamic/ sedimentary environments displaying markedly different scour characteristics. This review also described field evidence for scour around a rectangular gravity base foundation (75 m by 80 m by 16 m high) located within the North Sea in 42 m water depth. Scour was measured as 2.5 to 3.5 m deep in 0.15 mm (i.e. fine) sand.

Scour protection is evidently a mature engineering concept and by design will both prevent primary scour and minimise secondary scour. The evidence base supporting the design of scour protection is therefore strong but is not relevant to this assessment. The evidence base concerning the environmental impacts of scour protection is more limited. Although multi-layered gravel and rock scour protection is being successfully used at the Thornton Bank offshore wind farm in conjunction with six gravity base foundations in a sandy environment with water depths (28 m, similar to depths encountered within the AyM array area) (ABPmer *et al.*, 2010).

5.4   Assessment

5.4.1   Outline of structures considered in assessment

The following foundation structures have been considered within the assessment presented in this section:

- Monopile foundations:
    - 15 m diameter (largest) and 13 m diameter (smallest);
- Jacket foundations:
    - 40 m x 40 m base with four 3.5 m diameter legs (largest) and 30 m x 30 m base with four 3.5 m diameter legs (smallest); and
- Gravity base foundations:
    - 55 m diameter base (largest) and 45 m diameter base (smallest).

For each foundation type, both the largest and smallest structures have been considered. This is because the former has the potential to cause the greatest extent of scour at the scale of individual foundations

whereas the latter may potentially be associated with the greatest extent of scour at the array scale, owing to the larger number of structures.

5.4.2 Factors affecting equilibrium scour depth

As summarised in Whitehouse (1998), a number of factors are known to influence equilibrium scour depth for monopiles, contributing to the range of observed equilibrium scour depths. These factors include the:

- Frequency and magnitude of ambient sediment transport;
- Ratio of monopile diameter to water depth;
- Ratio of monopile diameter to peak flow speed;
- Ratio of monopile diameter to sediment grain size;
- Sediment grain size, gradation and the geotechnical properties of sedimentary units; and
- The thickness of erodible sediment overlying more erosion resistant sublayers.

The influence of these factors where they do apply is to generally reduce the depth, extent and volume of the predicted scour, hence providing a less conservative estimate. For example, a greater frequency and magnitude of sediment transport can actually reduce the equilibrium scour depth, as the scour hole is also simultaneously being (partially) in-filled by ambient sediment transport.

The above factors have been considered in the context of the AyM array area and (all except one) were not found to significantly or consistently reduce the predicted values for the purposes of EIA. The thickness of erodible sediment in the northern half of the AyM array area is limited to a thin veneer (<2 m thick) in many locations. The underlying glacial tills are more erosion resistant and would not be expected to continue scouring after the overlying sediment veneer has been locally eroded. In practice, this will fundamentally limit maximum potential scour depth in most of the array area. The following assessment conservatively assumes that foundations will be located in areas of deeper erodible sediment where the full equilibrium scour depth might eventually occur.

The next greatest influence on local scour depth would arise from the installation of scour protection. If correctly designed and installed, scour protection will essentially prevent the development of local primary scour as described in this section. The dimensions and nature of scour protection may vary between designs but, given its purpose, would likely cover an area of seabed approximately similar to the predicted extent of the scour.

Interaction between ambient currents and the scour protection may lead to the development of secondary scour at its edges. The local dimensions of secondary scour are highly dependent upon the specific shape, design and placement of the protection. These parameters are highly variable and so there is no clear quantitative method or evidence base for accurately predicting the dimensions of secondary scour. However, as for foundations, the approximate scale of the scour depth and extent is likely to be proportional to the much smaller size of the individual elements comprising the protection.

5.4.3 Time for scour to develop around the foundation options

Scour depth can vary significantly under combined current and wave conditions through time (Harris *et al.* 2010). Monitoring of scour development around monopile foundations in UK offshore wind sites suggest that the time-scale to achieve equilibrium conditions can be of the order of 60 days in environments with a potentially mobile seabed (Harris *et al.*, 2011). However, as previously stated, equilibrium scour depths may not be reached for a period of several months or even a few years where erosion resistant sediments/ geology are present. These values account for tidal variations as well as the

influence of waves. (Near) symmetrical scour will only develop following exposure to both flood and ebb tidal directions.

Under waves or combined waves and currents an equilibrium scour depth for the conditions existing at that time may be achieved over a period of minutes, whilst typically under tidal flows alone equilibrium scour conditions may take several months to develop.

5.4.4   Spatial extent of scour

At the Scroby Sands offshore wind farm, narrow, elongated scour features have been observed to extend over tens or hundreds of metres from individual foundations, leading to a more extensive impact than would normally be predicted. The development of elongate scour features at Scroby Sands is considered to have occurred due to the strongly rectilinear nature of the tidal currents (a very well defined tidal current axis with minimal deviation during each half tidal cycle) which allows the narrow turbulent wake behind each foundation to persist over the same areas of seabed for a greater proportion of the time, leading to net erosion in these areas. Due to a relatively higher rate of tidal rotation, the development of such elongate scour features is less likely to occur within the AyM array area.

5.4.5   Results

Table 11 and Table 12 summarize the key results of the first-order scour assessment undertaken using the methodological approach set out in Appendix C. Results conservatively assume maximum equilibrium scour depths are symmetrically present around the perimeter of the structure in a uniform and frequently mobile sedimentary environment. Derivative calculations of scour extent, footprint and volume assume an angle of internal friction = 32 deg. Scour extent is measured from the structure's edge. Scour footprint excludes the footprint of the structure. Scour pit volumes for gravity base foundation structures are calculated as the volume of an inverted truncated cone, minus the structure volume; scour pit volume for the jacket foundations are similarly calculated but as the sum of that predicted for each the corner piles.

Table 11.   **Summary of predicted maximum scour dimensions for largest individual turbine foundation structures**

Parameter		Foundation type		
		Monopile (15 m diameter)	Multi-leg (40 m base, 4 x 3.5 m legs)	Gravity Base (55 m diameter)
Equilibrium Scour Depth (m)^	Steady current	19.5	4.6	3.1
	Waves	Insufficient for scour	Insufficient for scour	2.2
	Waves and current	19.5	4.6	3.5
	Global scour		1.4	
Extent from foundation* (m)	Local scour	31.2	7.3	4.9
	Global scour	N/A	40.0	N/A
Footprint* (m²)	Structure alone	177	38	2,376
	Local scour (exc. Structure)	4,530	987	929
	Global scour (exc. Structure)	N/A	4,988	N/A
Volume* (m³)	Local scour (exc. Structure)	34,224	1,739	1,392
	Global scour (exc. local scour and structure)	N/A	6,983	N/A
^ Results assume erodible bed and absence of geological controls				
* Based upon the scour depth for steady currents. Footprint and volume values are per foundation.				

Table 12.   Total seabed footprint of the different foundation types with and without Scour

Parameter	Monopiles		Multi-leg		Gravity Base	
	(13 m diameter)	(15 m diameter)	(30 m base length)	(40 m base length)	(45 m diameter)	(55 m diameter)
Maximum number of foundations	50 x WTG 2 x OSP	34 x WTG 2 x OSP	50 x WTG 2 x OSP	34 x WTG 2 x OSP	50 x WTG 2 x OSP	34 x WTG 2 x OSP
Seabed footprint of all foundations (m²)	6,990	6,362	2,040	1,424	84,273	85,530
Proportion of array area* (%)	<0.1%	<0.1%	<0.1%	<0.1%	0.1	0.1
Seabed footprint of all local scour (m²)	179,187	163,080	52,286	36,502	32,291	33,439
Proportion of array area* (%)	0.2	0.2	0.1	<0.1%	<0.1%	<0.1%
Seabed footprint of all foundations + local scour (m²)	186,177	169,442	54,326	37,926	116,564	118,969
Proportion of array area* (%)	0.2	0.2	0.1	<0.1%	0.1	0.2
Seabed footprint of all global scour (m²)	NA	NA	155,040	185,187	NA	NA
Proportion of array area* (%)	NA	NA	0.2	0.2	NA	NA
Seabed footprint of all scour protection (m²)	185,415	188,420	78,548	54,836	519,190	513,045
Proportion of array area* (%)	0.2	0.2	0.1	0.1	0.7	0.7
Seabed footprint of all foundations + scour protection (m²)	192,405	194,782	80,588	56,260	603,463	598,575
Proportion of array area* (%)	0.2	0.2	0.1	0.1	0.8	0.8
All scour dimensions are based upon the scour depth for steady currents. Results assume erodible bed and absence of geological controls * Corresponding proportion of the AyM array area (88.3 km²).						

In the following section, the term 'local scour' refers to the local response to individual structure members. 'Global scour' refers to a region of shallower but potentially more extensive scour associated with a multi-member foundation resulting from the change in flow velocity through the gaps between members of the structure and turbulence shed by the entire structure. Global scour does not imply scour at the scale of the wind farm array.

Key findings are summarised below:

- Overall, scour development within the AyM array area is expected to be dominated by the action of tidal currents;
- In practice, the thickness of unconsolidated (and more easily erodible) surficial Holocene sediment is spatially variable across the AyM array, with the greatest thicknesses found in central and eastern areas of the array (Fugro, 2020a). In the west, pre-Holocene material is at or close to the surface and may limit the extent to which scour can occur. (Detailed geotechnical information is not currently available so the extent to which this is the case remains unknown at this stage);
- Of all the turbine foundation options under consideration, a 15 m diameter monopile foundation has the potential to cause the greatest equilibrium local scour depth (19.5 m), footprint (4,530 m^2) and volume (up to 34,224 m^3), but only in areas where the seabed is potentially erodible by the action of scour to that depth;
- The greatest individual turbine foundation global scour footprint is associated with the larger (40 m base length) piled jacket foundation (4,002 m^2), although with a relatively small average depth (1.4 m);
- For the AyM array as a whole, the greatest total turbine foundation local scour footprint is associated with an array of 50 smaller (13 m diameter) WTG monopile foundations and two OSP monopile foundations (15 m diameter) (179,187 m^2, equivalent to only approximately 0.2% of the array area); and
- For the AyM array as a whole, the greatest total turbine foundation global scour footprint is associated with an array of 34 larger (40 m base length) piled jacket foundations and two OSP piled jacket foundations (50 m base length) (185,187 m^2), equivalent to only approximately 0.2% of the array area.

6   References

ABPmer, HR Wallingford and Cefas, (2010). Further review of sediment monitoring data'. (COWRIE ScourSed-09).

Becker, J., van Eekelen, E., van Wiechen, J., de Lange, W., Damsma, T., Smolders, T., van Koningsveld, M. (2015). Estimating source terms for far field dredge plume modelling. Journal of Environmental Management. Volume 149 p282-293.

Det Norske Veritas (DNV), (2016). Support structures for Wind Turbines. Offshore Standard DNVGL-ST-0126, 182pp.

EMODnet: ███████████████████████

Fugro (2020a). WPM1 Main Array Area -Seafloor and Shallow Geological Results Report. Doc Ref 003616043-04

Fugro (2020b). WPM2& WPM3 – ECR East A and B- Seafloor and Shallow Geological Results Report. Doc Ref 003700854-02

Harris, J.M., Whitehouse, R.J.S. and Benson, T. (2010). The time evolution of scour around offshore structures. Proceedings of the Institution of Civil Engineers, Maritime Engineering, 163, March, Issue MA1, pp. 3 – 17.

Harris, J.M., Whitehouse, R.J.S. and Sutherland, J. (2011). Marine scour and offshore wind - lessons learnt and future challenges. Proceedings of the ASME 2011 30th International Conference on Ocean, Offshore and Arctic Engineering, OMAE2011, June 19-24, 2011, Rotterdam, The Netherlands, OMAE2011-50117.

HR Wallingford, ABPmer and Cefas. (2007). Dynamics of scour pits and scour protection - Synthesis report and recommendations. (Sed02)

RWE Npower (2005). Gwynt y Môr Offshore Wind Farm Environmental Statement.

SeaScape Energy (2008). Burbo Offshore Wind Farm: Construction Phase Environmental Monitoring Report. CMACS for SeaScape Energy. April 2008.

Soulsby, R. (1997). Dynamics of Marine Sands. Thomas Telford, London. pp249.

Whitehouse, R.J.S., (1998). Scour at marine structures: A manual for practical applications. Thomas Telford, London, 198 pp

Whitehouse RJS, Sutherland J., Harris. (2011). Evaluating scour at marine gravity foundations. Proceedings of the ICE. Maritime Engineering 164(4) 143-157.
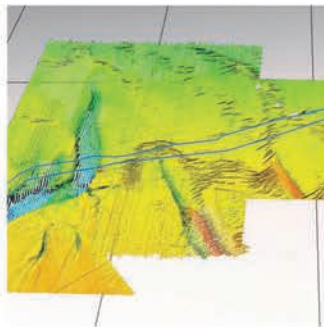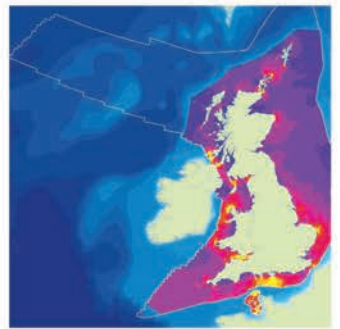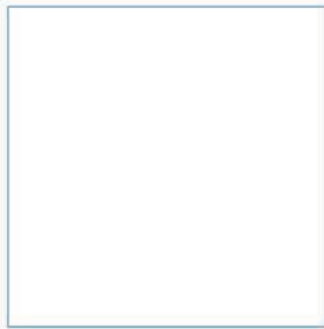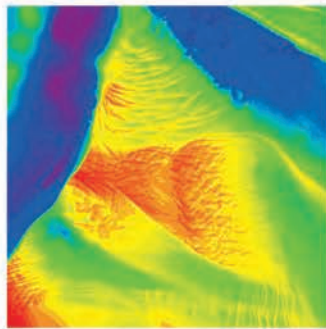
7   Abbreviations/Acronyms

AyM	Awel y Môr
BGS	British Geological Survey
COWRIE	Collaborative Offshore Wind Research Into The Environment
CurSpd	Current Speed
D	Diameter
DNV	Det Norske Veritas
DTI	Department of Trade
ECC	Export Cable Corridor
EIA	Environmental Impact Assessment
EMODnet	European Marine Observation and Data Network
FM	Flexible Mesh (MIKE21 Model)
G/D	Gap to Pile Diameter Ratio
GoBe	GoBe Consultants Ltd
GyM	Gwynt y Môr
HD	Hydrodynamic (MIKE21 Model)
Hs	Significant Wave Height
KC	Keulegan-Carpenter
LAT	Lowest Astronomical Tide
MDS	Maximum Design Scenario
MFE	Mass Flow Excavator
MW	Megawatt(s)
°N	Degrees North
OSP	Offshore Substation Platform
OWF	Offshore Wind Farm
PEIR	Preliminary Environmental Information Report
RP	Return Period
RWE	RWE Npower
SSC	Suspended Sediment Concentration
Sextent	Scour Extent
Sfootprint	Scour Footprint
ST	Sand Transport (MIKE21 Model)
SW	Spectral Wave (MIKE21 Model)
Tp	Peak Wave Period
TSHD	Trailing Suction Hopper Dredger
Tz	Zero Crossing Period
UK	United Kingdom
UTM	Universal Transverse Mercator
VORF	Vertical Offshore Reference Frames
WGS	World Geodetic System
WTG	Wind Turbine Generator

Cardinal points/directions are used unless otherwise stated.

SI units are used unless otherwise stated.
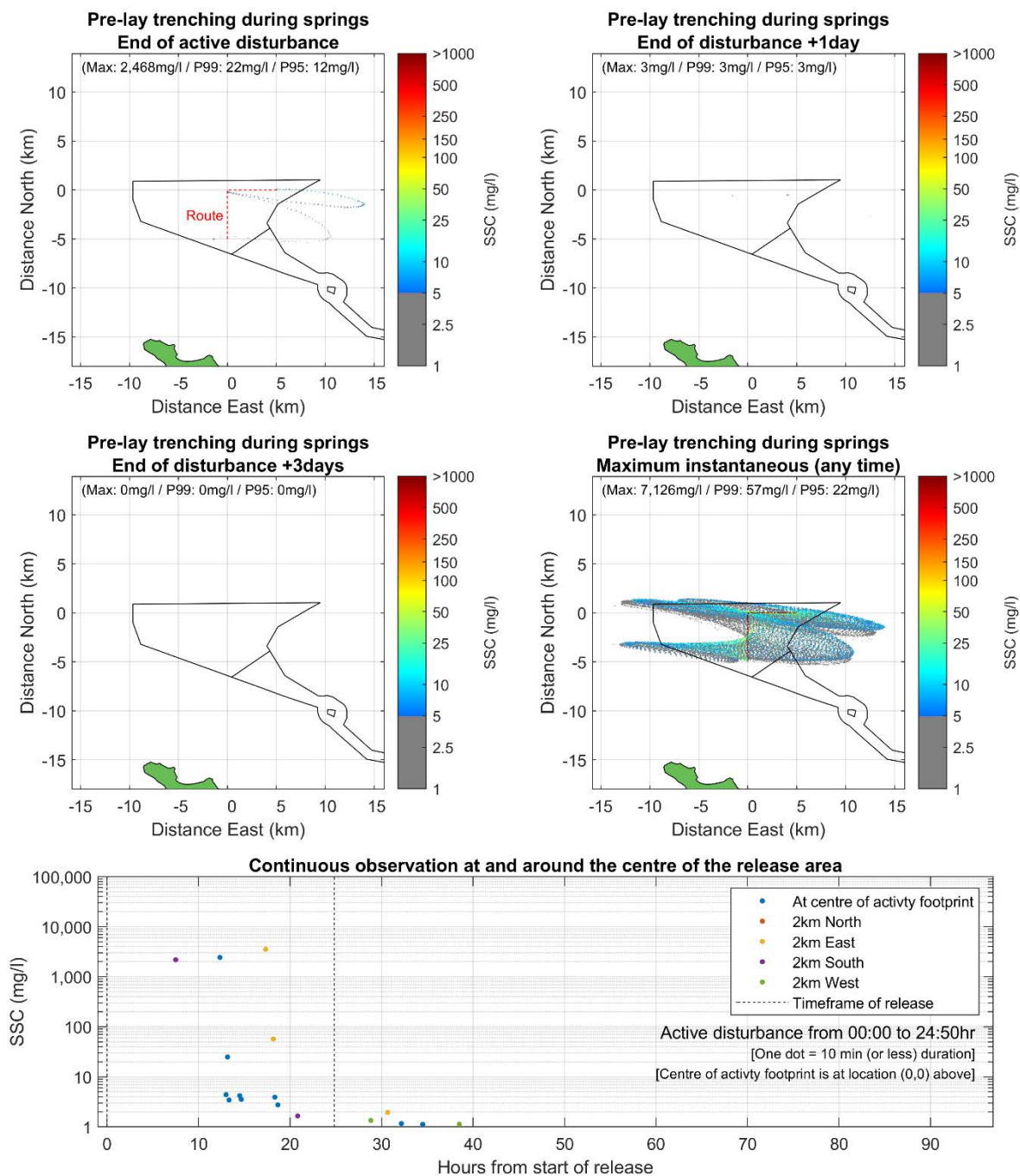
Appendices

Innovative Thinking - Sustainable Solutions

ABP mer

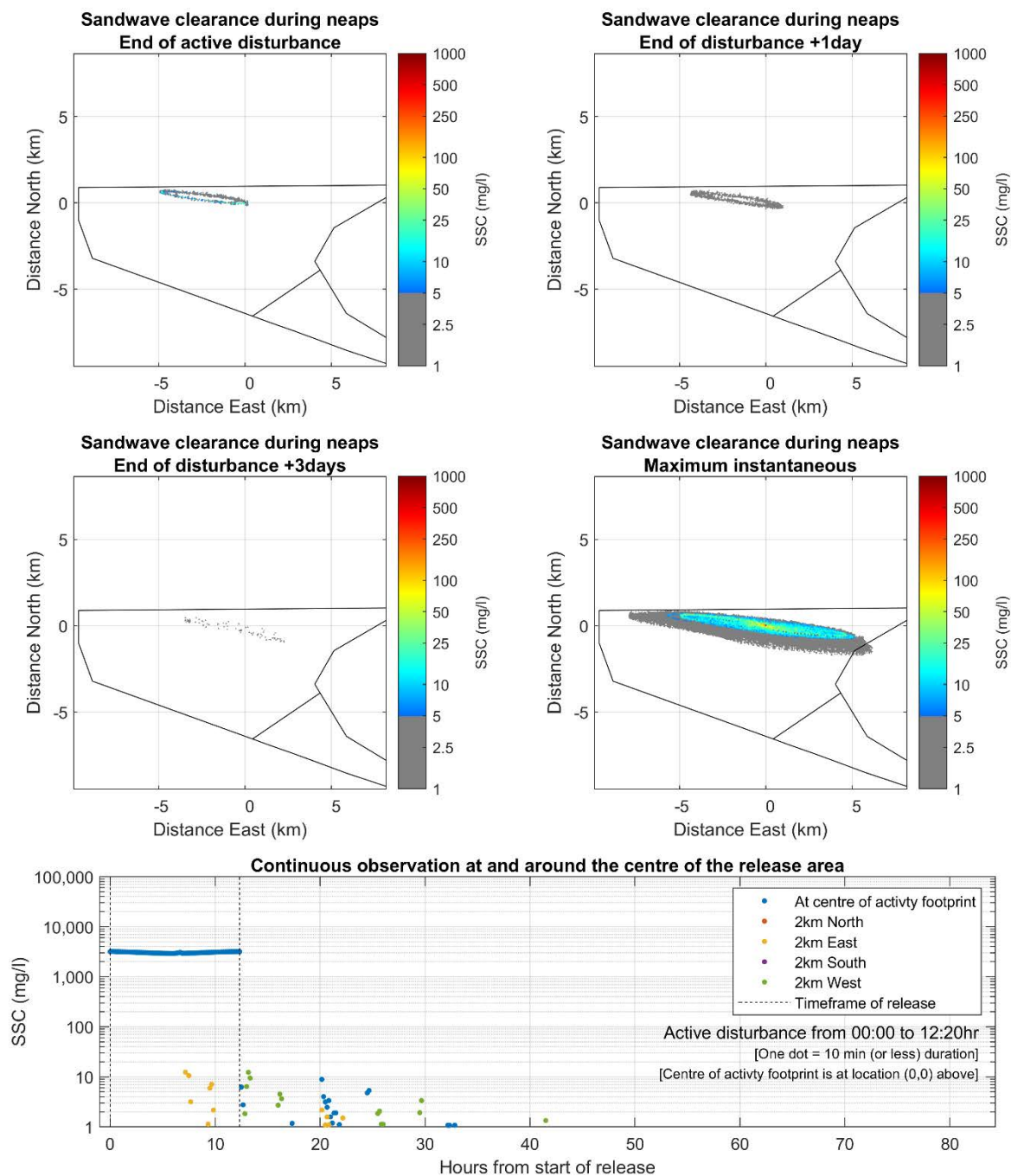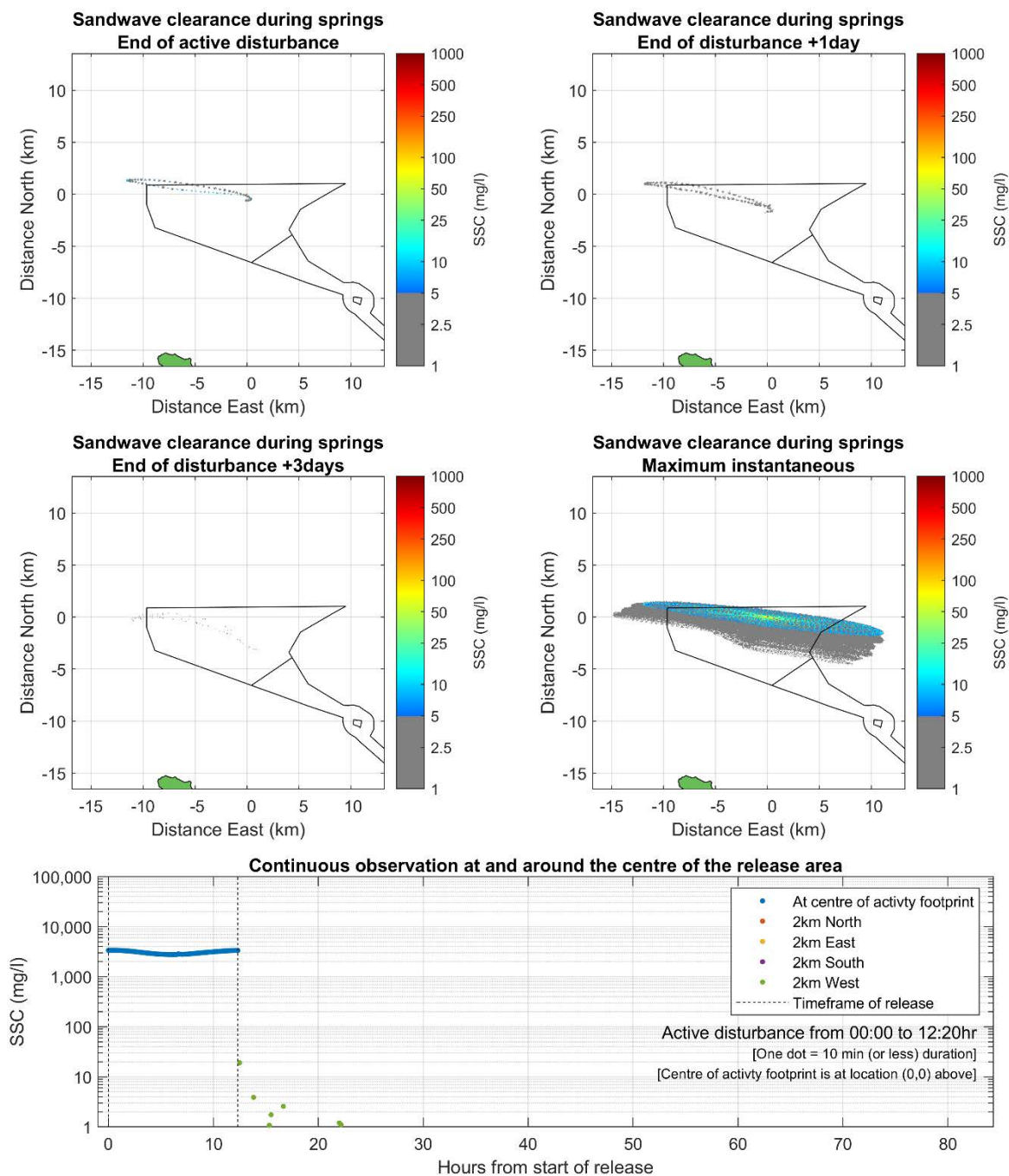# A   Suspended Sediment Concentration Figures

The trencher follows a route from (easting/northing (km): [0,-5; 0,0; 5,0] (red dotted line in top left panel).
The line that is visible along the trencher route in the 'Maximum Instantaneous' image is the locally very high SSC associated with sands and gravels before they are rapidly redeposited to the seabed within a short distance of the trencher.
The outline of the (older PEIR) AyM array area and offshore ECC are shown as solid black lines.

Figure A1.   Increase in suspended sediment concentration as a result of Scenario 1: pre-lay trenching using an MFE in the AyM array area. Mean neap tide
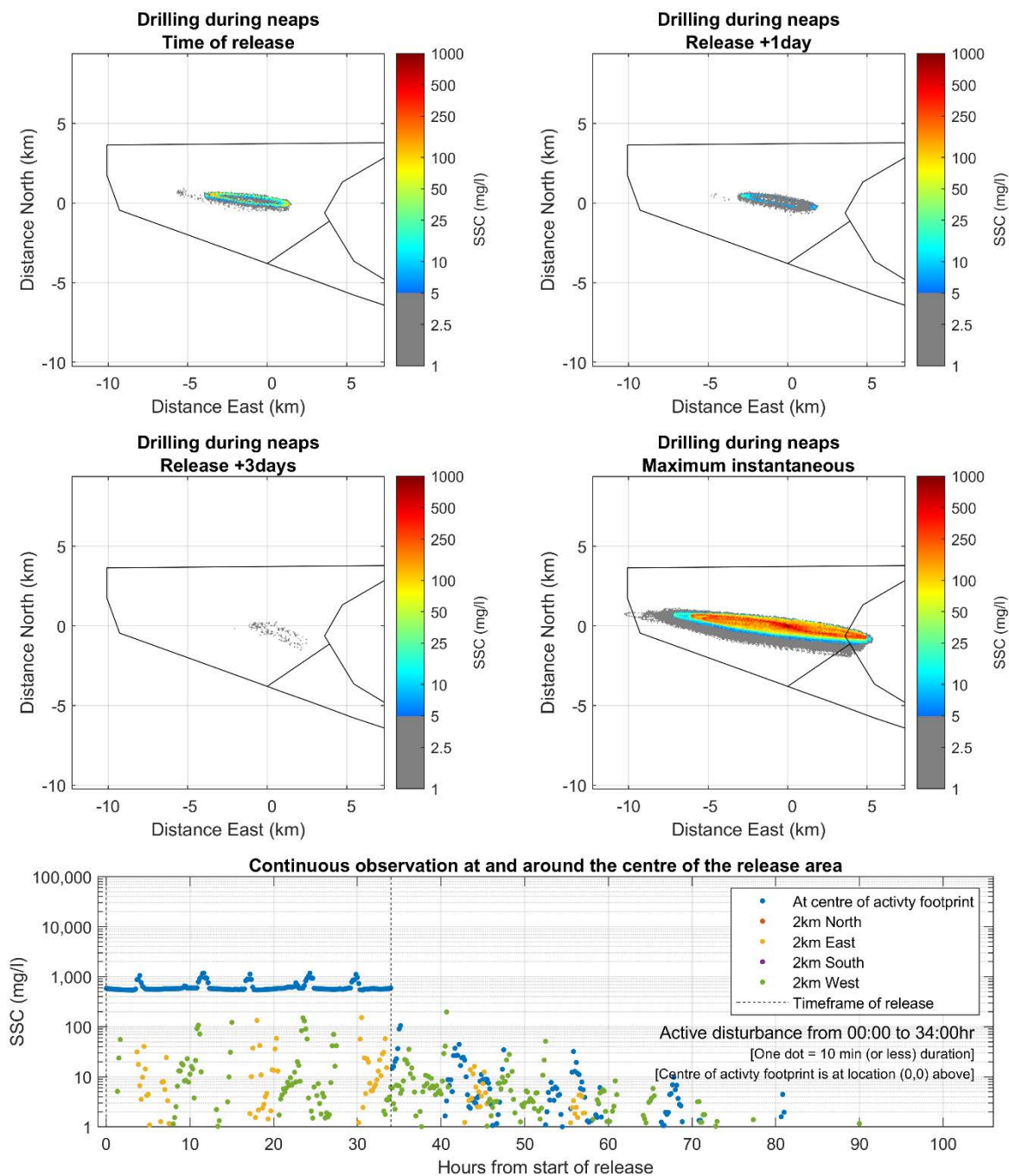
The trencher follows a route from (easting/northing (km): [0,-5; 0,0; 5,0] (red dotted line in top left panel).
The line that is visible along the trencher route in the 'Maximum Instantaneous' image is the locally very high SSC associated
with sands and gravels before they are rapidly redeposited to the seabed within a short distance of the trencher.
The outline of the (older PEIR) AyM array area and offshore ECC are shown as solid black lines.

Figure A2.   Increase in suspended sediment concentration as a result of Scenario 2: pre-lay trenching using an MFE in the AyM array area. Mean spring tide

The sand wave clearance occurs at location easting/northing (km): [0,0].
The outline of the (older PEIR) AyM array area and offshore ECC are shown as solid black lines.
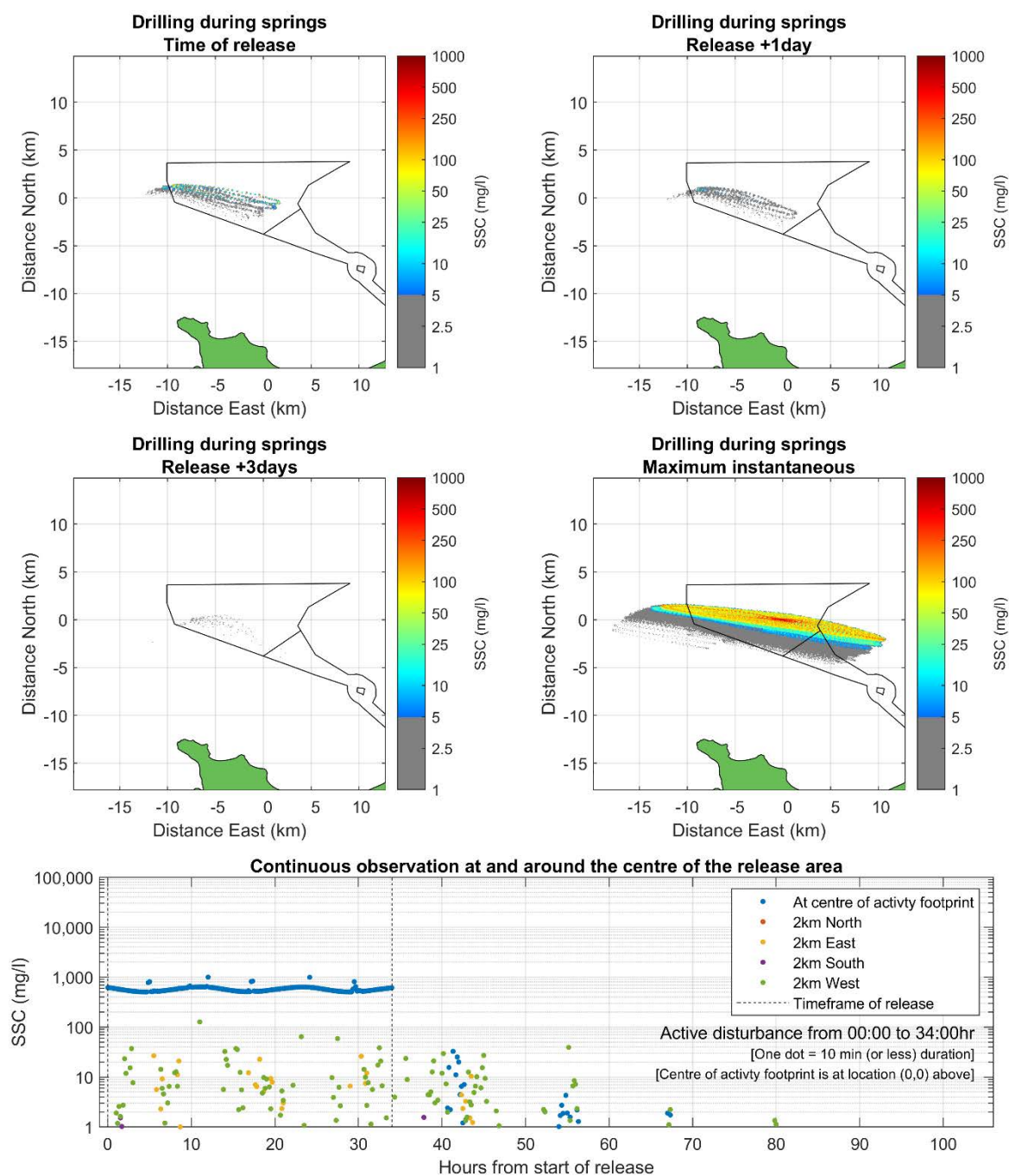
Figure A3.　　Increase in suspended sediment concentration as a result of Scenario 3: sand wave clearance using an MFE in the AyM array area. Mean neap tide

The sand wave clearance occurs at location easting/northing (km): [0,0].
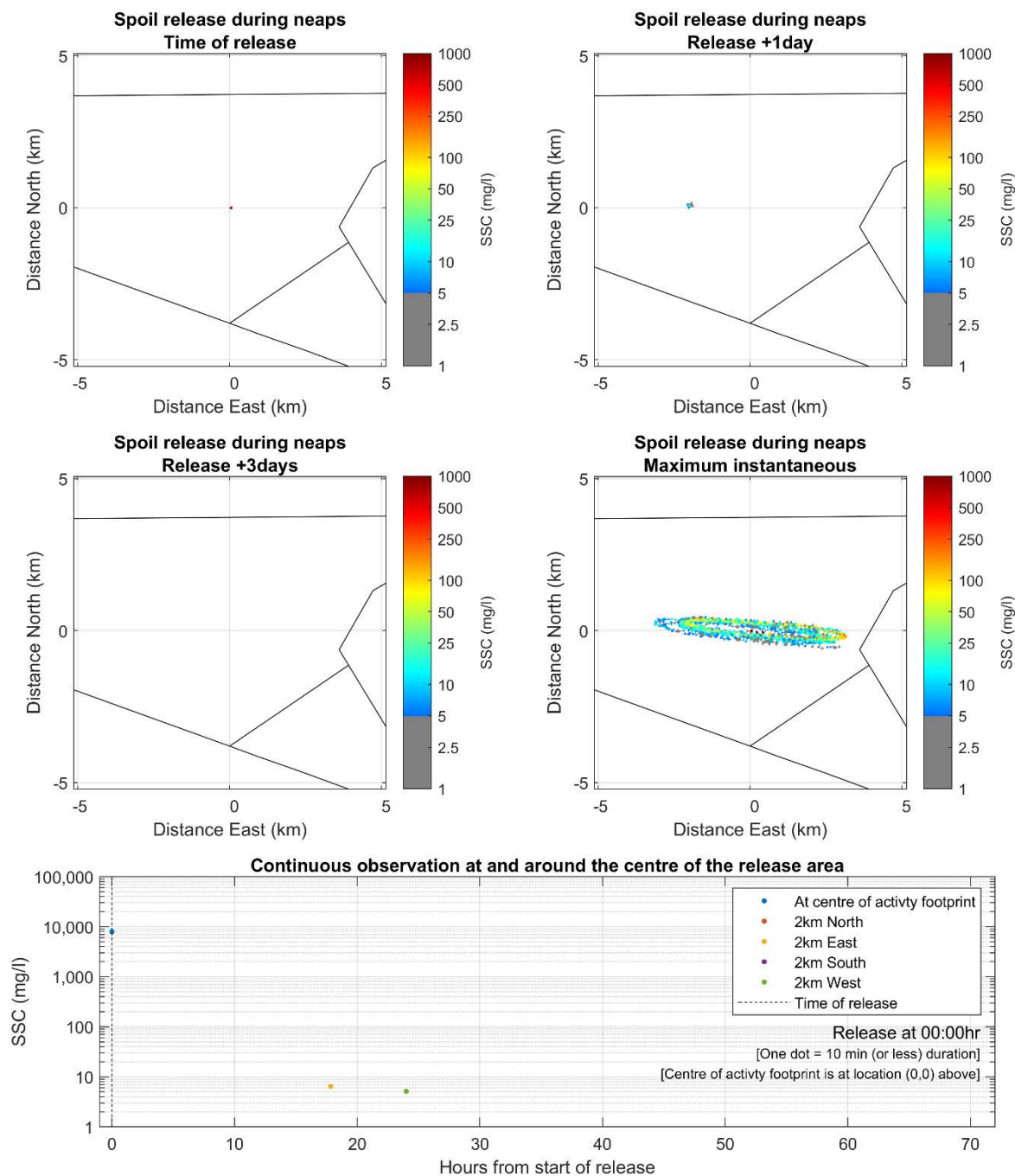The outline of the (older PEIR) AyM array area and offshore ECC are shown as solid black lines.

Figure A4.   Increase in suspended sediment concentration as a result of Scenario 4: sand wave clearance using an MFE in the AyM array area. Mean spring tide

The drilling occurs at location easting/northing (km): [0,0].
The outline of the (older PEIR) AyM array area and offshore ECC are shown as solid black lines.

Figure A5.   **Increase in suspended sediment concentration as a result of Scenario 5: drilling a large monopile (drilled hole 16 m diameter x 69 m depth) in the AyM array area. Mean neap tide**

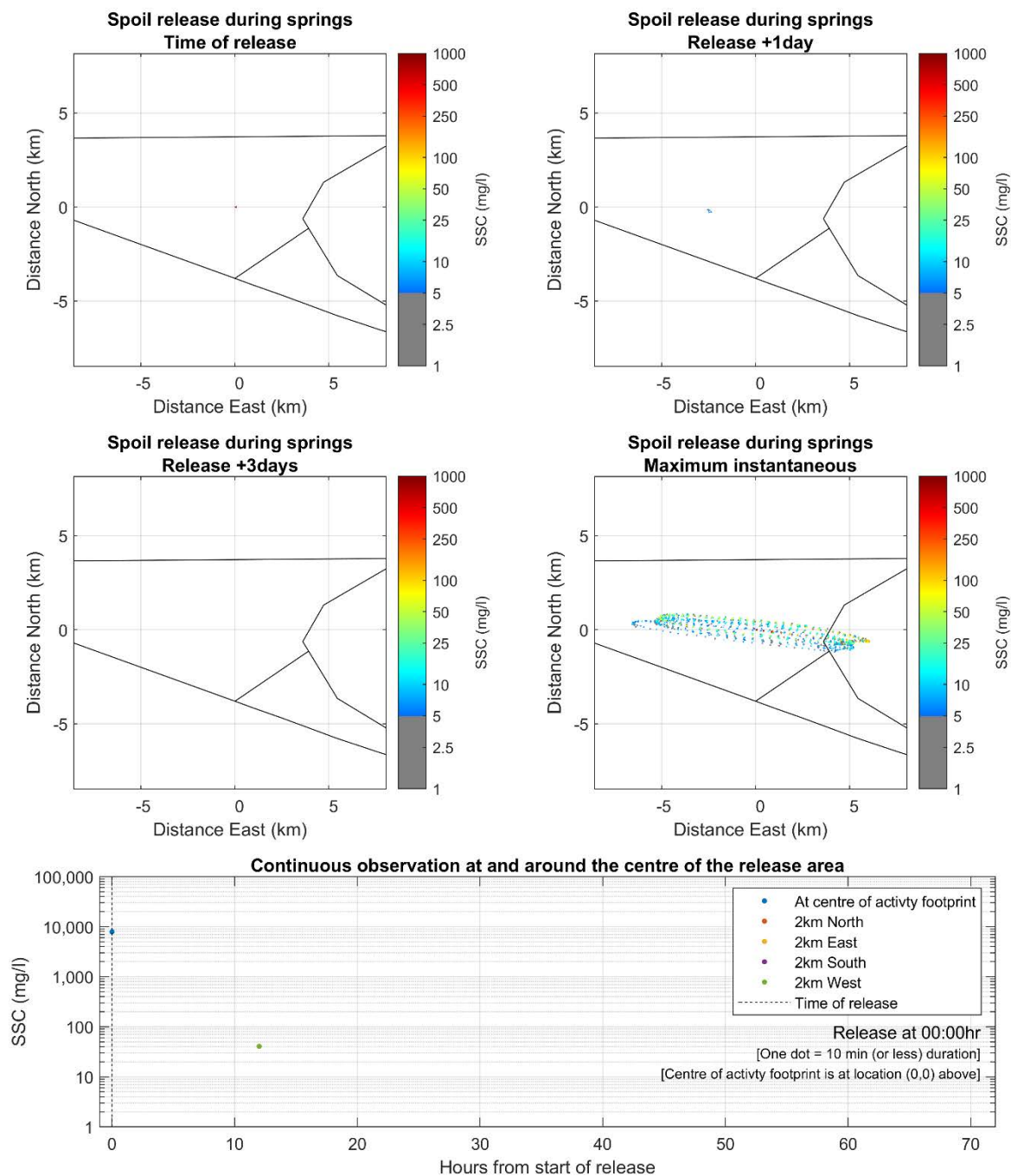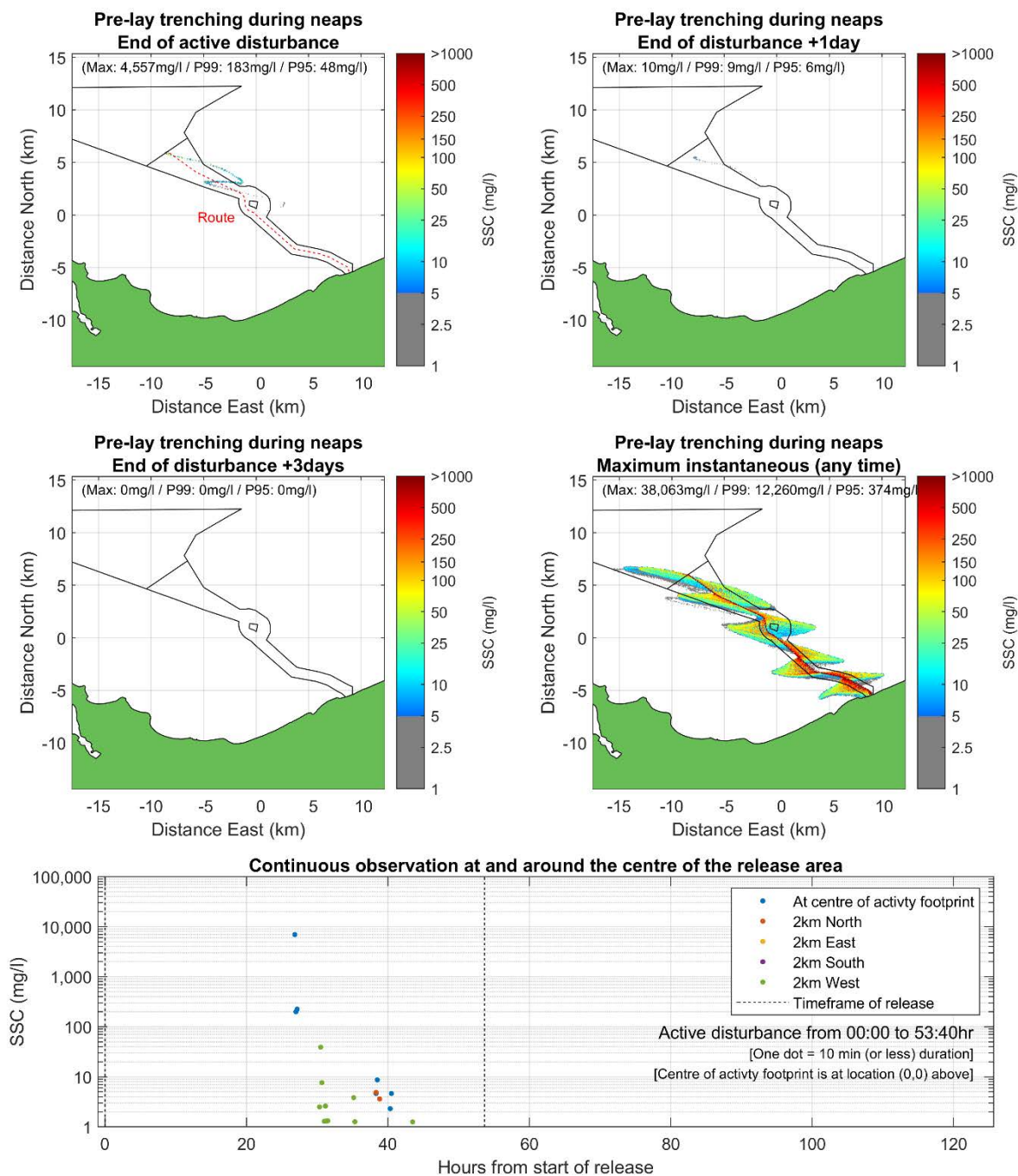The drilling occurs at location easting/northing (km): [0,0].
The outline of the (older PEIR) AyM array area and offshore ECC are shown as solid black lines.

Figure A6.   Increase in suspended sediment concentration as a result of Scenario 6: drilling a large monopile (drilled hole 16 m diameter x 69 m depth) in the AyM array area. Mean spring tide
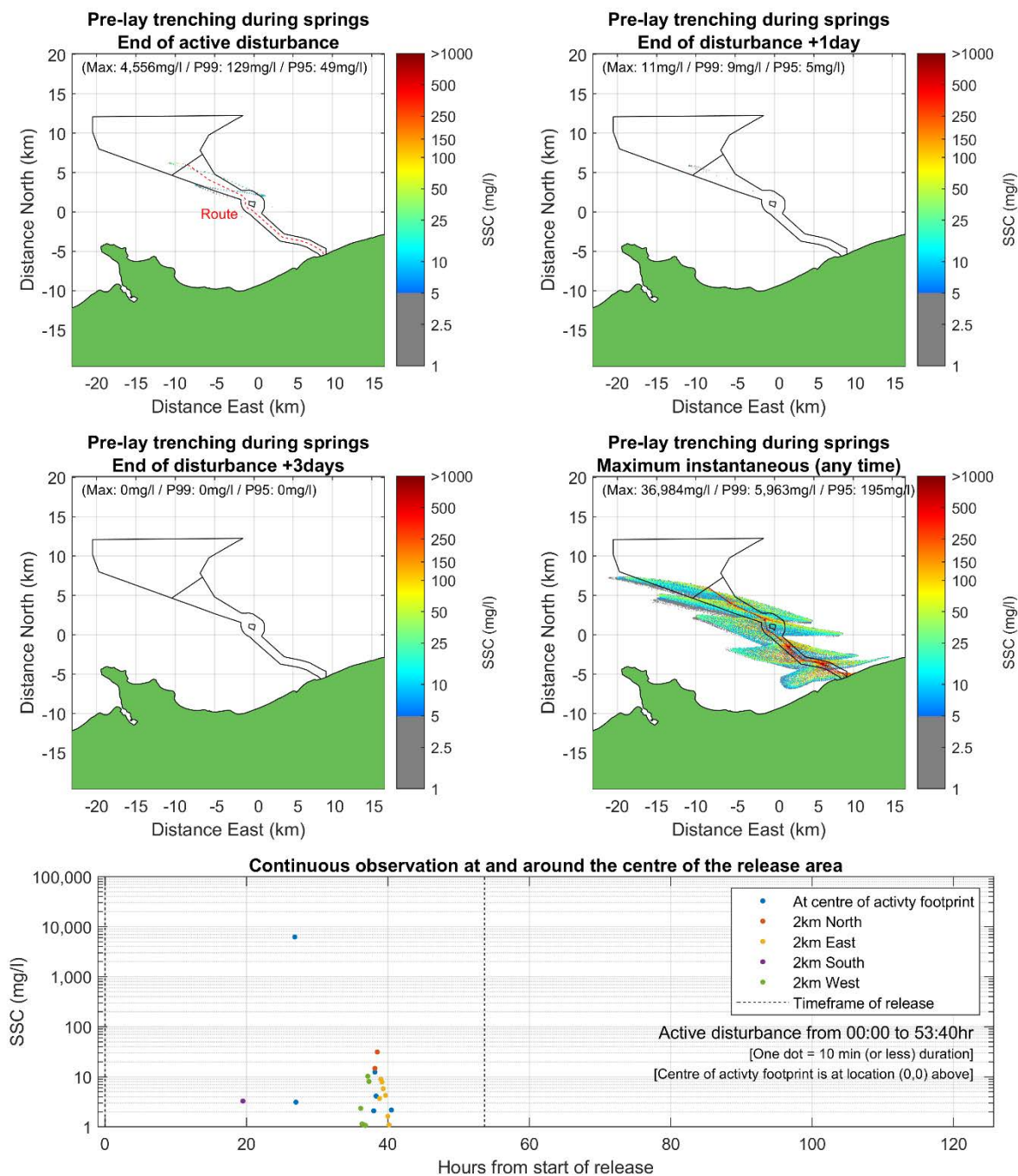
The dredge spoil disposal occurs at location easting/northing (km): [0,0].
The outline of the (older PEIR) AyM array area and offshore ECC are shown as solid black lines.

Figure A7.   Increase in suspended sediment concentration as a result of Scenario 7: dredge spoil disposal in the AyM array area. Mean neap tide

The dredge spoil disposal occurs at location easting/northing (km): [0,0].
The outline of the (older PEIR) AyM array area and offshore ECC are shown as solid black lines.

Figure A8.   **Increase in suspended sediment concentration as a result of Scenario 8: dredge spoil disposal in the AyM array area. Mean spring tide**

The trencher follows a central route along the full length of the export cable corridor (red dotted line in top left panel).
The line that is visible along the trencher route in the 'Maximum Instantaneous' image is the locally very high SSC associated
with sands and gravels before they are rapidly redeposited to the seabed within a short distance of the trencher.
The outline of the (older PEIR) AyM array area and offshore ECC are shown as solid black lines.

Figure A9. Increase in suspended sediment concentration as a result of Scenario 9: pre-lay trenching using an MFE along the length of the AyM export cable corridor. Mean neap tide

The trencher follows a central route along the full length of the export cable corridor (red dotted line in top left panel).
The line that is visible along the trencher route in the 'Maximum Instantaneous' image is the locally very high SSC associated
with sands and gravels before they are rapidly redeposited to the seabed within a short distance of the trencher.
The outline of the (older PEIR) AyM array area and offshore ECC are shown as solid black lines.

Figure A10.   Increase in suspended sediment concentration as a result of Scenario 10: -lay trenching using an MFE along the length of the AyM export cable corridor. Mean spring tide

The sand wave clearance occurs at location easting/northing (km): [0,0].
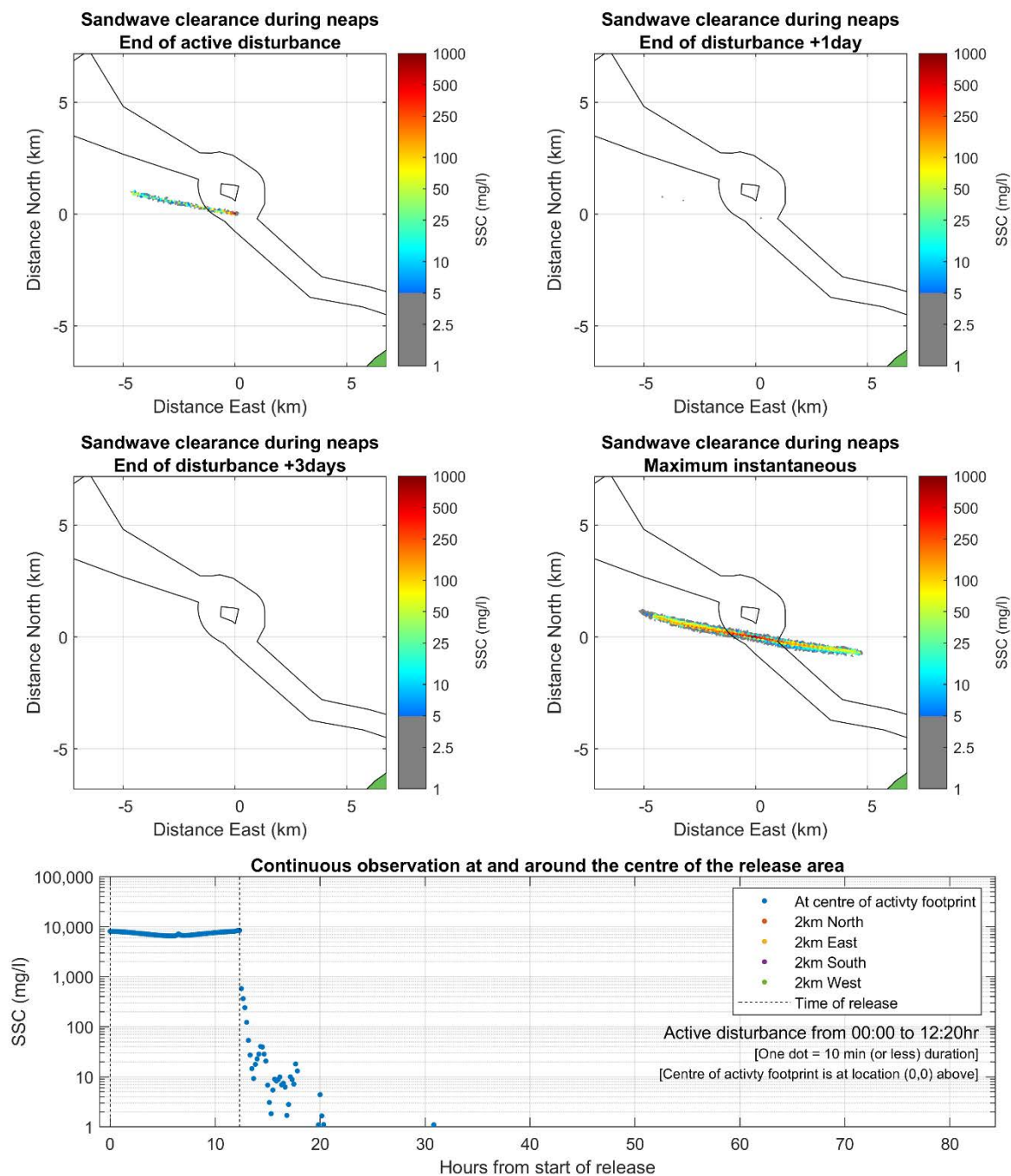The outline of the (older PEIR) AyM array area and offshore ECC are shown as solid black lines.

Figure A11.   Increase in suspended sediment concentration as a result of Scenario 11: sand wave clearance using an MFE at a central location in the AyM export cable corridor. Mean neap tide
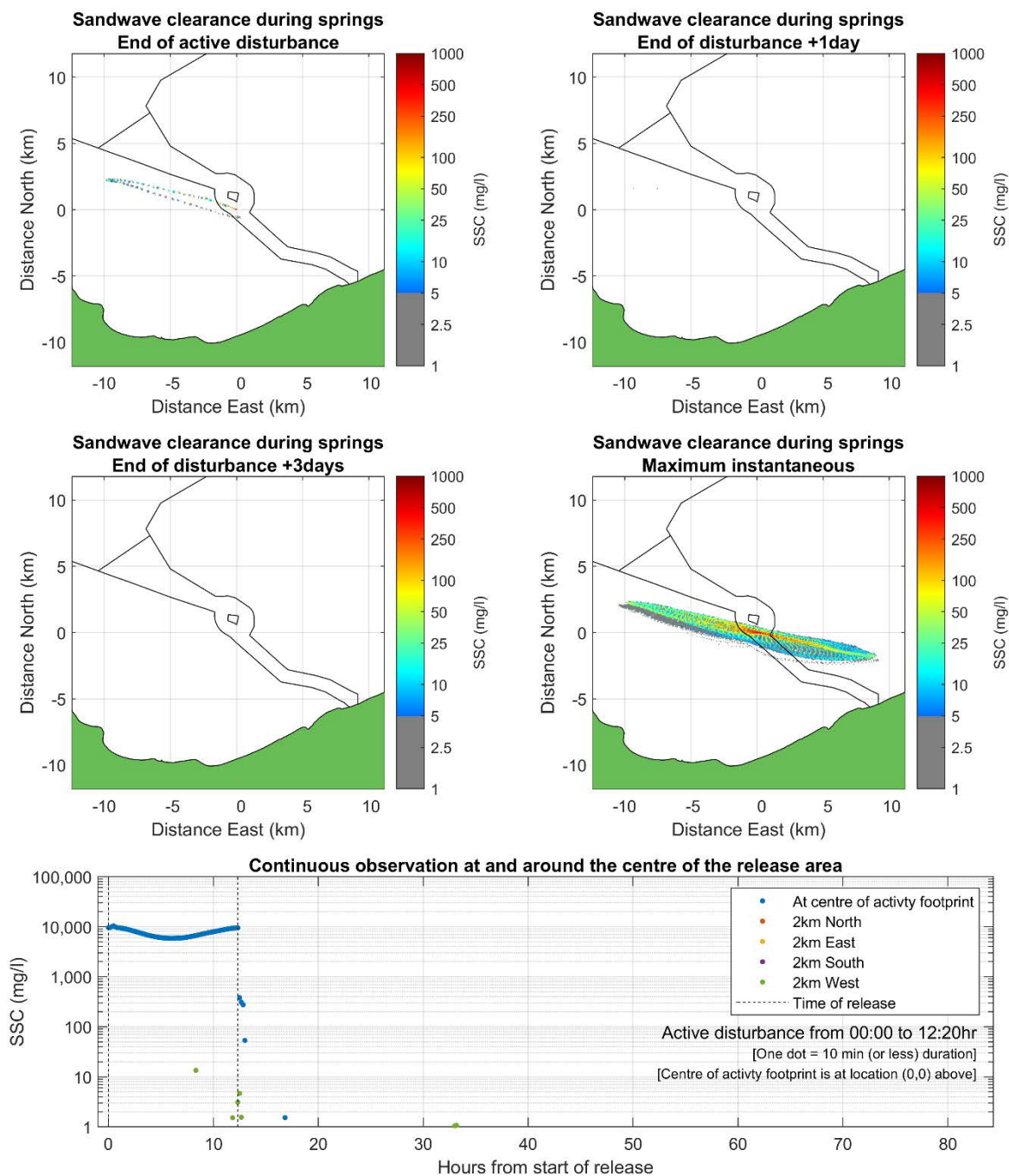
The sand wave clearance occurs at location easting/northing (km): [0,0].
The outline of the (older PEIR) AyM array area and offshore ECC are shown as solid black lines.
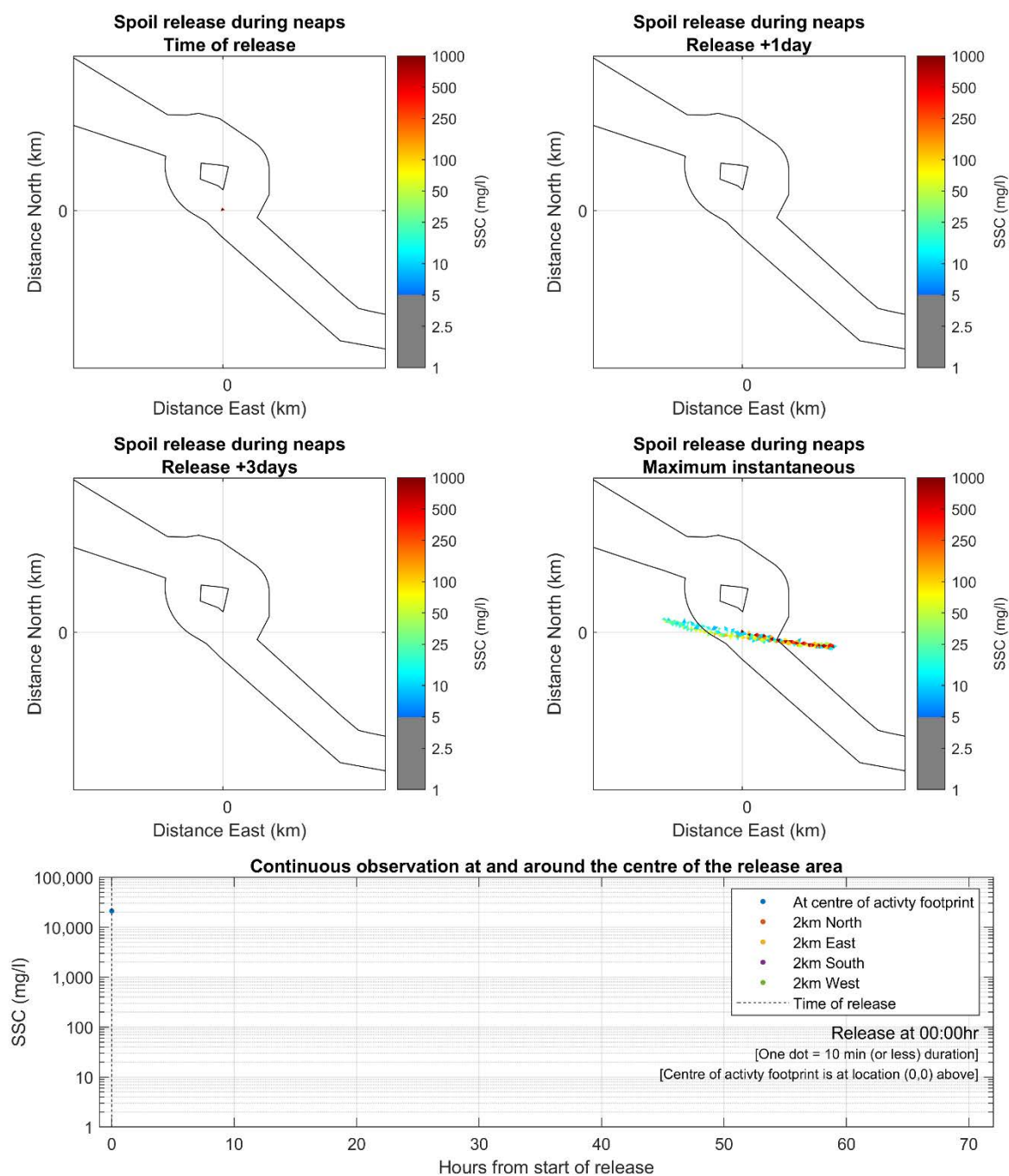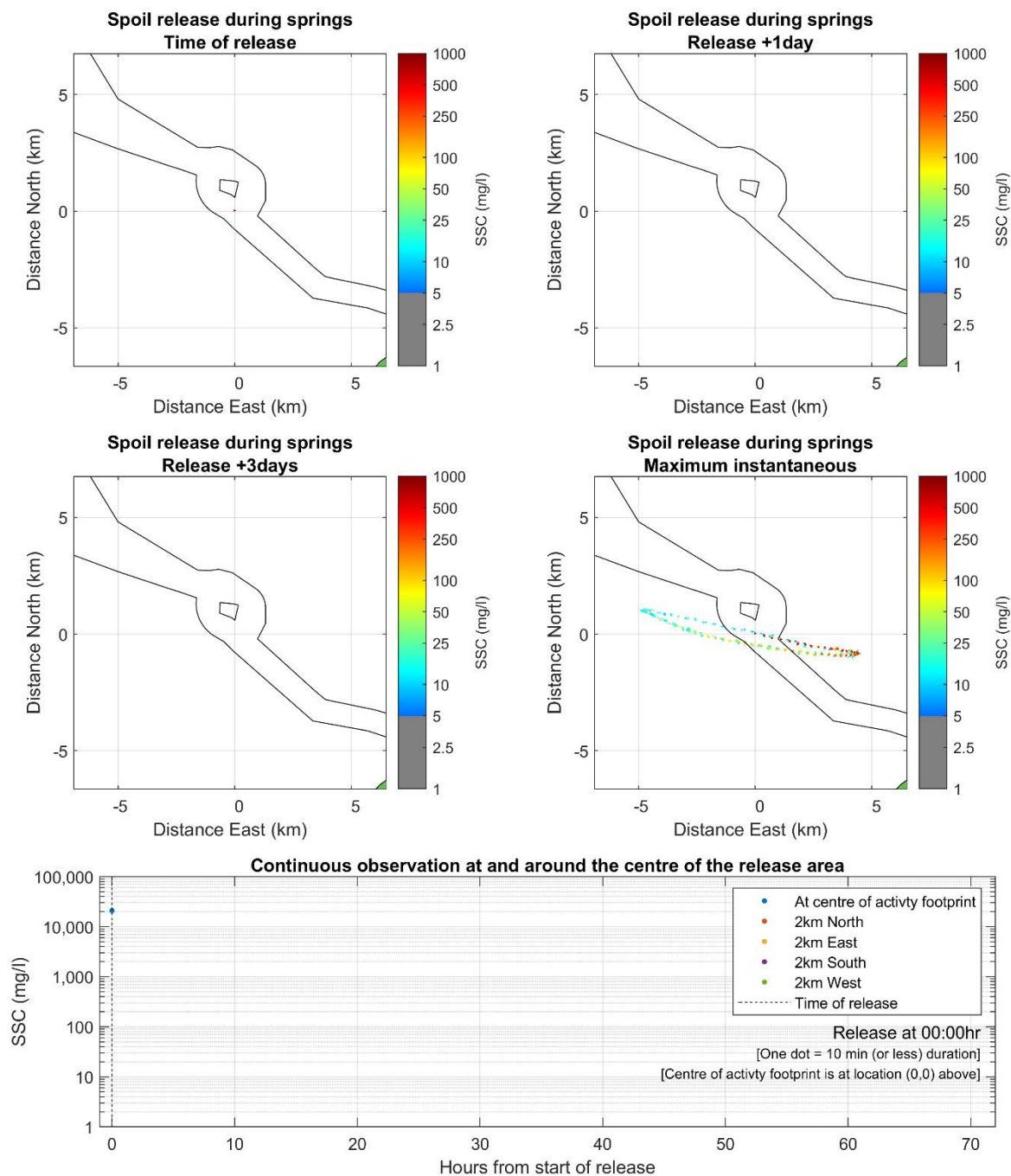
Figure A12.   Increase in suspended sediment concentration as a result of Scenario 12: sand wave clearance using an MFE at a central location in the AyM export cable corridor. Mean spring tide
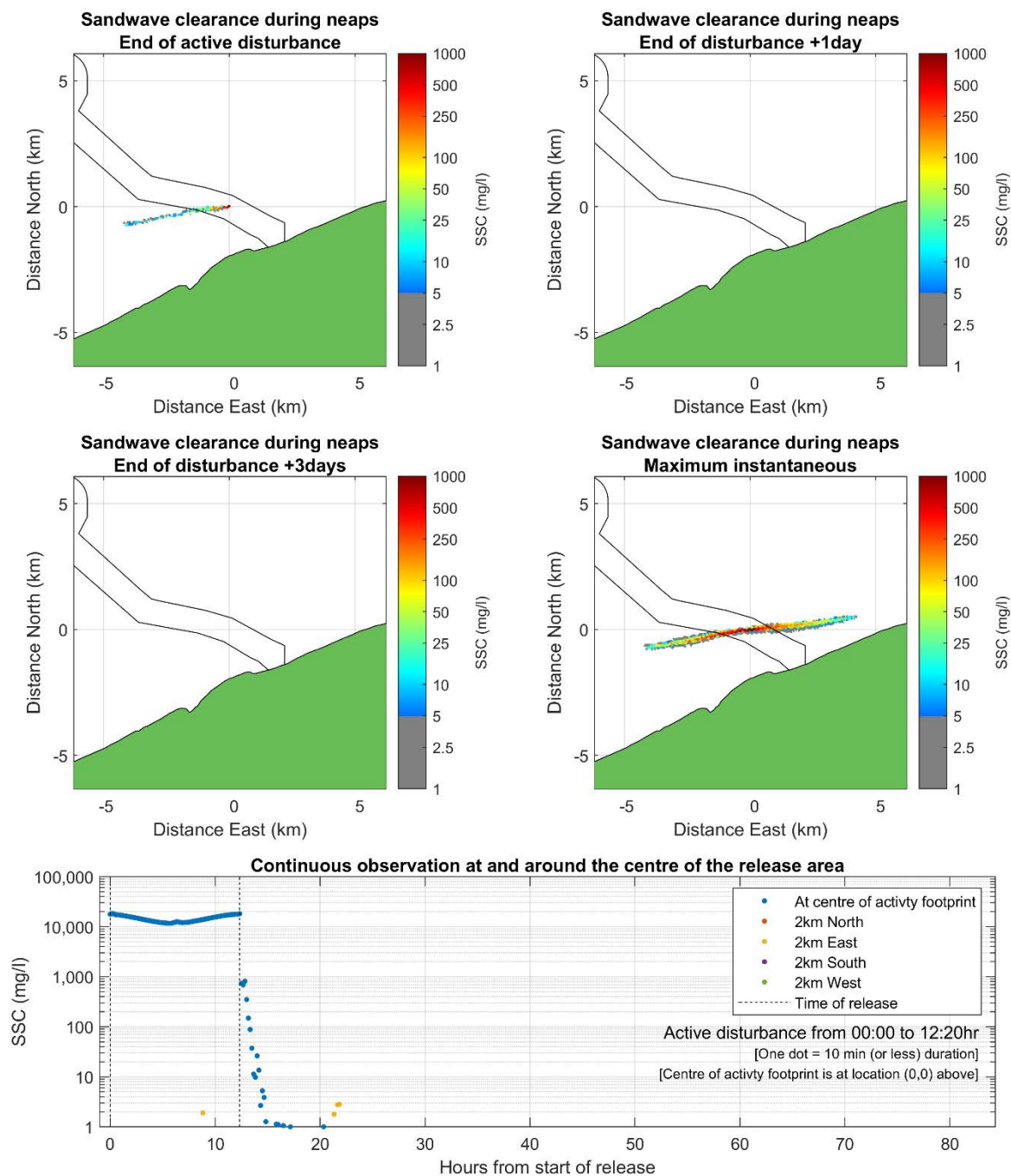
The dredge spoil disposal occurs at location easting/northing (km): [0,0].
The outline of the (older PEIR) AyM array area and offshore ECC are shown as solid black lines.

Figure A13.   Increase in suspended sediment concentration as a result of Scenario 13: dredge spoil disposal at a central location in the AyM export cable corridor. Mean neap tide
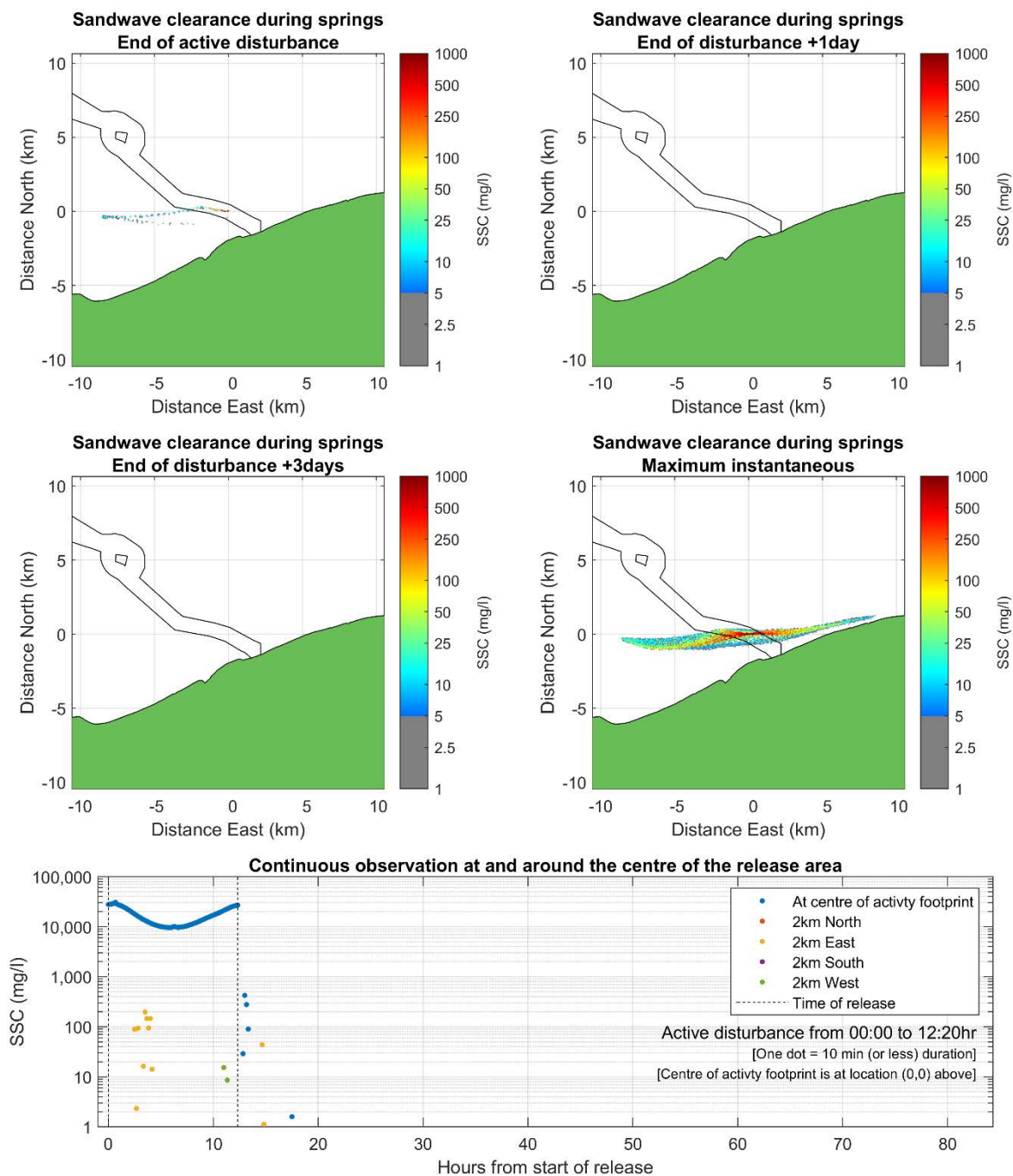
The dredge spoil disposal occurs at location easting/northing (km): [0,0].
The outline of the (older PEIR) AyM array area and offshore ECC are shown as solid black lines.

Figure A14.   Increase in suspended sediment concentration as a result of Scenario 14: dredge spoil disposal at a central location in the AyM export cable corridor. Mean spring tide

The sand wave clearance occurs at location easting/northing (km): [0,0].
The outline of the (older PEIR) AyM array area and offshore ECC are shown as solid black lines.

Figure A15.   **Increase in suspended sediment concentration as a result of Scenario 15: sand wave clearance using an MFE at a nearshore location in the AyM export cable corridor. Mean neap tide**
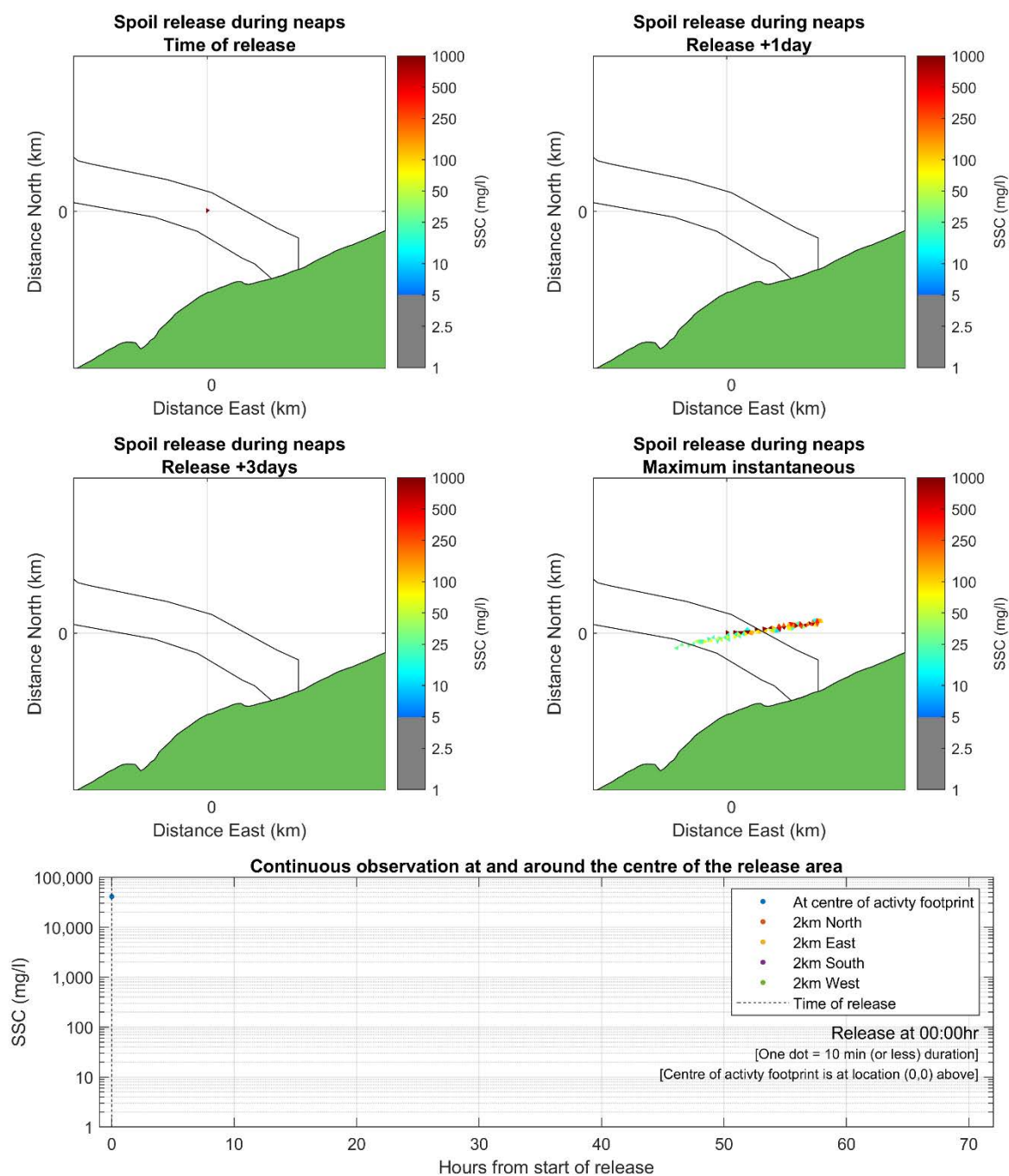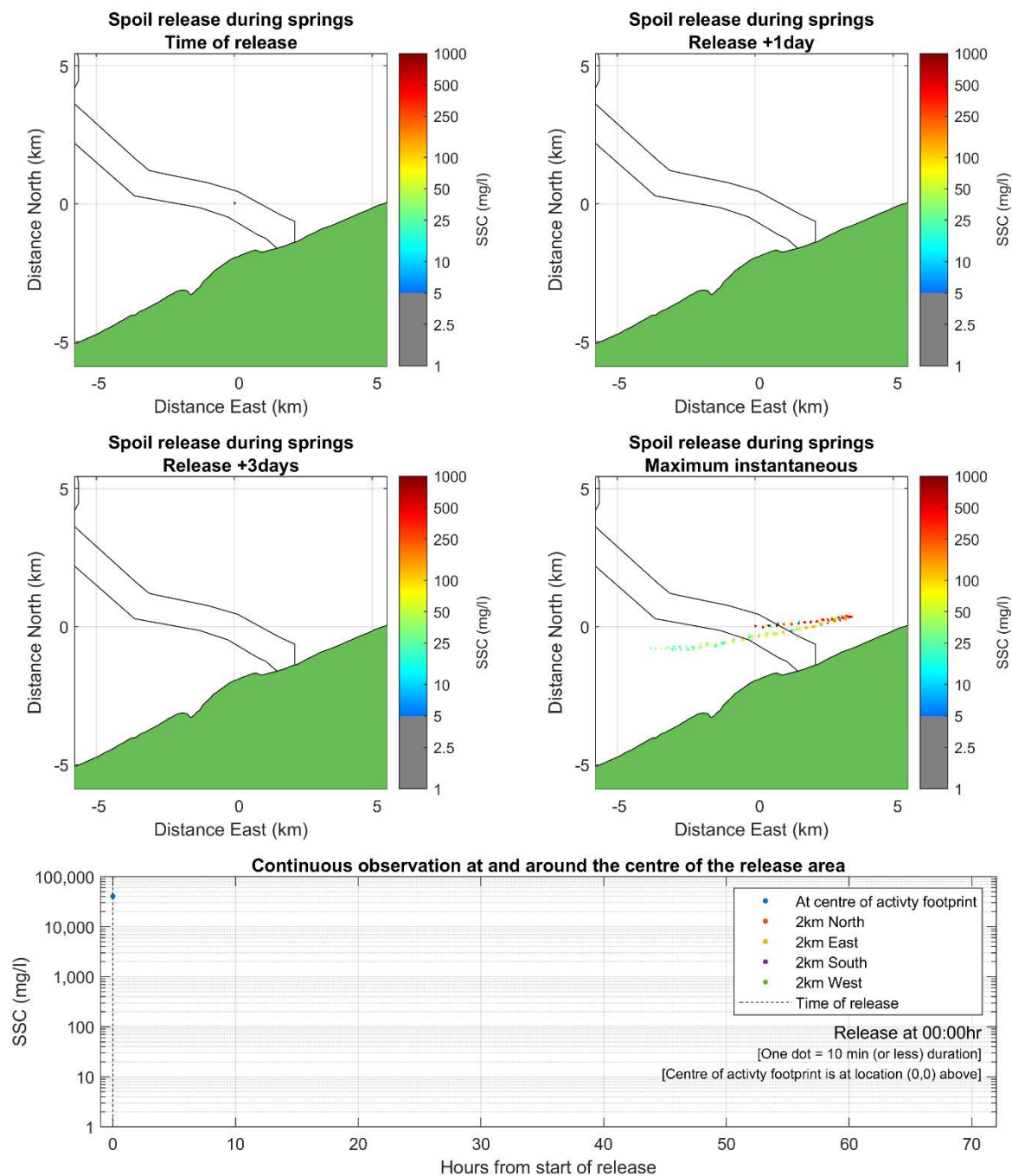
The sand wave clearance occurs at location easting/northing (km): [0,0].
The outline of the (older PEIR) AyM array area and offshore ECC are shown as solid black lines.

Figure A16. Increase in suspended sediment concentration as a result of Scenario 16: sand wave clearance using an MFE at a nearshore location in the AyM export cable corridor. Mean spring tide

The dredge spoil disposal occurs at location easting/northing (km): [0,0].
The outline of the (older PEIR) AyM array area and offshore ECC are shown as solid black lines.

Figure A17. Increase in suspended sediment concentration as a result of Scenario 17: dredge spoil disposal at a nearshore location in the AyM export cable corridor. Mean neap tide

The dredge spoil disposal occurs at location easting/northing (km): [0,0].
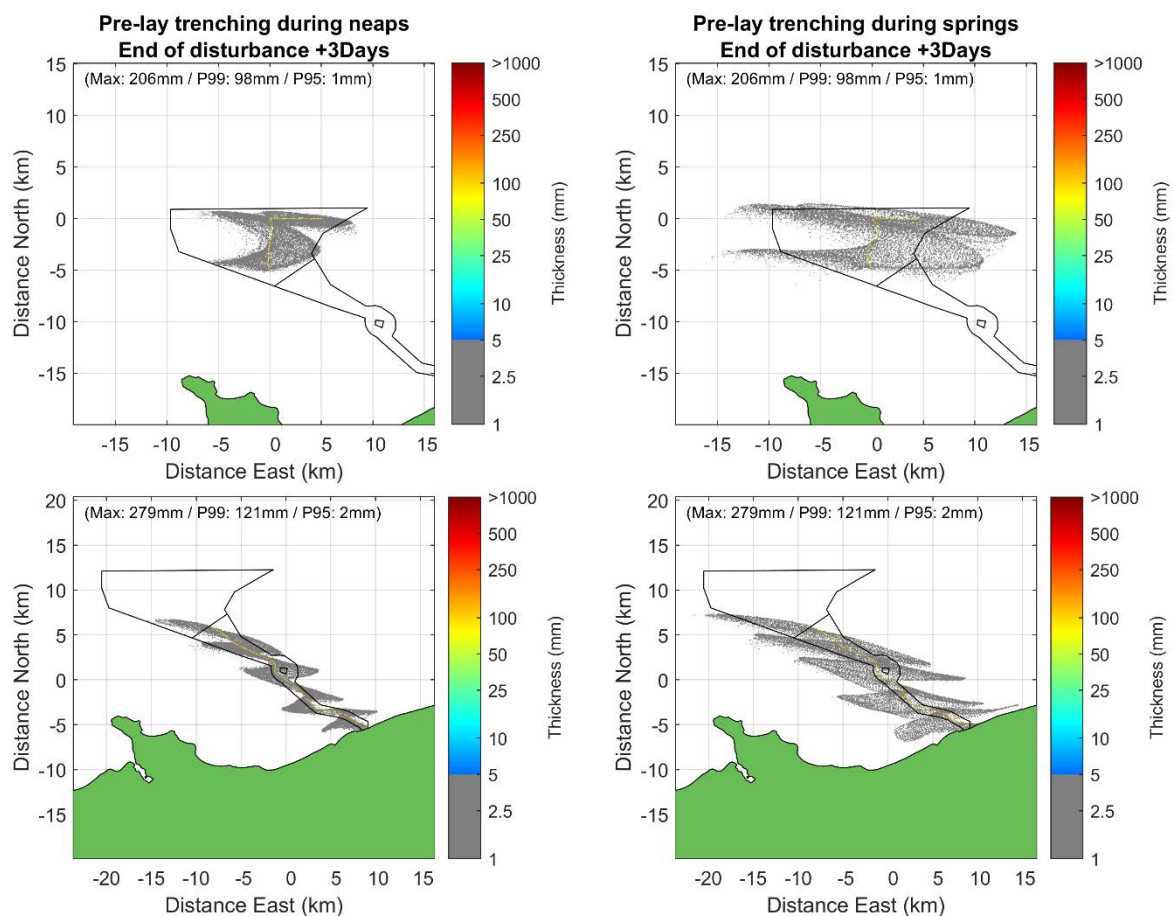The outline of the (older PEIR) AyM array area and offshore ECC are shown as solid black lines.

Figure A18.   Increase in suspended sediment concentration as a result of Scenario 18: dredge spoil disposal at a nearshore location in the AyM export cable corridor. Mean spring tide

B   Seabed Deposition Thickness Figures

The trencher follows a route from (easting/northing (km): [0,-5; 0,0; 5,0] and a central route along the full length of the export cable corridor (shown as red dotted lines in the top left panels of Figures A.1, A.2, A9 and A10).
The line that is visible (mainly under neap conditions) along the trencher route is the locally greater deposition thickness associated with sands and gravels that are rapidly redeposited to the seabed within a short distance of the trencher.
The outline of the (older PEIR) AyM array area and offshore ECC are shown as solid black lines.

Figure B1.   Sediment settlement thickness as a result of pre-lay trenching using an MFE in the AyM array area and export cable corridor. Mean spring and mean neap tides

The sand wave clearance occurs at location easting/northing (km): [0,0].
The outline of the (older PEIR) AyM array area and offshore ECC are shown as solid black lines.

Figure B2.   Sediment settlement thickness as a result of sand wave clearance using an MFE in the AyM array area and export cable corridor. Mean spring and mean neap tides

The dredge spoil disposal occurs at location easting/northing (km): [0,0].
The outline of the (older PEIR) AyM array area and offshore ECC are shown as solid black lines.

Figure B3.   Sediment settlement thickness as a result of the passive phase plume from dredge spoil disposal in the AyM array area. Mean spring and mean neap tides

The drilling occurs at location easting/northing (km): [0,0].
The outline of the (older PEIR) AyM array area and offshore ECC are shown as solid black lines.

Figure B4. Sediment settlement thickness as a result of drilling a large monopile in the AyM array area. Mean spring and mean neap tides

Awel y Môr Offshore Windfarm Environmental Impact Assessment:
Volume 4, Annex 2.3: Marine Geology, Oceanography and Physical Processes Technical Assessment

GoBe Consultants Ltd

C Wave Model Baseline and Results Figures

The array area outlines of AyM and other nearby operational wind farms, and the offshore ECC of AyM are shown as solid lines. The defined area of Constable Bank is indicated as a thin dotted line.

Figure C1.　　Baseline significant wave height, waves from the west, all return periods

Awel y Môr Offshore Windfarm Environmental Impact Assessment:
Volume 4, Annex 2.3: Marine Geology, Oceanography and Physical Processes Technical Assessment

GoBe Consultants Ltd

The array area outlines of AyM and other nearby operational wind farms, and the offshore ECC of AyM are shown as solid lines. The defined area of Constable Bank is indicated as a thin dotted line.

Figure C2. **Baseline significant wave height, waves from the west-north-west, all return periods**

Awel y Môr Offshore Windfarm Environmental Impact Assessment:
Volume 4, Annex 2.3: Marine Geology, Oceanography and Physical Processes Technical Assessment

GoBe Consultants Ltd

The array area outlines of AyM and other nearby operational wind farms, and the offshore ECC of AyM are shown as solid lines. The defined area of Constable Bank is indicated as a thin dotted line.

Figure C3. **Baseline significant wave height, waves from the north-west, all return periods**

Awel y Môr Offshore Windfarm Environmental Impact Assessment:
Volume 4, Annex 2.3: Marine Geology, Oceanography and Physical Processes Technical Assessment
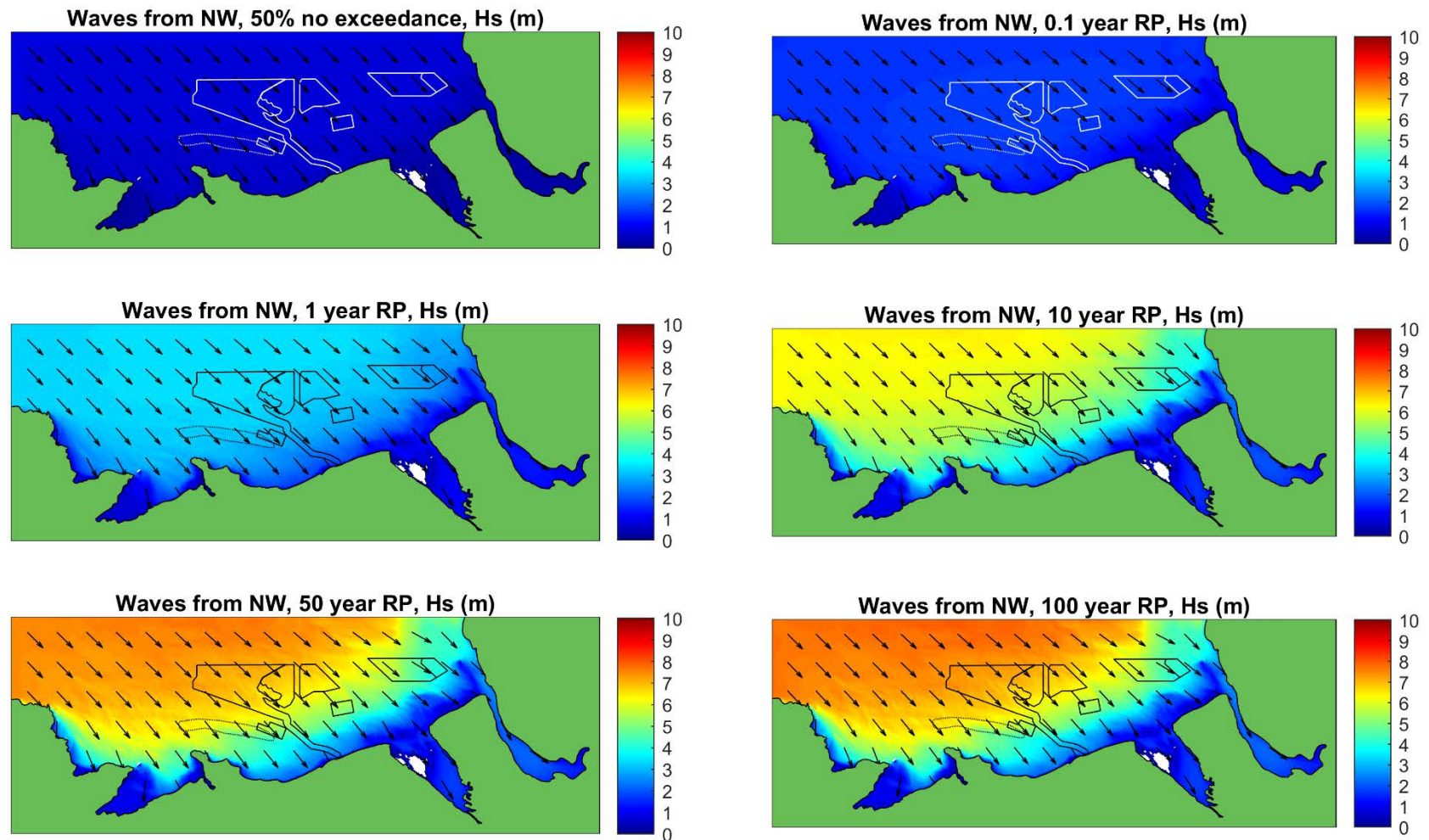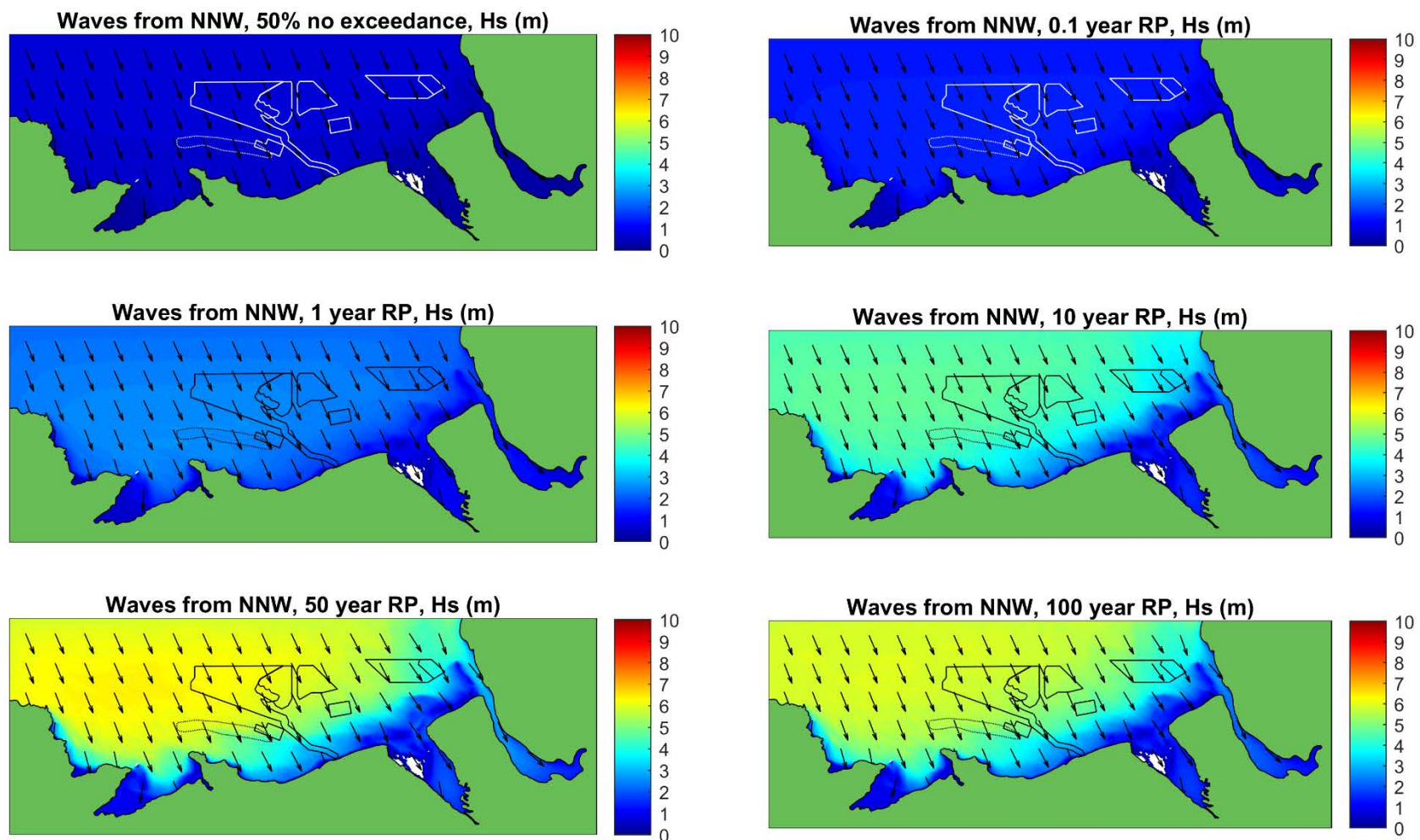
GoBe Consultants Ltd

The array area outlines of AyM and other nearby operational wind farms, and the offshore ECC of AyM are shown as solid lines. The defined area of Constable Bank is indicated as a thin dotted line.

Figure C4. **Baseline significant wave height, waves from the north-north-west, all return periods**

Awel y Môr Offshore Windfarm Environmental Impact Assessment:
Volume 4, Annex 2.3: Marine Geology, Oceanography and Physical Processes Technical Assessment
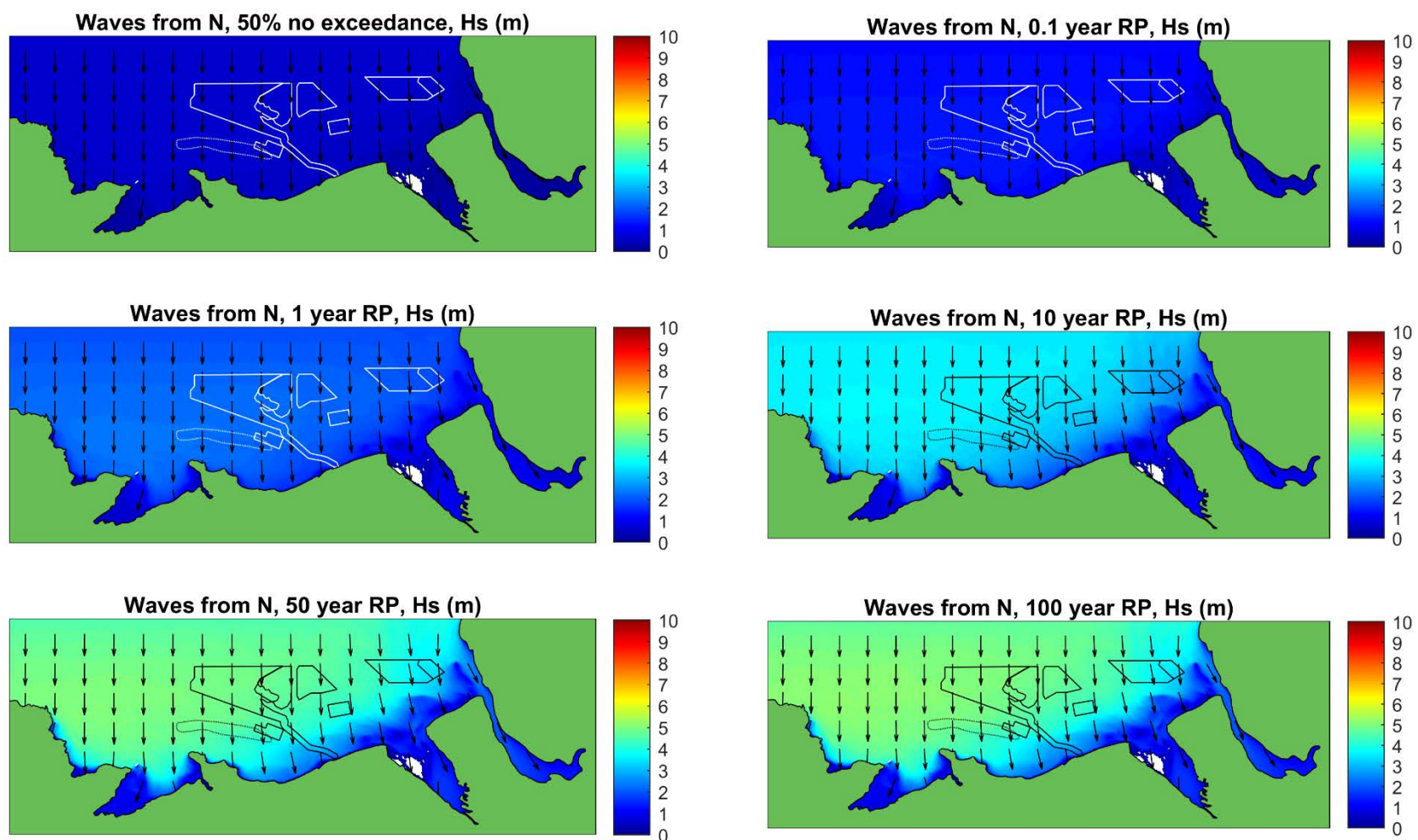
GoBe Consultants Ltd

The array area outlines of AyM and other nearby operational wind farms, and the offshore ECC of AyM are shown as solid lines. The defined area of Constable Bank is indicated as a thin dotted line.

Figure C5.   Baseline significant wave height, waves from the north, all return periods

Awel y Môr Offshore Windfarm Environmental Impact Assessment:
Volume 4, Annex 2.3: Marine Geology, Oceanography and Physical Processes Technical Assessment
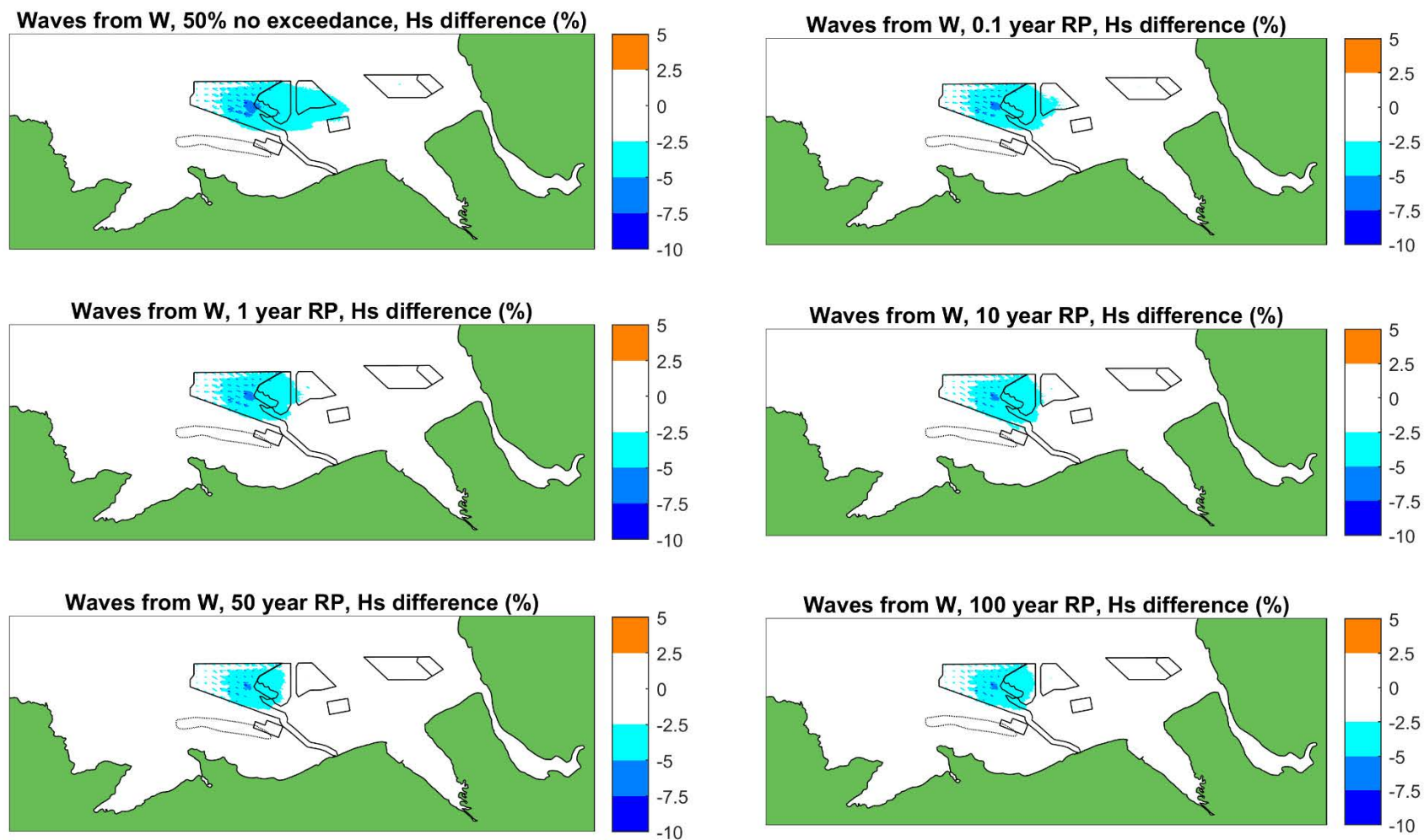
GoBe Consultants Ltd

The array area outlines of AyM and other nearby operational wind farms, and the offshore ECC of AyM are shown as solid lines. The defined area of Constable Bank is indicated as a thin dotted line.

Figure C6. Percentage difference in significant wave height (scheme minus baseline as a proportion of baseline values), operational phase, waves from the west, all return periods. Negative values are a reduction in wave height as a result of the installed infrastructure: MDS for Awel y Môr and as built for Gwynt y Môr, Rhyl Flats, North Hoyle, Burbo Bank and Burbo Bank Extension

Awel y Môr Offshore Windfarm Environmental Impact Assessment:
Volume 4, Annex 2.3: Marine Geology, Oceanography and Physical Processes Technical Assessment
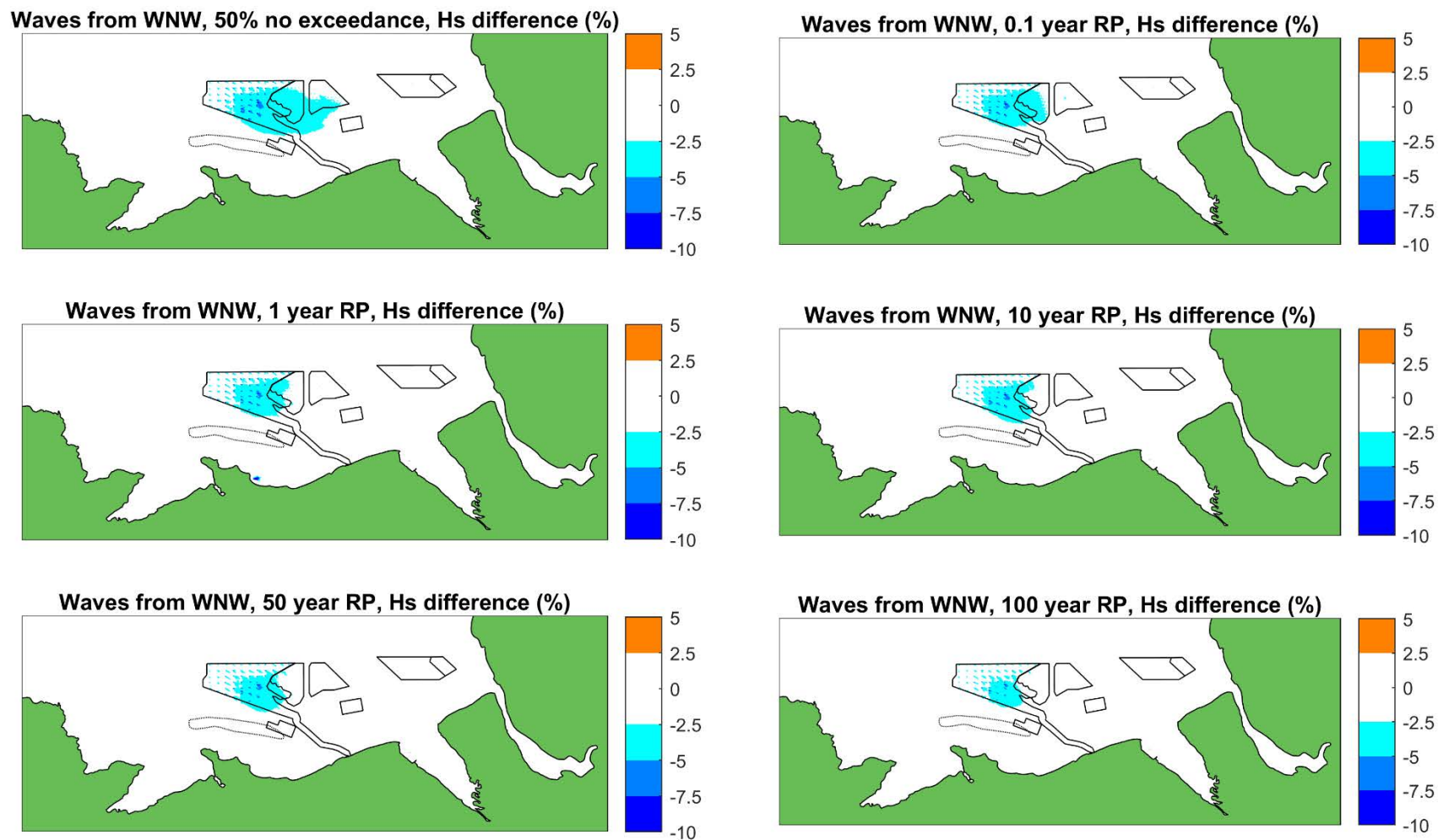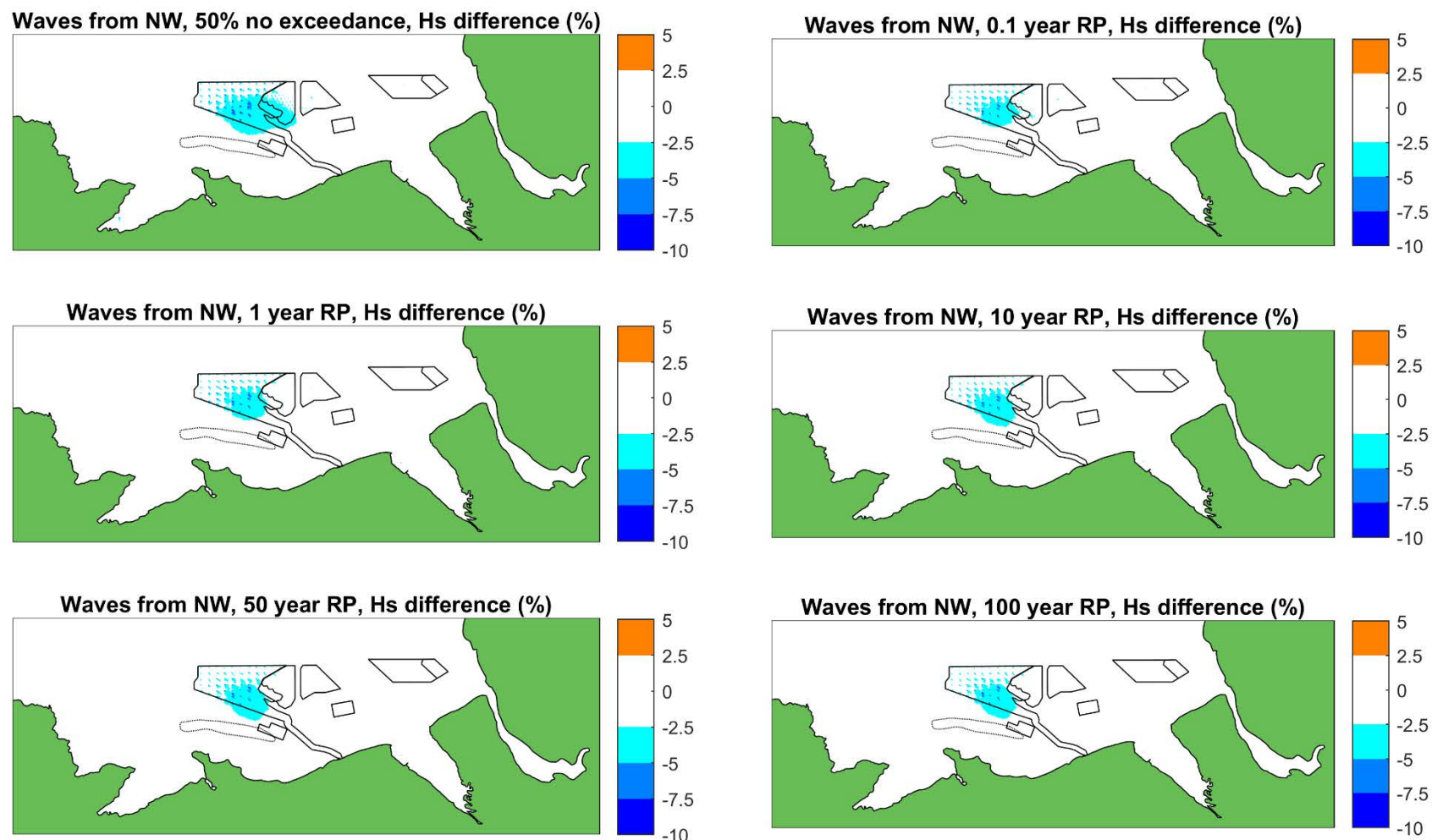
GoBe Consultants Ltd

The array area outlines of AyM and other nearby operational wind farms, and the offshore ECC of AyM are shown as solid lines. The defined area of Constable Bank is indicated as a thin dotted line.

Figure C7. Percentage difference in significant wave height (scheme minus baseline as a proportion of baseline values), operational phase, waves from the west-north-west, all return periods. Negative values are a reduction in wave height as a result of the installed infrastructure: MDS for Awel y Môr and as built for Gwynt y Môr, Rhyl Flats, North Hoyle, Burbo Bank and Burbo Bank Extension

Awel y Môr Offshore Windfarm Environmental Impact Assessment:
Volume 4, Annex 2.3: Marine Geology, Oceanography and Physical Processes Technical Assessment
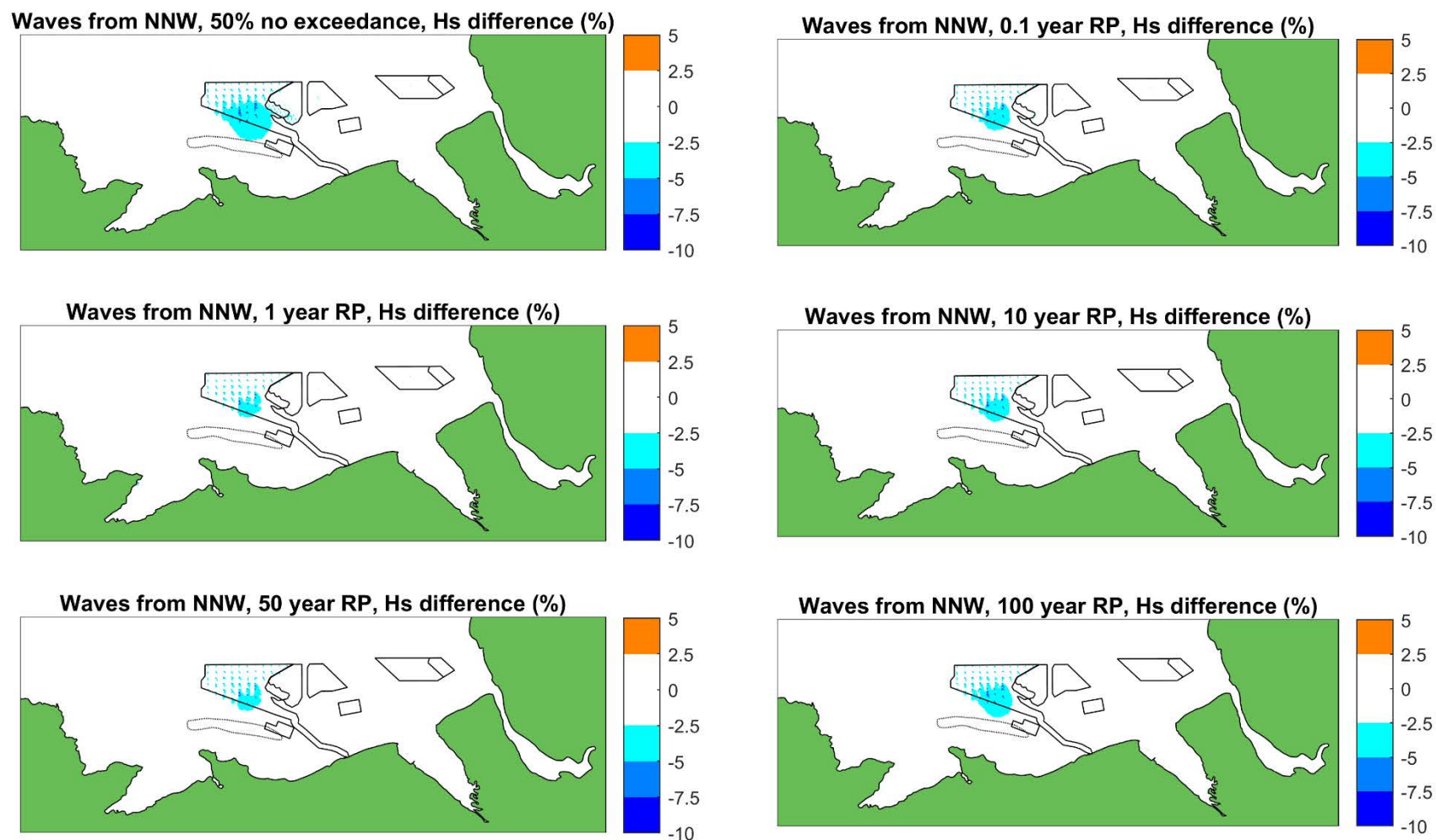
GoBe Consultants Ltd

The array area outlines of AyM and other nearby operational wind farms, and the offshore ECC of AyM are shown as solid lines. The defined area of Constable Bank is indicated as a thin dotted line.

Figure C8.   Percentage difference in significant wave height (scheme minus baseline as a proportion of baseline values), operational phase, waves from the north-west, all return periods. Negative values are a reduction in wave height as a result of the installed infrastructure: MDS for Awel y Môr and as built for Gwynt y Môr, Rhyl Flats, North Hoyle, Burbo Bank and Burbo Bank Extension

Awel y Môr Offshore Windfarm Environmental Impact Assessment:
Volume 4, Annex 2.3: Marine Geology, Oceanography and Physical Processes Technical Assessment
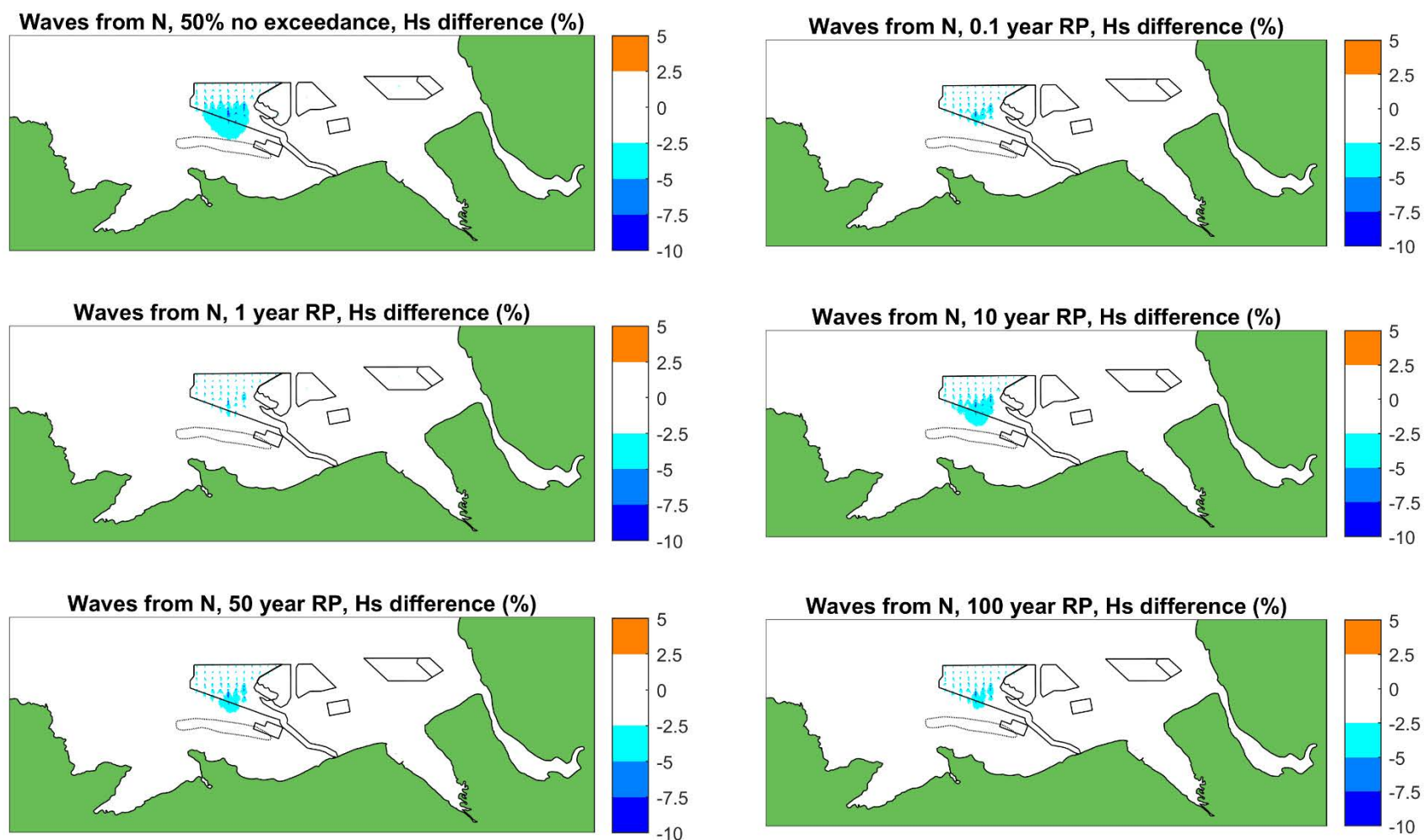
GoBe Consultants Ltd

The array area outlines of AyM and other nearby operational wind farms, and the offshore ECC of AyM are shown as solid lines. The defined area of Constable Bank is indicated as a thin dotted line.

Figure C9. Percentage difference in significant wave height (scheme minus baseline as a proportion of baseline values), operational phase, waves from the north-north-west, all return periods. Negative values are a reduction in wave height as a result of the installed infrastructure: MDS for Awel y Môr and as built for Gwynt y Môr, Rhyl Flats, North Hoyle, Burbo Bank and Burbo Bank Extension

Awel y Môr Offshore Windfarm Environmental Impact Assessment:
Volume 4, Annex 2.3: Marine Geology, Oceanography and Physical Processes Technical Assessment

GoBe Consultants Ltd

The array area outlines of AyM and other nearby operational wind farms, and the offshore ECC of AyM are shown as solid lines. The defined area of Constable Bank is indicated as a thin dotted line.
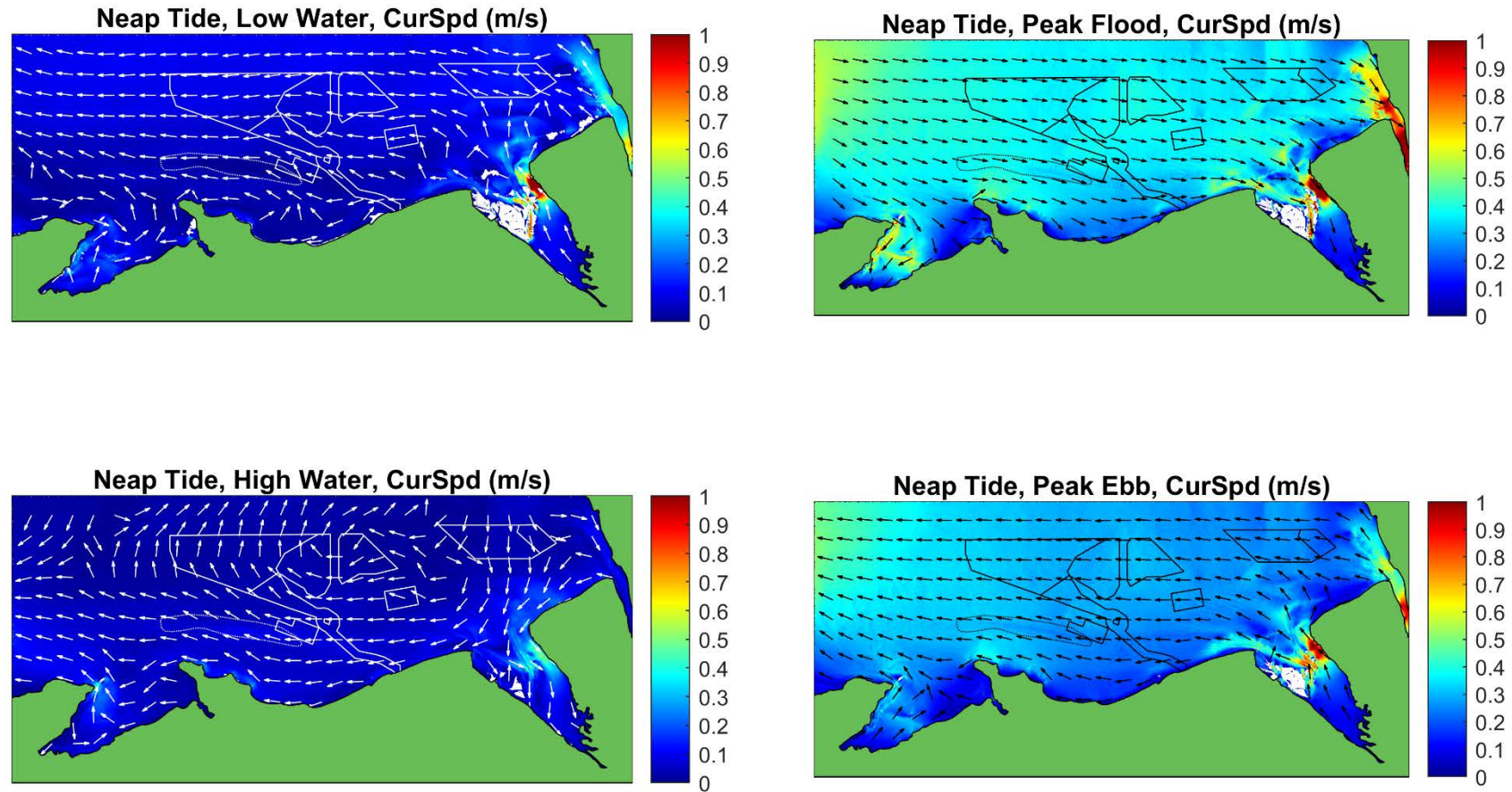
Figure C10. Percentage difference in significant wave height (scheme minus baseline as a proportion of baseline values), operational phase, waves from the north, all return periods. Negative values are a reduction in wave height as a result of the installed infrastructure: MDS for Awel y Môr and as built for Gwynt y Môr, Rhyl Flats, North Hoyle, Burbo Bank and Burbo Bank Extension

Awel y Môr Offshore Windfarm Environmental Impact Assessment:
Volume 4, Annex 2.3: Marine Geology, Oceanography and Physical Processes Technical Assessment

GoBe Consultants Ltd

D   Tidal Model Baseline and Results Figures

White areas in the Dee Estuary and elsewhere are where sandbanks and coastlines dry out to varying extents at different tidal water levels.
A combination of black and white site outlines and vector arrows are used to improve visual contrast against the underlying colourmap.
The (older PEIR) array area outlines of AyM and other nearby operational wind farms, and the (older PEIR) offshore ECC of AyM are shown as solid lines.
The defined area of Constable Bank is indicated as a thin dotted line.

Figure D1.   Baseline tidal current speed and direction during a representative neap tidal condition

Awel y Môr Offshore Windfarm Environmental Impact Assessment:
Volume 4, Annex 2.3: Marine Geology, Oceanography and Physical Processes Technical Assessment
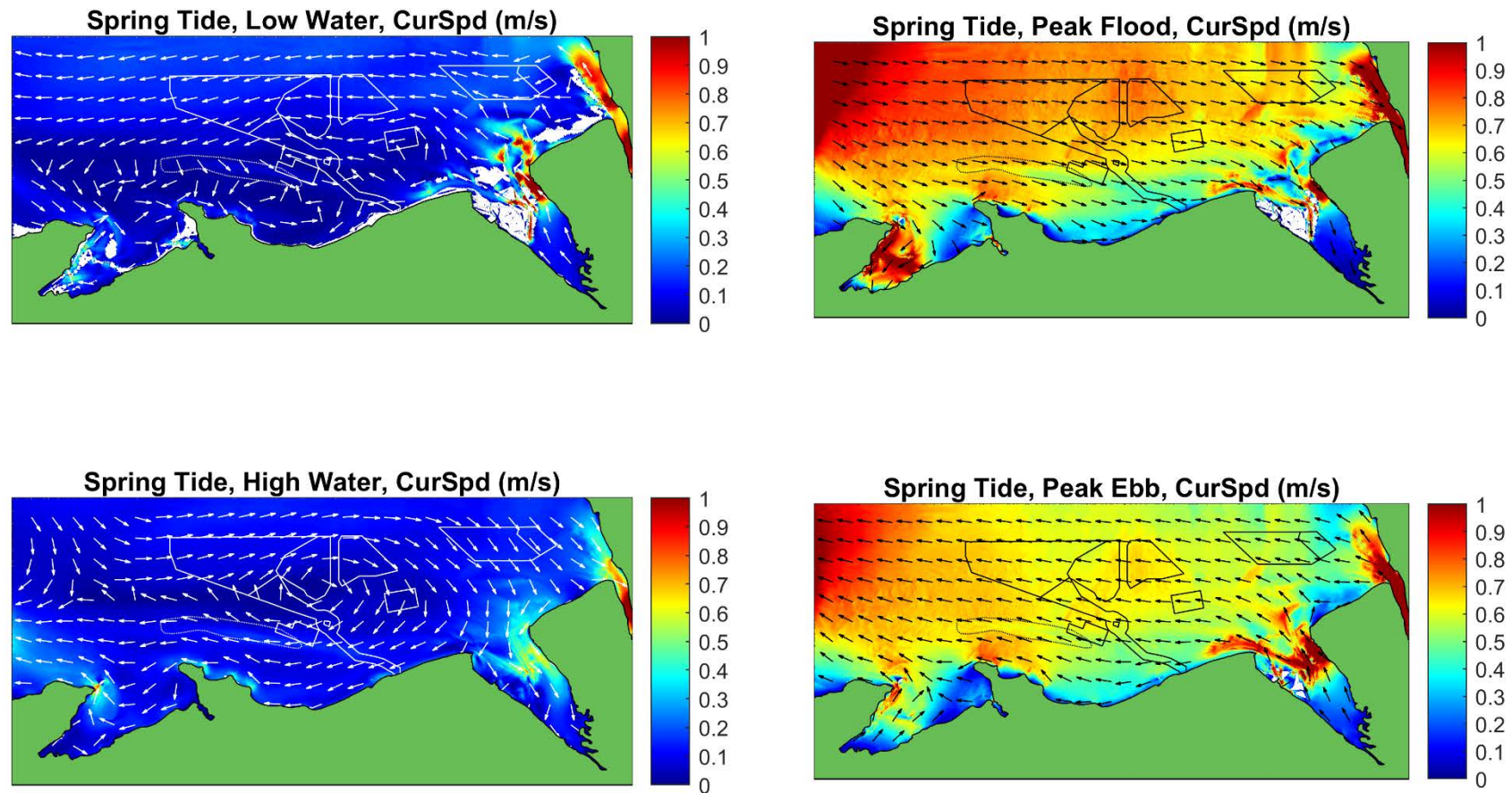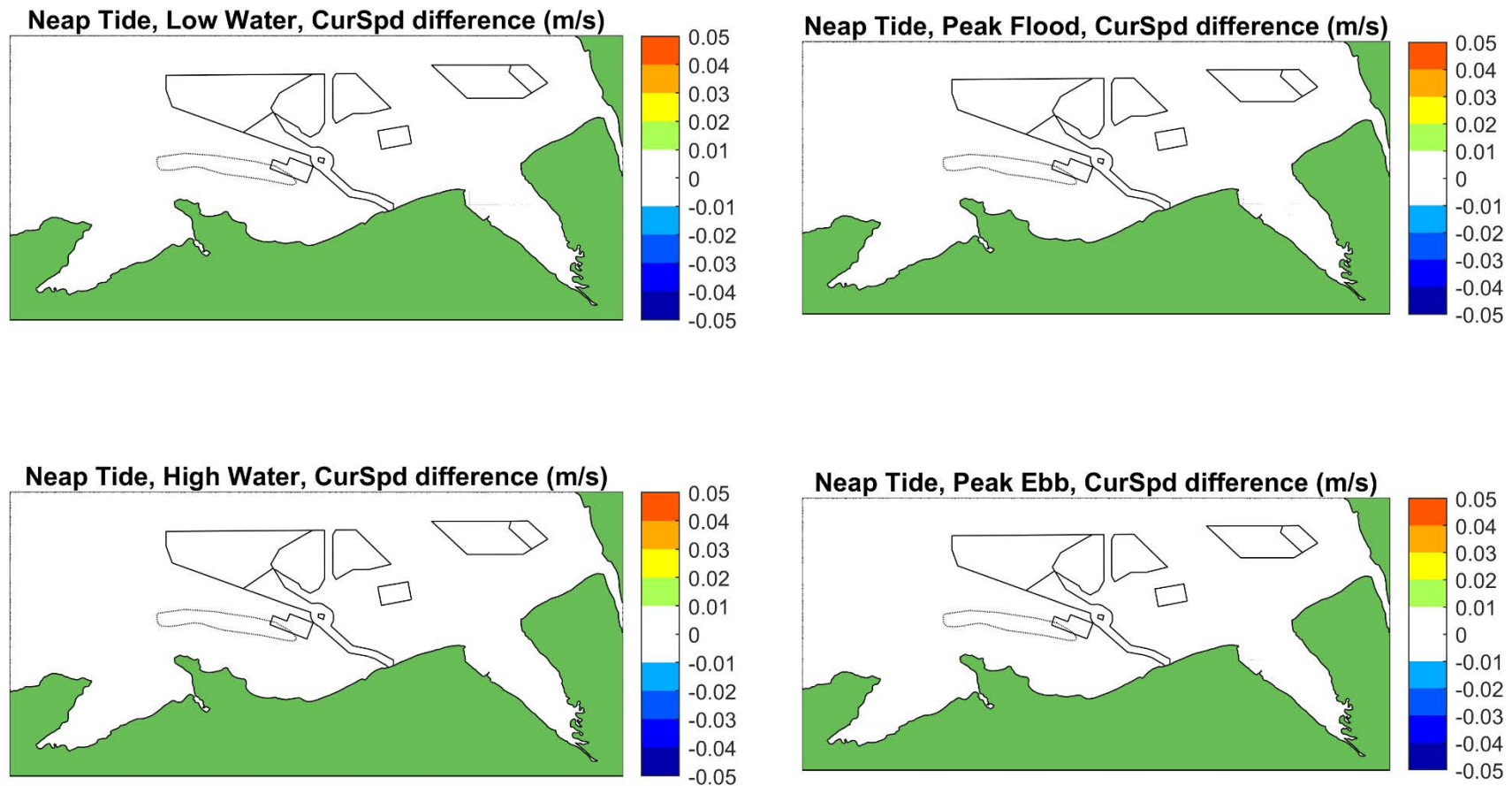
GoBe Consultants Ltd

White areas in the Dee Estuary and elsewhere are where sandbanks and coastlines dry out to varying extents at different tidal water levels.
A combination of black and white site outlines and vector arrows are used to improve visual contrast against the underlying colourmap.
The (older PEIR) array area outlines of AyM and other nearby operational wind farms, and the (older PEIR) offshore ECC of AyM are shown as solid lines.
The defined area of Constable Bank is indicated as a thin dotted line.

Figure D2.   Baseline tidal current speed and direction during a representative spring tidal condition

Awel y Môr Offshore Windfarm Environmental Impact Assessment:
Volume 4, Annex 2.3: Marine Geology, Oceanography and Physical Processes Technical Assessment

GoBe Consultants Ltd

The plots indicate no change greater than ±0.01 m/s at any location at any state of the tide, within the resolution of the model (approximately 100 m).
The (older PEIR) array area outlines of AyM and other nearby operational wind farms, and the (older PEIR) offshore ECC of AyM are shown as solid lines.
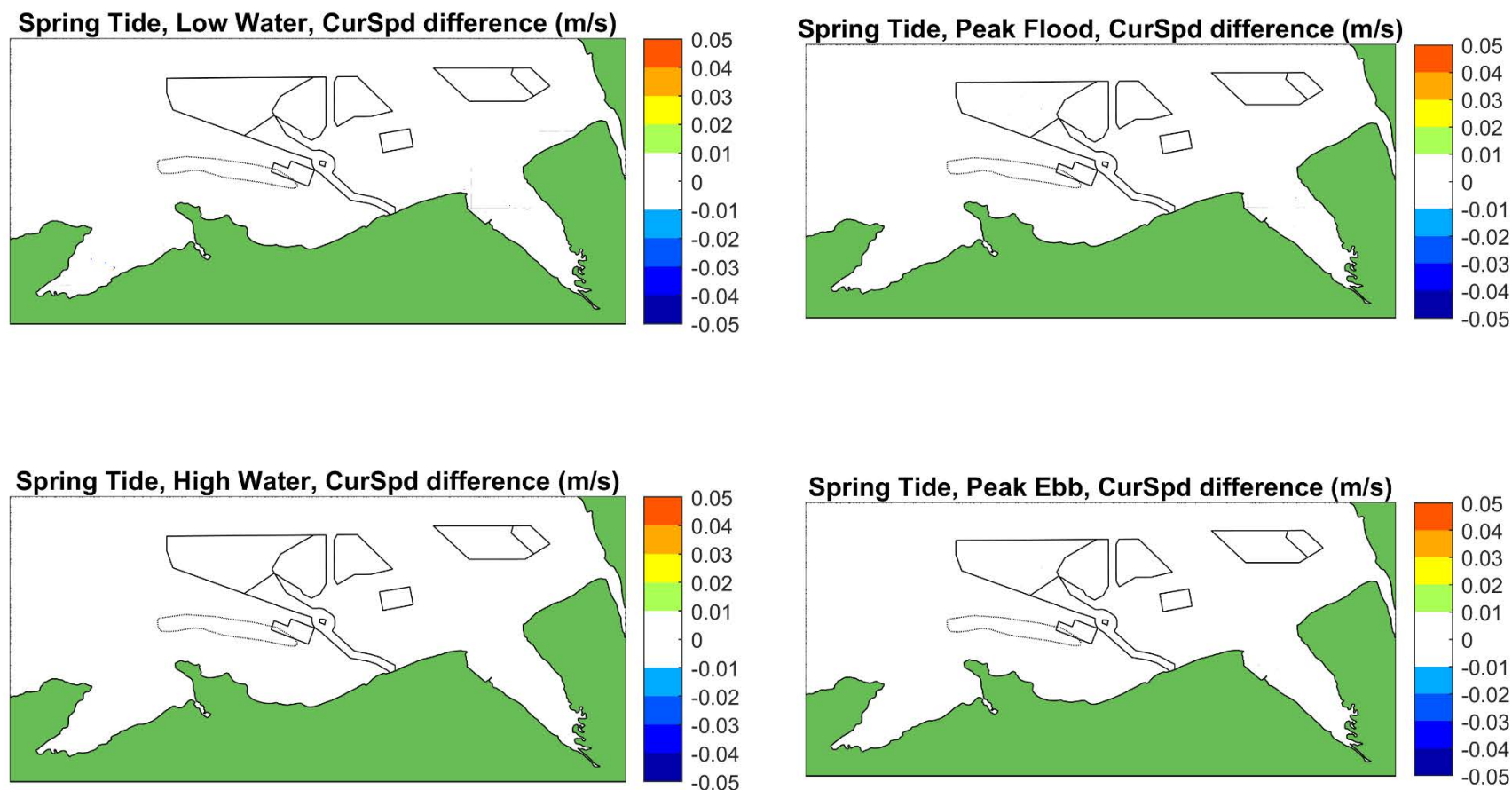The defined area of Constable Bank is indicated as a thin dotted line.

Figure D3. **Absolute difference in tidal current speed (scheme minus baseline), operational phase, during a representative neap tidal condition. Negative and positive values are a reduction or increase in time average current speed, respectively, as a result of the installed infrastructure: MDS for Awel y Môr and as built for Gwynt y Môr, Rhyl Flats, North Hoyle, Burbo Bank and Burbo Bank Extension**

Awel y Môr Offshore Windfarm Environmental Impact Assessment:
Volume 4, Annex 2.3: Marine Geology, Oceanography and Physical Processes Technical Assessment
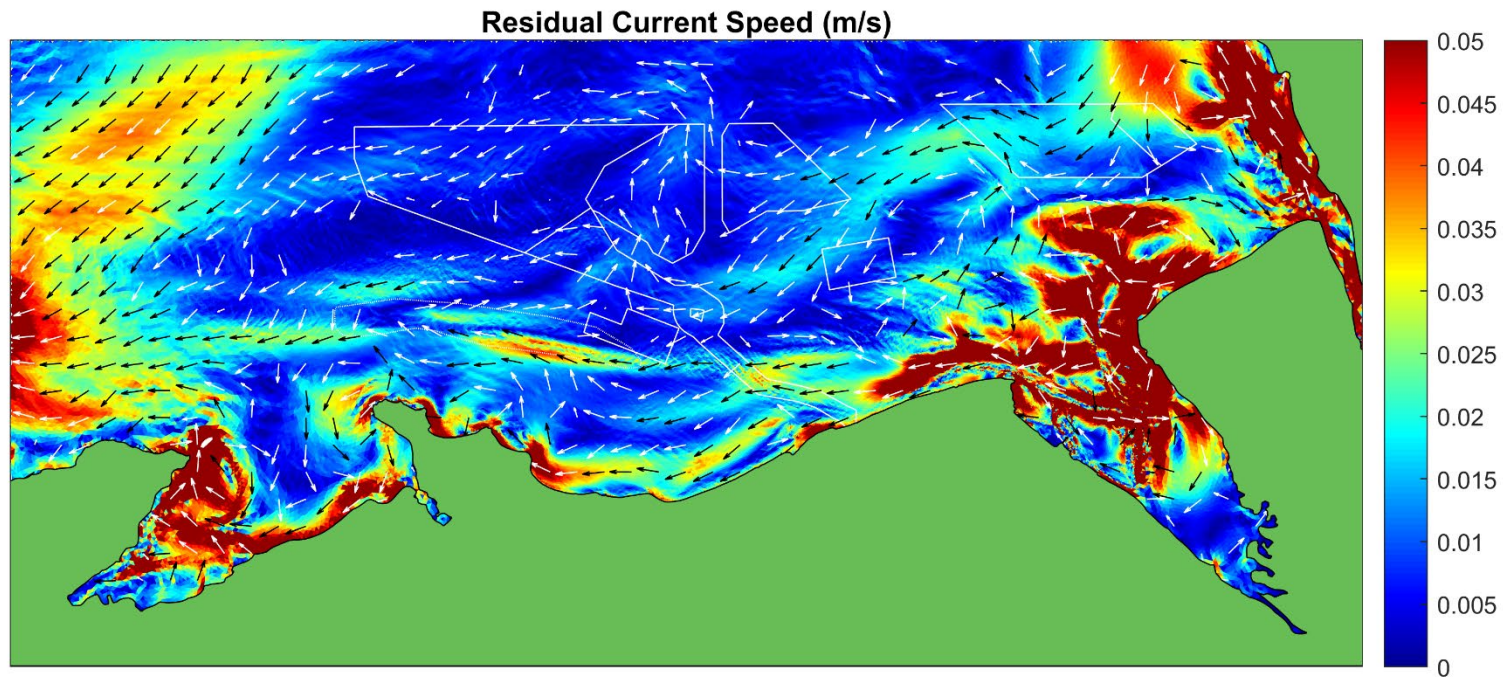
GoBe Consultants Ltd

The plots indicate no change greater than ±0.01 m/s at any location at any state of the tide, within the resolution of the model (approximately 100 m).
The (older PEIR) array area outlines of AyM and other nearby operational wind farms, and the (older PEIR) offshore ECC of AyM are shown as solid lines.
The defined area of Constable Bank is indicated as a thin dotted line.

Figure D4. Absolute difference in tidal current speed (scheme minus baseline), operational phase, during a representative spring tidal condition. Negative and positive values are a reduction or increase in time average current speed, respectively, as a result of the installed infrastructure: MDS for Awel y Môr and as built for Gwynt y Môr, Rhyl Flats, North Hoyle, Burbo Bank and Burbo Bank Extension
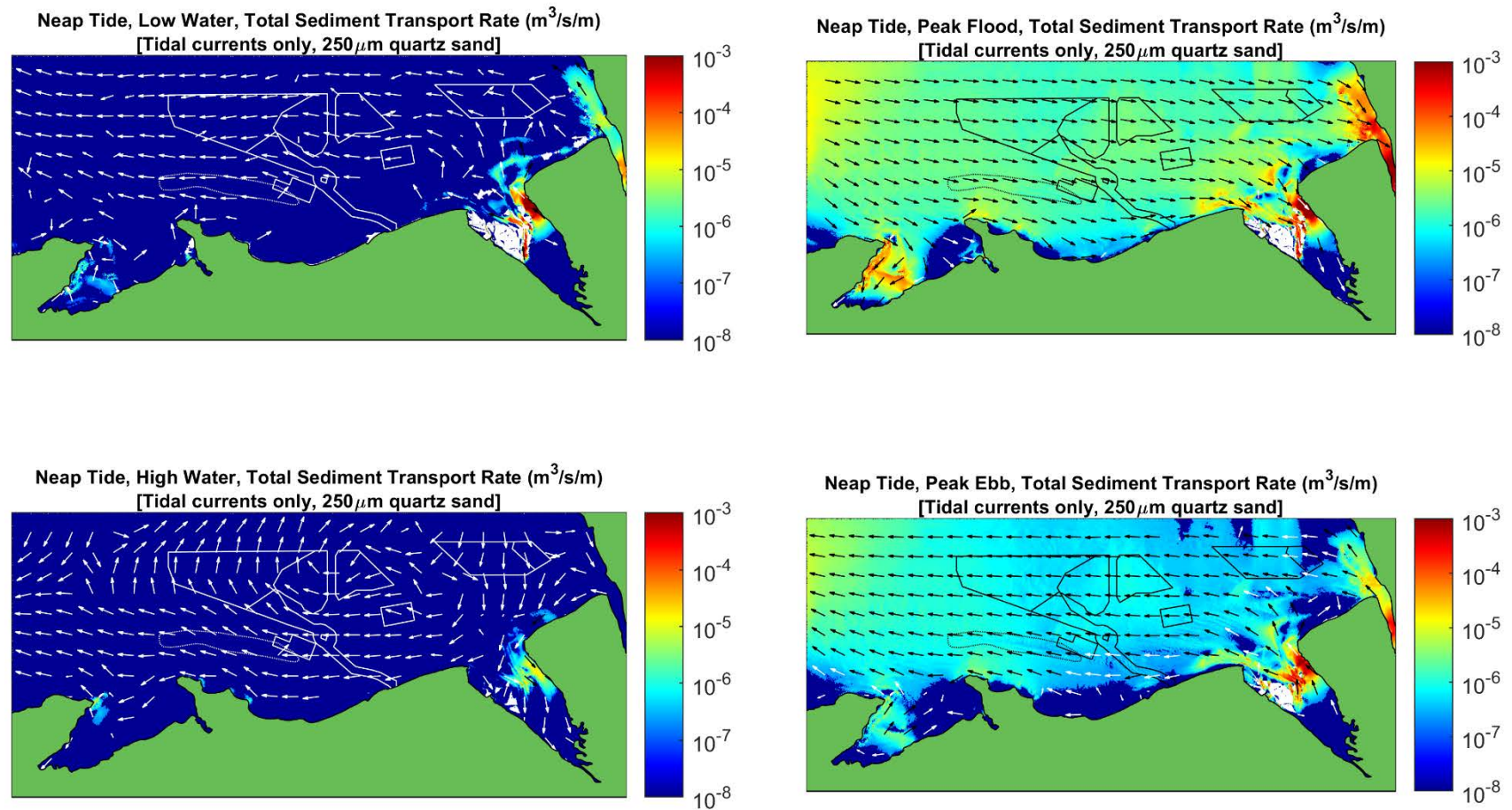
Awel y Môr Offshore Windfarm Environmental Impact Assessment:
Volume 4, Annex 2.3: Marine Geology, Oceanography and Physical Processes Technical Assessment

GoBe Consultants Ltd

Residual Current Speed (m/s)

A combination of black and white site outlines and vector arrows are used to improve visual contrast against the underlying colourmap.
The (older PEIR) array area outlines of AyM and other nearby operational wind farms, and the (older PEIR) offshore ECC of AyM are shown as solid lines.
The defined area of Constable Bank is indicated as a thin dotted line. Direction is not indicated for residual current speeds less than 0.01 m/s.

Figure D5.   **Baseline residual tidal current speed and direction measured over a representative spring-neap tidal period**

Awel y Môr Offshore Windfarm Environmental Impact Assessment:
Volume 4, Annex 2.3: Marine Geology, Oceanography and Physical Processes Technical Assessment

GoBe Consultants Ltd

White areas in the Dee Estuary and elsewhere are where sandbanks and coastlines dry out to varying extents at different tidal water levels.
A combination of black and white site outlines and vector arrows are used to improve visual contrast against the underlying colourmap.
The (older PEIR) array area outlines of AyM and other nearby operational wind farms, and the (older PEIR) offshore ECC of AyM are shown as solid lines.
The defined area of Constable Bank is indicated as a thin dotted line.

Figure D6. Baseline sediment transport rate and direction, for 250 µm quartz sand, during a representative neap tidal condition

Awel y Môr Offshore Windfarm Environmental Impact Assessment:
Volume 4, Annex 2.3: Marine Geology, Oceanography and Physical Processes Technical Assessment
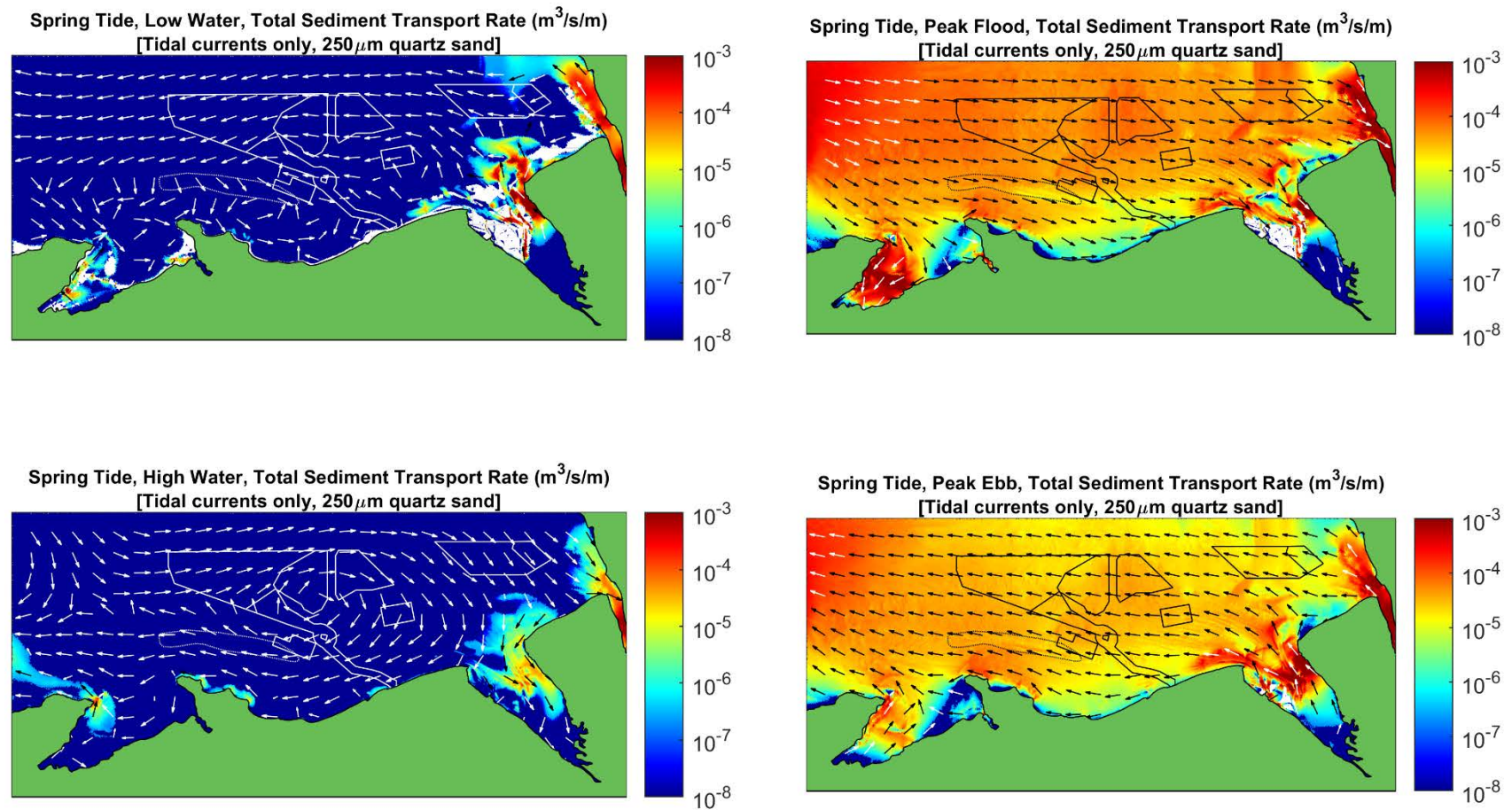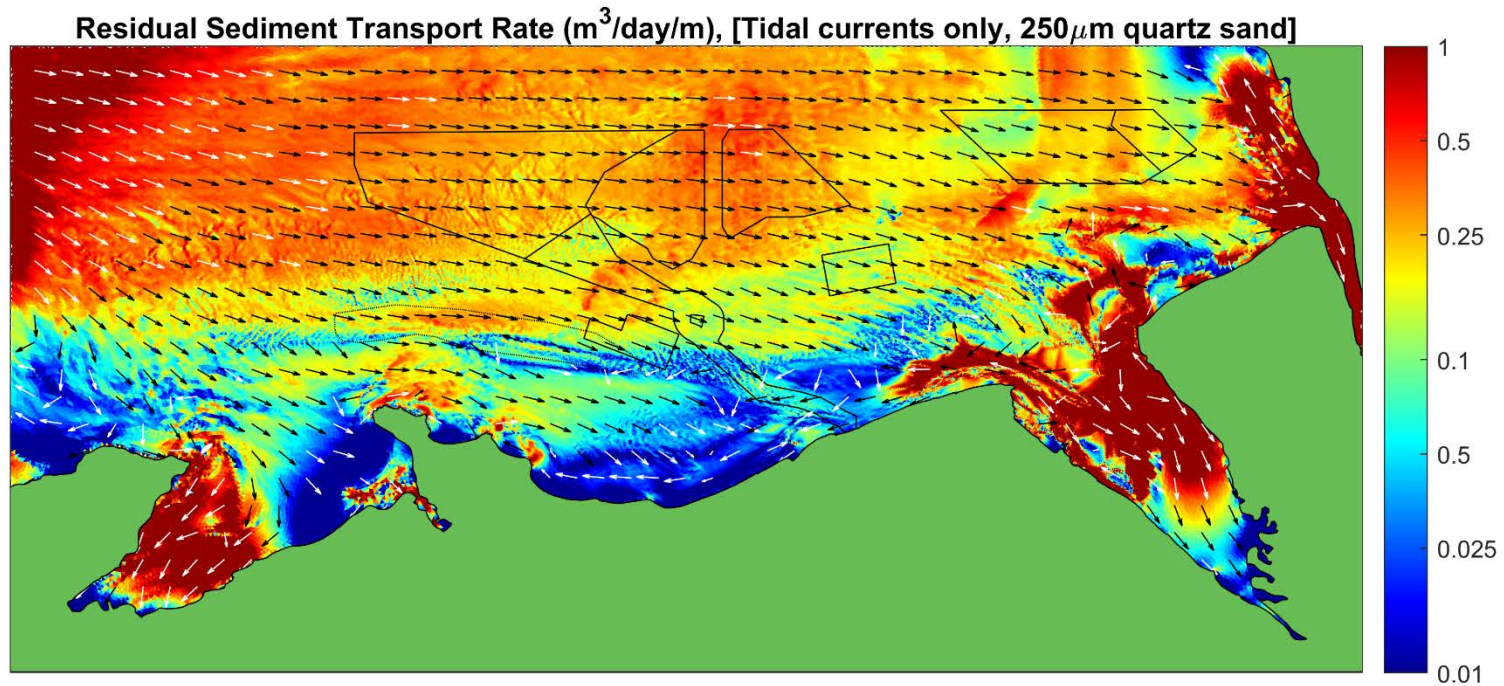
GoBe Consultants Ltd

White areas in the Dee Estuary and elsewhere are where sandbanks and coastlines dry out to varying extents at different tidal water levels.
A combination of black and white site outlines and vector arrows are used to improve visual contrast against the underlying colourmap.
The (older PEIR) array area outlines of AyM and other nearby operational wind farms, and the (older PEIR) offshore ECC of AyM are shown as solid lines.
The defined area of Constable Bank is indicated as a thin dotted line.

Figure D7. Baseline sediment transport rate and direction, for 250 μm quartz sand, during a representative spring tidal condition

Awel y Môr Offshore Windfarm Environmental Impact Assessment:
Volume 4, Annex 2.3: Marine Geology, Oceanography and Physical Processes Technical Assessment

GoBe Consultants Ltd

Residual Sediment Transport Rate (m³/day/m), [Tidal currents only, 250μm quartz sand]

A combination of black and white site outlines and vector arrows are used to improve visual contrast against the underlying colourmap.
The (older PEIR) array area outlines of AyM and other nearby operational wind farms, and the (older PEIR) offshore ECC of AyM are shown as solid lines.
The defined area of Constable Bank is indicated as a thin dotted line.

Figure D8. Baseline residual sediment transport rate and direction, for 250 μm quartz sand, measured over a representative spring-neap tidal period

E   Scour Calculations

E.1   Overview

In order to quantify the area of seabed that might be affected by scour (either the footprint of scour or scour protection), estimates of the theoretical maximum depth and extent of scour are provided below. Estimates are made of the primary scour, i.e. the scour pit directly associated with the presence of the main obstacle.

The equilibrium primary scour depth for each foundation type has been conservatively calculated assuming the absence of any scour protection, using empirical relationships described in Whitehouse (1998). This analysis considers scour resulting from the characteristic wave and current regime, both alone and in combination.

The project description (Volume 2, Chapter 1: Offshore Project Description) provides Maximum Adverse Scenario extents of scour protection for each foundation type. Scour protection might be applied around the base of some or all foundations depending upon the seabed conditions and other engineering requirements. By design, scour protection will largely prevent the development of primary scour, but may itself cause smaller scale secondary scour due to turbulence at the edges of the scour protection area.

E.2   Assumptions

The following scour assessment for AyM reports the estimated equilibrium scour depth, which assumes that there are no limits to the depth or extent of scour development by time or the nature of the sedimentary or metocean environments. As such, the results of this study are considered to be conservative and provide an (over-) estimation of the maximum potential scour depth, footprint and volume. Several factors may naturally reduce or restrict the equilibrium scour depth locally, with a corresponding reduction in the area and volume of change.

This study makes the basic assumption that the seabed comprises an unlimited thickness of uniform non-cohesive and easily eroded sediment. In practice, the thickness of unconsolidated (and more easily erodible) surficial Holocene sediment is spatially variable across the AyM array, with the greatest thicknesses found in central and eastern areas of the array (Fugro, 2020). In the west, pre-Holocene material is at or close to the surface and may limit the extent to which scour can occur.

The foundation types, dimensions and numbers used in the assessment are consistent with the project design information provided in Volume 2; Chapter 1.

Reported observations of scour under steady current conditions (e.g. in rivers) generally show that the upstream slope of the depression is typically equal to the angle of internal friction for the exposed sediment (typically 32 deg in loose medium sand; Hoffmans and Verheil, 1997) but the downstream slope is typically less steep.

In reversing (tidal) current conditions, both slopes will develop under alternating upstream and downstream forcing and so will tend towards the less steep or an intermediate condition. For the purposes of the present study a representative angle of internal friction (32 deg) will be used as the characteristic slope angle for scour development.

E.3   Equilibrium scour depth

The maximum equilibrium scour depth (Se) is defined as the depth of the scour pit adjacent to the structure, below the mean ambient or original seabed level. The value of Se is typically proportional to the diameter of the structure and so is commonly expressed in units of structure diameter (D).

Scour depth decreases with distance from the edge of the foundation. The scour extent (Sextent) is defined as the radial distance from the edge of the structure (and the point of maximum scour depth) to the edge of the scour pit (where the bed level is again equal to the mean ambient or original seabed level). This is calculated on the basis of a linear slope at the angle of internal friction for the sediment, i.e.:

$$S_{extent} = \frac{S_e}{\tan 32°} \approx S_e \times 1.6$$

(Eq. 1)
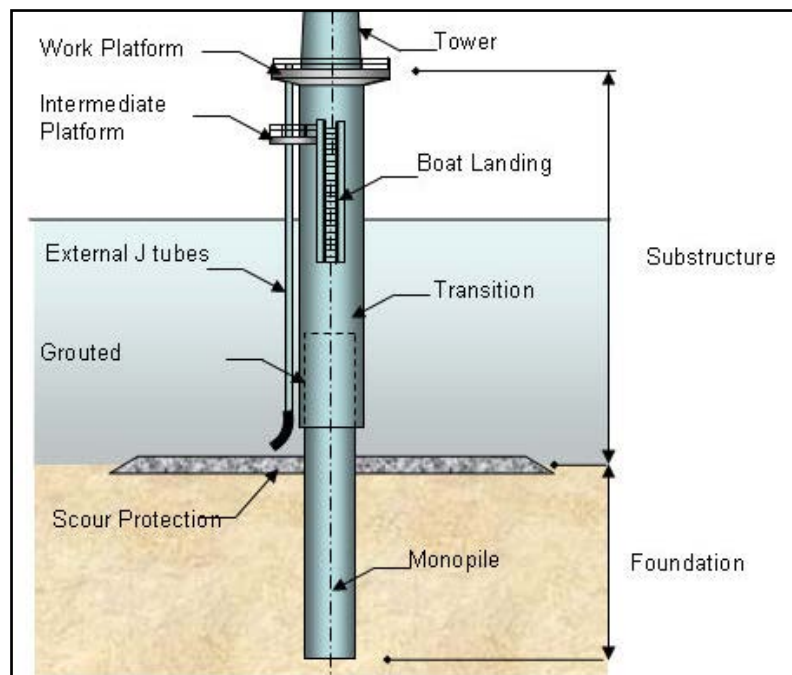
The scour footprint (Sfootprint) is defined as the seabed area affected by scour, excluding the foundation's footprint, i.e.:

$$S_{footprint} = \pi \left(S_{extent} + \left(\frac{D}{2} \right) \right)^2 - \pi \left(\frac{D}{2} \right)^2$$

(Eq. 2)

The scour pit volume is calculated as the volume of an inverted truncated cone described by Equations 1 and 2 above, accounting for the presence of the foundation but excluding its volume.

E.4   Scour assessment method: monopiles

The outline design of the proposed monopile structure is shown in Figure E1.

Source: Garrad Hassan and Partners Ltd)

Figure E1.   Outline design of a typical steel monopile foundation (with scour protection)

Compared to other more complex foundation types, scour around upright slender monopile structures in steady currents is relatively well-understood in the literature and is supported by a relatively large empirical evidence base from the laboratory and from the field. The maximum equilibrium scour depth, adjacent to the structure, below the mean seabed level (Sc), is typically proportional to the diameter of the monopile and is therefore expressed in units of monopile diameter (D).

E.4.1 Under steady currents

Breusers *et al*. (1977) presented a simple expression for scour depth under live-bed scour (i.e. scour occurring in a dynamic sediment environment) which was extended by Sumer *et al*. (1992) who assessed the statistics of the original data to show that:

$$\frac{S_c}{D} = 1.3 \pm \sigma_{Sc/D}$$

(Eq. 3)

Where $\sigma Sc/D$ is the standard deviation of observed ratio Sc /D. Based on the experimental data, $\sigma Sc/D$ is approximately 0.7, hence, 95 % of observed scour falls within two standard deviations, i.e. in the range 0 < Sc/D < 2.7. Based on the central value Sc = 1.3 D (as also recommended in DNV, 2016), the maximum equilibrium depth of scour for the largest diameter monopile (15 m) is estimated to be 19.5 m. The equivalent value for the smallest diameter monopile (12 m) is 15.6 m.

E.4.2 Under waves and combined wave-current forcing

The mechanisms of scour associated with wave action are limited when the oscillatory displacement of water at the seabed is less than the length or size of the structure around which it is flowing. This ratio is typically parameterised using the Keulegan-Carpenter (KC) number:

$$KC = \frac{U_{0m}T}{D}$$

(Eq. 4)

Where U_{0m} is the peak orbital velocity at the seabed (e.g. using methods presented in Soulsby, 1997) and T is the corresponding wave period. Sumer and Fredsøe (2001) found that for KC < 6, wave action is insufficient to cause significant scour in both wave alone and combined wave-current scenarios.

Values of KC are < 6 for monopiles in the AyM array area, for a range of extreme wave conditions (see Table E1) and for the full expected range of tidally affected water depths across the site (approximately -15 mLAT to -42 mLAT). Therefore, it is predicted that waves do not have the potential to contribute to scour development around monopiles in the AyM area.
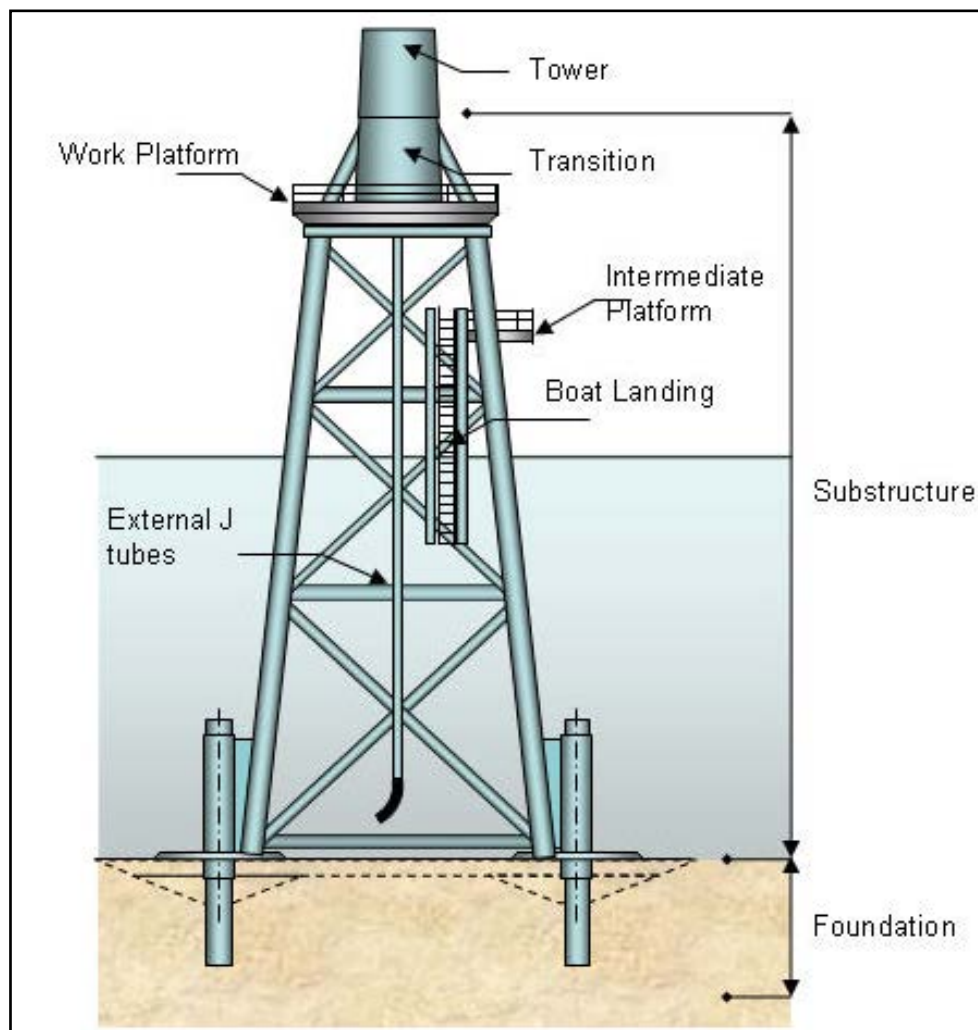
Table E1.   Extreme omni-directional wave conditions considered

Return Period (years)	Significant Wave Height, Hs (m)	Zero Crossing Period, Tz (s)
1:1	4.4	6.26
1:10	6.16	7.41
1:50	7.26	8.05

The value of U_{0m} for given (offshore or deep water) wave conditions depends upon the local water depth, which varies between approximately -15 mLAT to -42 mLAT within the array due to variations in absolute bathymetry and relative water level; the influence of shoaling and wave breaking have been ignored in the present study (a conservative assumption).

E.5   Scour assessment method: jacket foundations

The outline design of the proposed four-legged jacket foundation for turbines is shown in Figure E2. Above the seabed jacket foundations comprise a lattice of vertical primary members and diagonal cross-member bracing, up to 3.5 m in diameter; it is assumed that either no near-bed horizontal cross-member bracing is required, or that it is sufficiently high above the bed to not induce significant local scour. The four-legged jacket foundation will have a nominally square plan view cross-section with base edge dimensions of between 30 m and 40 m (Volume 2; Chapter 1).

Source: Garrad Hassan and Partners Ltd

Figure E2.   Outline design of a typical jacket foundation

The jacket foundation is anchored to the seabed at each corner by a pile driven into the seabed, 3.5 m in diameter. A jacket foundation structure may result in the occurrence of both local and group or global scour. The local scour is the local response to individual structure members.

E.5.1 Under steady currents

Under steady currents alone, the equilibrium scour depth around the vertical members of the structure base can be assessed using the same methods as for monopiles, unless significant interaction between individual members occurs. The potential for such interaction is discussed below.

The main scour development will be in proportion to the size of the largest exposed member near to the seabed. In this case, the largest exposed member will be the jacket leg which will have a diameter of up to 3.5 m. Using Equation 3, the scour depth for the largest jacket foundation is therefore estimated as 4.6 m.

In the case of currents, inter-member interaction has been shown to be a factor when the gap to pile diameter ratio (G/D) is less than 3. In this case limited experiments by Gormsen and Larson (1984) have shown that the scour depth might increase by between 5 % and 15%. However, in the case of the present study the gap ratio for members at the base of the jacket foundation structure is much greater than 3, and so no significant in-combination change is expected.

Empirical relationships also presented in Sumer and Fredsøe (2002) indicate that the depth of group scour (measured from the initial sediment surface to the new sediment surface surrounding local scour holes) for an array of piles similar to a jacket foundation (2x2) can be approximated as 0.4 D (i.e. approximately 1.4 m based on 3.5 m diameter jacket leg). On the basis of visual descriptions of group scour pits, their extent from the edge of the structure is estimated as half the width of the structure and following a broadly similar plan shape to that of the jacket foundation (i.e. square).

Together, the predicted maximum scour depth at the corner piles (4.6 m) and the group scour (1.4 m) is conservatively consistent with evidence from the field reported in Whitehouse (1998), summarising another report that scour depths of between 0.6 m and 3.6 m were observed below jacket structures in the Gulf of Mexico (although these could potentially be constrained from the maximum possible equilibrium scour depth by environmental factors and could also be subject to uncertainties in the seabed reference datum against which to measure the scour).

On the basis of the proposed jacket design, the diagonal bracing members are not predicted to induce seabed scouring due to the distance of separation from the seabed.

E.5.2 Under waves and combined wave-current forcing

Values of the KC parameter (Eq. 4) were calculated for a 3.5 m diameter jacket leg from the extreme wave conditions found at the site (Table E1)). Values of KC are less than 6 over the full expected range of tidally affected water depths across the site (approximately -15 mLAT to -42 mLAT) and so it is predicted that waves do not have the potential to contribute to scour development around the base of the jacket foundations.

The diagonal bracing members will have a smaller diameter and so a larger KC value. However, they are again not predicted to induce seabed scouring due to the likely distance of separation from the seabed. For moderate KC numbers a sufficient distance to avoid scour is approximately one diameter for a horizontal member, increasing to approximately three diameters under increasing KC numbers.
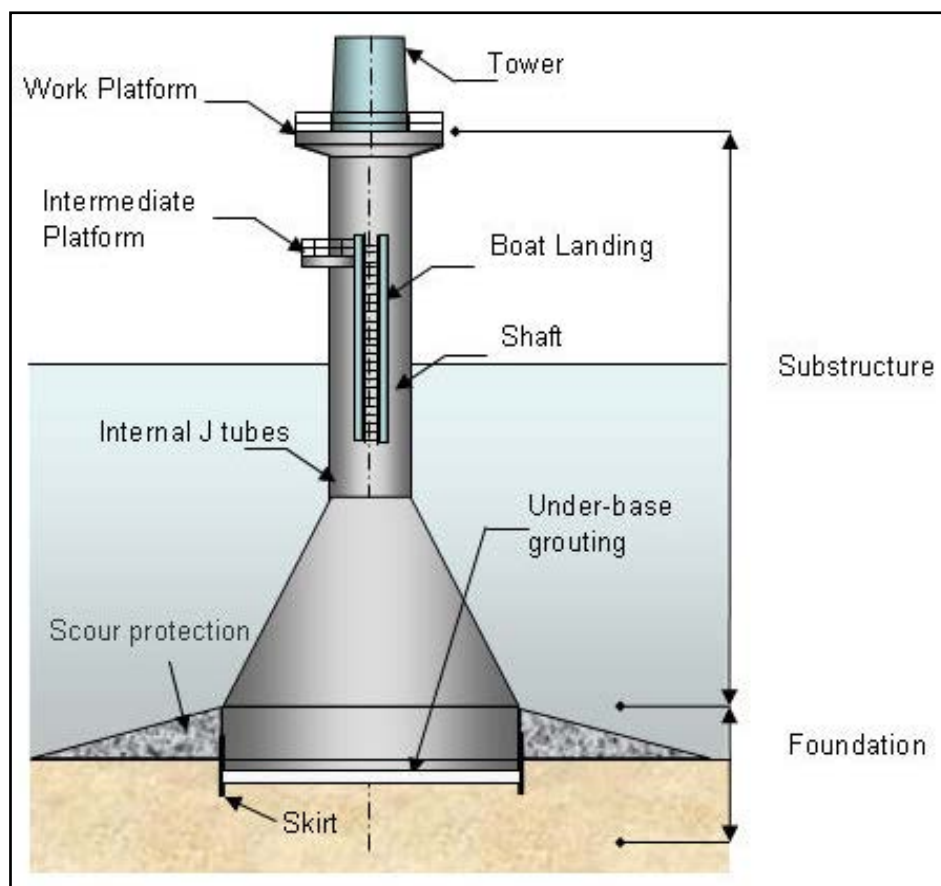
As such, little or no significant additional scour is predicted to result from waves, either alone or in combination with currents.

E.6   Scour assessment method: gravity base foundations

The outline design of the proposed gravity base foundation is shown in Figure E3. The foundation is characterised as a round base plate upon which sits a circular cross-section cone with a base diameter of between 45 m (for the smallest option) and 55 m (for the largest).

The evidence base for scour associated with gravity base foundation installations is relatively limited in comparison to that for monopiles and typically refers to oil and gas platforms which have a wide range of shapes and designs. Attempts to produce empirical relationships are complicated by this diversity of gravity base foundation structures.

The pattern and extent of scouring and the location of the point of maximum scouring may also vary depending upon the gravity base foundations relative size and shape. For the purposes of the present assessment, scour is assumed to be equally present at the predicted depth around the whole perimeter of the gravity base foundation, decreasing in depth with distance from the base edge to the ambient bed level at the angle of internal friction for the sediment (32 deg).

Source: Garrad Hassan and Partners Ltd)

Figure E3.   Outline design of a gravity base foundation

E.6.1 Under steady currents

Hoffmans and Verheij (1997) presented the Khalfin (1983) current-only scour predictor for a gravity base foundation with the following modified features:

- The pile diameter was replaced by a characteristic length, Dc, taken as the average of the length and breadth of the gravity base foundation;
- The flow depth, h, in the water depth to diameter ratio h/Dc was replaced by the gravity base foundation height, hc; and
- The undisturbed depth-averaged flow velocity was multiplied by αc/2 with αc = 2 for a circular structure, and αc = 2.3 for a rectangular gravity base foundation expressing the additional turbulence generated at the corners of the structure. The coefficient αc is an influence factor that represents the flow enhancement near the structure caused by the structure.

The equilibrium scour depth, S, is then given by:

$$\frac{S}{D_c} = 8.96\left(2\frac{0.5\,a_c U}{U_{cr}} - 1\right)\left(\frac{h_c}{D_c}\right)^{1.43}\left(\frac{(0.5\,a_c U)^2}{gh}\right)^N$$

With   U/Ucr = 1 for U > Ucr

$$N = 0.83\left(\frac{h_c}{D_c}\right)^{0.34}$$

And

Where:
- Ucr   is the value of depth-averaged flow velocity for initiation of sediment motion (m/s); and
- g   is the gravitational acceleration constant (9.81 m/s2)

(Eq. 5)

Assuming hc = h = 33 m and U > Ucr, the maximum equilibrium depth of scour for the largest diameter gravity base foundation (Dc = 55 m) is estimated to be 3.1 m. The equivalent value for the smallest diameter gravity base foundation (Dc = 45 m) is 2.5 m.

E.6.2 Under waves and combined wave-current forcing

The large scale of the gravity base foundation structures in relation to both water depth and wave orbital excursion length mean that the processes governing structure-flow interaction and scour are different from that described in relation to monopile and jacket structures. As such, relationships for scour associated with a shallow conical top gravity base foundation for waves alone are also not readily available from the literature. However, Whitehouse (2004) provides a relationship for a 'girder top' gravity base foundations, predicting equilibrium scour depth in response to waves alone of:

Se = 0.04D

(Eq. 6)

Yielding a value of between 1.8 m and 2.2 m for a 45 m and 55 m diameter gravity base foundation, respectively. Empirical results from physical model testing by Whitehouse (2004) suggest that the maximum scour depth around a conical top gravity base foundation (broadly similar to that proposed here) under combined wave-current conditions will be:

Se = 0.064D

(Eq. 7)

Yielding a value of between 2.9 m and 3.5 m for a 45 m and 55 m diameter gravity base foundation, respectively.

E.7   References

Breusers, H.N.C, Nicollet, G. and Shen, H.W., (1977). Local scour around cylindrical piers. J. of Hydraulic Res., IAHR, Vol. 15, No. 3, pp. 211 252.

Det Norske Veritas (DNV), (2016). Support structures for Wind Turbines. Offshore Standard DNVGL-ST-0126, 182pp.

Fugro, 2020. WPM1 Main Array Area -Seafloor and Shallow Geological Results Report. Doc Ref 003616043-04

Gormsen, C. and Larsen, T., (1984). Time development of scour around offshore structures. ISVA, Technical University of Denmark, 139pp. (In Danish).

Hoffmans, G.J.C.M. and Verheij, H.J. (1997). Scour Manual. Balkema.

Khalfin I.Sh.(1983). Local scour around ice-resistant structures caused by wave and current effect. Proceedings of the Seventh International Conference on Port and Ocean Engineering under Arctic Conditions, Helsinki, Finland, 5-9 April 1983 vol 2. VTT Symposium 28, 992-1002.

Soulsby, R. (1997). Dynamics of Marine Sands. Thomas Telford, London. pp249

Sumer, B.M. and Fredsøe, J., (2002). The mechanics of scour in the marine environment. Advanced series in Ocean Engineering - Volume 17.

Sumer, B.M., Fredsøe, J. and Christiansen, N., (1992). Scour around a vertical pile in waves. J. Waterway, Port, Coastal, and Ocean Engineering. ASCE, Vol. 118, No. 1, pp. 15 - 31.

Sumer, B.M. and Fredsøe, J., (2001). Wave scour around a large vertical circular cylinder. J. Waterway, Port, Coastal, and Ocean Engineering. May/June 2001.

Whitehouse, R.J.S., (2004). Marine scour at large foundations. In: Proc. 2nd Int. Conf. On Scour and Erosion, (eds). Chiew, Y-M., Lim, S-Y. and Cheng, N-S., Singapore, 14 - 17 Nov, Vol. 2, pp. 455 - 463.

Whitehouse, R.J.S., (1998). Scour at marine structures: A manual for practical applications. Thomas Telford, London, 198 pp.

Contact Us

ABPmer

Quayside Suite,
Medina Chambers
Town Quay, Southampton
SO14 2AQ

T +44 (0) 23 8071 1840
F +44 (0) 23 8071 1841
E enquiries@abpmer.co.uk

www.abpmer.co.uk

ABP mer

Fferm Wynt Alltraeth

AWEL Y MÔR
Offshore Wind Farm

RWE Renewables UK
Swindon Limited

Windmill Hill Business Park
Whitehill Way
Swindon
Wiltshire SN5 6PB
T +44 (0)8456 720 090
www.rwe.com

Registered office:
RWE Renewables UK
Swindon Limited Windmill
Hill Business Park Whitehill
Way
Swindon